LOW TEMPERATURE CRACKING RESISTANCE CHARACTERISTICS OF RECYCLED ASPHALT PAVEMENT BINDER

FHWA-RIDOT-RTD-02-6
August 31, 2002

K. Wayne Lee, Ph.D., P.E.
Arun Shukla, Ph.D.
Nikone Soupharath
James Wilson

College of Engineering
University of Rhode Island

Sponsored By

Rhode Island
Department of Transportation

Research and Technology Development

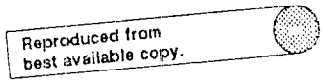

Technical Report Documentation Page

1. Report No.	2. Government Accession No.	3. Recipient's Catalog No.
FHWA-RI-RTD-02-6		

4. Title and Subtitle	5. Report Date
Low Temperature Cracking Resistance Characteristics of Recycled Asphalt Pavement Binder	August 31, 2002
	6. Performing Organization Code
7. Author (s)	8. Performing Organization Report No.
K. Wayne Lee, Arun Shukla, Nikone Soupharath, and James Wilson	URI-CVET-99-2
9. Performing Organization Name and Address	10. Work Unit No. (TRAIS)
College of Engineering University of Rhode Island Kingston, RI 02881	11. Contract or Grant No. SPR-225-2240
	13. Type of Report and Period Covered
12. Sponsoring Agency Name and Address	14. Sponsoring Agency Code
Research and Technology Development Rhode Island Department of Transportation Providence, RI 02903	

15. Supplementary Notes

16. Abstract

An attempt was made to evaluate the rheological and mechanical properties of asphalt blended with binder extracted from recycled asphalt pavement (RAP). This report presents results of the investigation dealing with resistance characteristics against permanent deformation, fatigue and low temperature cracking. Two base asphalt binders (PG 58-28 and PG 64-22) typically used in Rhode Island were blended with RAP binders obtained from two sources at percentage of 0, 10, 20, 30, 40, 50, 75, and 100% based on the total weight of blended asphalt binder. The Dynamic Shear Rheometer (DSR) was used to evaluate the blended asphalt binders at high temperatures, i.e., 52, 58, 64, 70, and 76°C and intermediate temperatures, i.e., 19, 22, 25, 28, and 31°C. A good linear relationship between log dynamic shear and the amount of RAP binders was obtained from this study. It was also observed that an increase in RAP binder content causes an increase in dynamic shear. It was found that the addition of RAP binder generally increases the resistance against permanent deformation. However, the Superpave criteria of $G^*\sin\delta$ may dictate the maximum amount of RAP addition not to have fatigue cracking. The Bending Beam Rheometer (BBR) test was performed to evaluate the resistance characteristics of blended asphalt binder against thermal cracking at low temperatures, i.e., -6, -12, -18, and –24 °C. It was observed that the creep stiffness increased and the m-value decreased for all temperatures as the amount of RAP binder content increased. It appears that the addition of RAP did not enhance the binder's resistance characteristic against low temperature cracking. Furthermore, the Superpave criteria of S(t) and m(t) may dictate the maximum amount of RAP not to have low temperature cracking.

For the mechanical properties, the fracture toughness test was performed to characterize the fracture behavior. A series of experiments was conducted at loading rate of 152.4 mm per minute to evaluate the fracture toughness of the blended asphalt binders at different temperatures i.e., 0, -10 and -20°C based on the principles of linear elastic fracture mechanics. It was observed that the fracture toughness decreased as a function of RAP binder content. The crack propagation became unstable as the RAP amount was increased and the temperature was decreased. Consequentially, the increase of RAP amount and the decrease of temperature reduced ductility, and brittle fast fracture occurred. The dynamic constitutive behavior of blended asphalt binders was evaluated using the Split Hopkinson Pressure Bar (SHPB) test. It was observed that the performance of the binder was not affected by the addition of RAP binder at room nor at low temperatures. At -20°C, there was no significant difference in the average maximum flow stresses, as the RAP binder amount was increased; and the maximum flow strain was decreased, as the RAP binder content was increased. The addition of RAP binder increased the degree of brittle failure.

17. Key Words	18. Distribution Statement
Recycled asphalt pavement, asphalt mixture, permanent deformation, fatigue cracking, rutting, low-temperature cracking, Superpave, rheological properties, bending beam rheometer, mechanical properties, fracture toughness, Split Hopkinson Pressure Bar.	

19. Security Classif. (of this report)	20. Security Classif. (of this page)	21. No. of Pages	22. Price
		124	

Form DOT F 1700.7 (8-72) Reproduction of completed page authorized (art.5/94)

DISCLAIMER

A University of Rhode Island (URI) research team prepared this report for the Rhode Island Department of Transportation (RIDOT). The contents of the report reflect the views of the URI research team, which is responsible for the accuracy of the facts and data presented herein. The contents are not to be construed as the official position of the RIDOT or URI. This document does not constitute a standard, specification or regulation.

Citation of trade or manufacturer's names does not constitute an official endorsement or approval of the use of such commercial products. Trade or manufacturer's names appear herein solely because they are considered essential to the object of this study.

PREFACE

This is the final report of the research project, entitled "Low Temperature Cracking Resistance Characteristics of Recycled Asphalt Pavement (RAP) Binder." This study dealt with the investigation of the rheological properties of RAP binder to evaluate the resistance to permanent deformation, fatigue cracking and low temperature cracking using the Strategic Highway Research Program (SHRP) products, i.e., Superpave binder specification. In addition, this laboratory investigation characterized the fracture behavior and dynamic response of asphalt blended with binder extracted from RAP. Results of this laboratory investigation help the engineers understand the resistance characteristics of asphalt containing RAP binder against permanent deformation, fatigue and low temperature cracking of asphalt pavements. The report presents the results of:

1. Investigation of the effect of RAP binder percentages on the physical and rheological properties of asphalt blended with binder extracted from the RAP;
2. Investigation of the effect of RAP source and variation on physical and rheological properties of asphalt blended with binder extracted from the RAP;
3. Evaluation of the permanent deformation, fatigue and low-temperature cracking resistance characteristics of asphalt blended with RAP binders by utilizing Superpave binder tests;
4. Determination of the Superpave performance based grading for asphalt blended with RAP binders;
5. Evaluation of the fracture toughness of the asphalt containing RAP binder; and
6. Evaluation of the dynamic constitutive behavior of asphalt blended with binder extracted from the RAP.

This research project was conducted by a research team of the College of Engineering at the University of Rhode Island (URI) under contract No. SPR-225-2240 (RIDOT-RTD-98-1) for the Rhode Island Department of Transportation (RIDOT). Funds were provided by RIDOT and the Federal Highway Administration (FHWA).

The work presented herein was accomplished by a team including Dr. K. Wayne Lee, Dr. Arun Shukla, Mr. Nikone Soupharath and Mr. James Wilson. Appreciation is due to Messrs. Brian Gray, Amphone Soupharath, Sekhar Vajjhala, Eugene Mozzoni, and Todd Brayton who assisted with laboratory work. Grateful recognition is forwarded to Mmes. Gail Paolino and Virginia Mulholland for manuscript preparation and administrative assistance. The authors express their gratitude to Cardi Corporation and Lynch & Sons Inc., which supplied RAPs, and Hudson Co., which provided asphalt binders. The authors wish to acknowledge the assistance and cooperation of the RIDOT in this study. In particular, the authors are indebted to Messrs. Colin Franco, Francis Manning and Mrs. Deborah Munroe of Research and Technology Development section, and Messrs. Mark Felag, Mike Byrne, David Clark, William Ringgold and Mike Foisey of the Materials section.

TABLE OF CONTENTS

LIST OF TABLES

LIST OF FIGURES

CHAPTER 1. INTRODUCTION

For over a century, paved roadways have been constructed using asphalt concrete mixtures in Rhode Island as well as across the United States. However, a major problem still exists in asphalt pavement involving premature distresses and failures, e.g., permanent deformation, fatigue cracking, and low temperature cracking. Since the early 1970s, many highway agencies have recycled old pavements in the overlay or major reconstruction of highways. Recently, the use of Recycled Asphalt Pavement (RAP) has significantly increased due to the protection of the environment, economy of construction/rehabilitation procedures, and the conservation of materials. However, the evaluation of RAP performance has not been well established.

The Strategic Highway Research Program (SHRP) developed a performance based specification for asphalt binder accompanied by a new system and testing procedures, as a component of "Superpave™," which stands for *Su*perior *Per*forming Asphalt *Pave*ment (McGennis et al. 1994). Six types of new binder testing equipment were recommended to measure the physical and/or rheological properties of modified as well as unmodified asphalt binders that can be related directly to field performance by engineering principles. Among the equipment, the Dynamic Shear Rheometer (DSR) was chosen to evaluate permanent deformation and fatigue cracking resistance characteristics by measuring the properties of asphalt binder at high and intermediate temperatures, respectively. The Bending Beam Rheometer (BBR) was chosen to evaluate the low temperature properties of the asphalt binders. Yet, Superpave did not include a comprehensive RAP mixture evaluation system. Therefore, an attempt was made to evaluate rheological properties of blended asphalt containing RAP binder by

utilizing the Superpave tool and to help engineers gain insight into the use of RAP in asphalt pavement.

Since SHRP performed a limited investigation related to fracture and crack propagation within asphalt mixtures, further mechanical characterization of asphalt binder and mixture is warranted. In the present study, single notched specimens were used for the fracture toughness testing. Split Hopkinson pressure bar (SHPB) equipment was utilized to characterize the dynamic constitutive behavior.

The goal of the present study was to investigate the relationship between rheological and mechanical properties and RAP binder percentage in blended asphalt for evaluation of performance. Specific objectives of the present study were:

1. To investigate the effect of RAP binder percentages on the physical and rheological properties of asphalt blended with binder extracted from the RAP;
2. To investigate the effect of RAP source and variation on physical and rheological properties of asphalt blended with binder extracted from the RAP;
3. To evaluate permanent deformation, fatigue cracking, and low-temperature cracking resistance characteristics of asphalt blended with RAP binders by utilizing Superpave binder tests;
4. To determine the Superpave performance based grading for asphalt blended with RAP binders;
5. To evaluate the fracture toughness of the asphalt containing RAP binder; and
6. To evaluate dynamic constitutive behavior of asphalt blended with binder extracted from the RAP.

CHAPTER 2. PERMANENT DEFORMATION

Permanent deformation or rutting is a type of distress, which can be found in the surface of asphalt pavement. Rutting mostly occurs along the wheel path of the traffic. The surface cross section is no longer in its design position. It is caused by many sources (e.g., traffic densification, abrasion, and underlaying hot mix asphalt (HMA) weakened by moisture damage), and has two principal causes (May and McGennis 1996). Firstly, the rutting is caused by high stress being applied to the subgrade and/or granular subbase layer below the asphalt layer.

Secondly, the rutting results from the asphalt mixture having too low a shear strength to resist repeated heavy loads. Typically, rutting occurs during the hot summer under high pavement temperatures. Although aggregates play the major roles in causing permanent deformation, the soft asphalt binder can be a contributing factor. Since rutting is an accumulation of very small permanent deformation, stiffer asphalt binder and mineral aggregates with a high degree of internal friction are needed to increase shear strength.

2.1 Physical and Rheological Properties

The present study investigated and analyzed the effect of RAP binder percentage on the physical and rheological properties of asphalt blended with extracted binders from the recycled asphalt pavement (RAP). Then, the rheological property was utilized to determine the resistance characteristics of blended asphalt binders against permanent deformation (rutting).

2.1.1 Experimental Plan

To examine the source variation, RAPs were procured from two HMA plants (C and L) in Rhode Island. Two base asphalts, i.e., PG 58-28 (or AC-10) and PG 64-22 (or AC-20) typically used in Rhode Island, were blended with different amounts of RAP binders, i.e., 0, 10, 20, 30, 40, 50, 75 and 100% based on the total weight of blended asphalt binders. The absolute viscosity was measured at 60°C (140°F) in accordance with the procedure of American Association of State Highway and Transportation Officials (AASHTO) T202-91("Standard" 1995). The Brookfield rotational viscosity at 135°C was recommended in the Superpave binder specification to determine the handling and pumping characteristics of the asphalt binder at the refinery, terminal, or hot mixing asphalt plant. The test was performed in accordance with the procedure of American Society for Testing and Materials (ASTM) D4402 ("Annual" 1997). Two replicates were tested in the present study.

Dynamic Shear Rheometer (DSR) tests were performed in accordance with the procedure of AASHTO TP5 at Superpave high temperatures, i.e., 52, 58, 64, 70, and 76°C ("Provisional" 1996). These binders were aged using the rolling thin film oven (RTFO), and DSR tests were performed. Values of $G^*/\sin\delta$ were determined to evaluate the rutting resistance characteristics of binders for all temperatures. The experimental design in the year of 1997 is summarized in Table 2.1. To study the variation from the same asphalt plant, other RAPs were secured from Plants C and L in 1998. RAP binders were blended with base asphalts similar to those used in 1997 study, and the absolute viscosity and DSR tests were performed with the same procedure used in the previous year study (Table 2.2).

2.1.2 Sample Preparation

RAP binders were recovered in accordance with the procedure of AASHTO T170-93 at the Rhode Island Department of Transportation (RIDOT) laboratory ("Standard" 1995). It may be noted that detailed information on the two RAP sources was not available, e.g., virgin asphalt properties, age, etc. The base asphalts were procured from a Rhode Island distributor, H. Virgin and RAP asphalt binders were heated to 135 and 160°C, respectively. The base asphalt was blended with the required amount of RAP binder using a mechanical stirrer.

2.1.3 Laboratory Testing

After absolute viscosity testing, the base asphalt and blended asphalts with different amounts of RAP binders were tested with DSR. DSR was used to characterize the viscous and elastic behavior of asphalt binders. The test measures the complex shear modulus (G*) and phase angle (δ) of the asphalt binder at high and intermediate temperatures when the dynamic (oscillatory) shear is applied to the sample using parallel plate test geometry (McGennis et al. 1994). G* is a measure of the total resistance of a material to deforming when repeatedly sheared. The delta (δ) is an indicator of the relative amounts of elastic (recoverable) and viscous (non-recoverable) deformation. The DSR tests were performed for unaged binders and RTFO aged binders.

The RTFO test was used to measure the effect of heat and air on the moving film of asphalt binders (Brown et al. 1996). This test was recommended in the Superpave binder specification to simulate short-term aging during mixing at the plant and lay down process. In accordance with the procedure of AASHTO Provisional Standard TP5, the

unaged and RTFO aged binders were tested using the 25mm plate and 1mm gap setting for DSR testing.

2.1.4 Test Results

From the test results in the year of 1997, it has been observed that the absolute viscosity test results for the asphalt binders blended with Plant C and L RAPs were increased as the amounts of RAP increased. Also, the rotational viscosities were increased as a function of RAP binder contents for both Plant C and L RAPs (Lee et al. 1998).

In 1998, the absolute viscosity tests were performed similar to the experiments in 1997. The test results are summarized in Table 2.3. The comparisons of the test results are shown in Figures 2.1 and 2.2, and it was observed that the viscosity increases as the amount of RAP increases.

The absolute viscosity values were plotted in a log-log scale on the Y-axis. A good linear correlation was observed between the log-log rheological properties of blended asphalt and RAP binder contents. It was found that the log-log transformation was not the best fit, statistically. However, it was used, because the Asphalt Institute recommended it to determine the viscosity of asphalt blended with new and recovered binder ("Mix-Design" 1993). The models and high R^2 values of AC-10 and AC-20 containing Plant C and L RAP indicated the good linear relationship between the viscosity as a function of RAP amount in asphalt binder. The viscosity values of Plant C RAP binder in 1998 were slightly higher than the ones of Plant L RAP binder, and implies that the former RAP binder is harder than the latter (Figures 2.1 and 2.2). This

was reversed to the results in 1997. The characteristic of RAP binder is dependent on the age of the RAP. The older the RAP, the harder the RAP binder due to the volatilization and oxidation. However, the age of RAP was not available, because the original sources of the RAP were not identifiable.

A constant stress mode was used for the DSR test in the present study. The rutting parameter, $G^*/\sin\delta$ was measured at 52, 58, 64, 70, and 76°C. Tables 2.4 and 2.5 show the DSR test results of unaged asphalt binder containing Plant C and L RAPs, respectively. Tables 2.6 and 2.7 provide the data for RTFO aged binder containing Plant C and L RAPs, respectively. The experimental data were also plotted for the comparative analysis purpose as shown in Figures 2.3 through 2.10. As expected, the values of $G/\sin\delta$ were increased as the content of RAP binder was increased at all temperatures. In addition, a series of statistical analysis was performed on the test data in 1998.

2.1.5 Analysis and Discussion

The Superpave binder specification requires the rutting factor, $G^*/\sin\delta$ to be a minimum of 1.00 kPa and 2.20 kPa for unaged and RTFO aged binders, respectively. The rutting factor reflects the total resistance of a binder to deform under repeated loading (G^*), and the relative energy dissipated into non-recoverable deformation ($\sin\delta$) during the loading cycle. A higher value of $G^*/\sin\delta$ implies that the binder behaves more like an elastic material, which is desirable for rutting resistance. Since the tenderness factor, $G^*/\sin\delta$ for unaged binder was higher than 1.00 kPa at Superpave high grading temperatures, unaged binder results were not considered seriously in the present study.

Rather, the rutting resistance was evaluated mainly by examining G*/sinδ values of RTFO aged binders (Lee et al. 1998).

Based on the visual observation, it was observed that the binder with Plant L RAP exhibited higher G*/sinδ values than the one with Plant C RAP at all corresponding temperatures in 1997. It was also noted that the slope for binder with Plant L RAP is steeper than the one for binder with Plant C RAP. Since all values of G*/sinδ for RTFO aged binders were higher than the minimum 2.2 kPa at 58 and 64°C for AC-10 and AC-20 base binders, respectively, it appeared that the addition of RAP binder would enhance the resistance against rutting.

Similar observations were observed from the experiments conducted in 1998. As can be seen from Figure 2.3 through 2.10, the values of G*/sinδ for unaged and RTFO aged binders were increased as the content of RAP binder was increased at all temperatures. It was also observed that there was no significant difference in the slope of the trends between RAP binder sources (Plant C and L) for both base asphalt binders (PG 58-28 and PG 64-22). This may indicate that the rheological properties of both RAP binders secured in 1998 were the same. In addition, the dynamic shear values of the base binder used in 1997 were compared with the one used in 1998, and it was found that the former was slightly higher than the latter one. The dynamic shear values of the 100% RAP binders (Plant C and L) were also compared between the year of 1997 and 1998. It was found that the dynamic shear values of Plant C RAP binder used in 1997 were lower than the ones used in 1998. Inversely, the values of Plant L RAP binder in 1997 were higher than the ones in 1998. This may lead to a conclusion that the binder properties vary, although the RAP came from the same asphalt plant.

To linearize the relationship between the G*/sinδ and the RAP binder content, data transformation has been carried out. The log transformation of G*/sinδ was found to give the best fit and could be applicable for all blended asphalt binders. Furthermore, the analysis of variance (ANOVA) was performed to investigate the effects of the controlled variables using Minitab. Mintab is the user-friendly statistical software for data analysis. As can be observed from the ANOVA table in Table 2.8, all four main effects were found to be statistically significant. All of the two-way interactions of the variables were found significant, except for the interaction of temperature with RAP source. The F-test shows that the interactions and the RAP source variables were found significantly lower than the main effect variables (RAP binder content, temperature, and asphalt type). Some of the terms in the full model were dropped to improve the model, i.e., RAP source and the interactions. The coefficient of determination (R^2) was found to be 99.2% for the reduced model, which is not significantly different than the R^2 value of 99.9% determined from the full model with interaction effects.

Table 2.8 also shows the linear regression models for different variables. The first reduced model containing all main effect variables gives an R^2 value of 99.2%, which is not significantly different than the second model without the RAP source variable. In the last model, the asphalt type variable was eliminated, and the R^2 value did not differ significantly from the other models. This statistical analysis indicates that the asphalt type and the RAP source are not important factors. It may be noted that if either asphalt type or RAP sources with more significant differences in their rheological properties will be used, the asphalt type and RAP source variables should be considered in the models. The interactions were found to be less important due to a high R^2 value.

The linear relationship between the increase in log $G^*/\sin\delta$ and blended asphalt binder content indicates that the effect of RAP binders can be reliably predicted using simple linear models. These models were observed to be valid for all combinations of RAP binder and asphalt. It may be noted that the above statistical analyses were performed only on the dynamic shear values of RTFO aged binder tested in 1998.

TABLE 2.1. Experimental Design to Evaluate Viscosities and Dynamic Shear Properties of Asphalt Blended with RAP Binders in 1997.

Tests	RAP Binder, %							
	0	10	20	30	40	50	75	100
Absolute Viscosity	4	4	4	4	4	4	4	4
Rotational Viscosity	4	4	4	4	4	4	4	4
DSR, Unaged	4	4	4	4	4	4	4	4
DSR, RTFO	4	4	4	4	4	4	4	4
DSR, PAV	4	4	4	4	4	4	4	4

NOTE: 1. 4 = 2 (RAP source) x 2 (base asphalts).
2. DSR tests were performed at the Superpave high and intermediate temperatures, i.e., 52, 58, 64, 70, 76°C and 19, 22, 25, 28, 31°C, respectively.
3. Two replicate samples were tested for all experimental cells.

TABLE 2.2. Experimental Design to Evaluate Viscosities and Dynamic Shear Properties of Asphalt Blended with RAP Binders in 1998.

Tests	RAP Binder, %							
	0	10	20	30	40	50	75	100
Absolute Viscosity	4	4	4	4	4	4	4	4
DSR, Unaged	4	4	4	4	4	4	4	4
DSR, RTFO	4	4	4	4	4	4	4	4
DSR, PAV	4	4	4	4	4	4	4	
BBR, PAV Aged	4	4	4	4	4	4	4	4

NOTE: 1. 4 = 2 (Plant C and L RAP) x 2 (PG 58-28 & PG 64-22).
2. DSR tests were performed at the Superpave high (52, 58, 64, 70, and 76°C) and intermediate temperatures (19, 22, 25, 28, and 31°C).
3. All BBR tests were performed at the Superpave low temperatures (-6, -12, -18, and - 24°C).
4. Two replicate samples were tested for all experimental cells.

Table 2.3 Absolute Viscosity Results of Asphalt Blended with RAP Binders.

RAP, %	Absolute Viscosity Values in 1997 (Poise)		Absolute Viscosity Values in 1998 (Poise)	
	AC-10 (PG 58-28)	AC-20 (PG 64-22)	AC-10 (PG 58-28)	AC-20 (PG 64-22)
RAP from Plant C				
0	1,035	2,209	1,053	2,151
10	1,225	2,623	1,390	2,819
20	1,625	2,864	1,833	3,956
30	2,133	3,241	2,610	5,444
40	2,700	4,446	3,609	7,071
50	3,902	5,769	5,880	9,177
75	10,011	12,033	16,721	19,660
100	18,640	18,640	37,477	37,477
RAP from Plant L				
0	1,035	2,209	1,053	2,151
10	1,689	3,383	1,295	2,721
20	3,114	5,146	1,522	3,825
30	4,303	6,672	2,638	4,471
40	7,453	14,422	3,465	6,138
50	13,170	19,965	4,996	8,776
75	77,818	103,165	11,356	14,987
100	463,836	463,836	26,789	26,789

Note: The test was performed at 60°C.

Table 2.4 DSR Test Results of Unaged Asphalt Binders Blended with Plant C-RAP in 1998.

RAP, %	Temps, C	Unaged					
		PG 58-28			PG 64-22		
		G*	δ	G*/sinδ	G*	δ	G*/sinδ
0	52	2.73	85.1	2.7	5.54	81.8	5.6
	58	1.21	86.5	1.21	2.53	84.1	2.54
	64	0.61	87.8	0.61	1.15	85.9	1.15
	70	0.31	88.7	0.31	0.59	87.3	0.59
	76	0.17	89.0	0.17	0.31	88.3	0.31
10	52	3.85	83.7	3.87	6.77	80.5	6.86
	58	1.67	85.7	1.67	3.11	82.7	3.13
	64	0.81	87.0	0.81	1.47	84.7	1.47
	70	0.41	88.2	0.41	0.74	86.5	0.74
	76	0.22	88.8	0.22	0.39	88.0	0.39
20	52	5.94	81.9	6	9.49	78.9	9.67
	58	2.68	84.0	2.7	3.94	81.3	3.99
	64	1.22	85.9	1.22	1.89	83.5	1.9
	70	0.61	87.3	0.61	0.96	85.1	0.96
	76	0.32	88.2	0.32	0.49	86.2	0.49
30	52	6.43	80.7	6.51	11.70	77.2	12
	58	2.80	83.0	2.82	5.41	79.5	5.5
	64	1.40	85.1	1.4	2.57	82.1	2.59
	70	0.67	86.9	0.67	1.21	83.6	1.21
	76	0.36	87.9	0.36	0.60	84.2	0.6
40	52	9.48	78.7	9.67	16.65	75.7	17.19
	58	4.13	81.3	4.18	7.32	78.6	7.47
	64	2.02	83.6	2.03	3.15	81.3	3.18
	70	0.99	85.4	0.99	1.53	83.7	1.53
	76	0.50	87.2	0.5	0.79	85.6	0.79
50	52	13.97	76.8	14.35	20.01	74.2	20.8
	58	5.79	79.7	5.88	8.59	77.3	8.81
	64	2.70	82.4	2.72	3.95	80.0	4.01
	70	1.33	84.4	1.34	1.91	83.0	1.92
	76	0.66	86.2	0.66	0.95	85.2	0.95
75	52	31.47	71.7	33.16	38.92	69.8	41.48
	58	14.03	74.9	14.53	17.97	73.6	18.73
	64	6.23	78.1	6.63	7.84	76.8	8.05
	70	2.90	80.9	2.94	3.58	80.0	3.63
	76	1.42	83.8	1.43	1.78	82.8	1.79
100	52	65.03	66.9	70.7	65.03	66.9	70.7
	58	29.56	70.7	31.32	29.56	70.7	31.32
	64	13.03	74.6	13.51	13.03	74.6	13.51
	70	6.30	78.1	6.44	6.30	78.1	6.44
	76	2.92	80.9	2.95	2.92	80.9	2.95

Table 2.5 DSR Test Results of Unaged Asphalt Binders Blended with Plant L-RAP in 1998.

RAP, %	Temps, C	Unaged					
		PG 58-28			PG 64-22		
		G*	δ	G*/sinδ	G*	δ	G*/sinδ
0	52	2.73	85.1	2.7	5.54	81.8	5.6
	58	1.21	86.5	1.21	2 53	84.1	2.54
	64	0.61	87.8	0.61	1.15	85.9	1.15
	70	0.31	88.7	0.31	0.59	87.3	0.59
	76	0.17	89.0	0.17	0.31	88.3	0.31
10	52	3.26	84.1	3.27	7.73	80.0	7.85
	58	1.54	86.2	1.54	3.48	82.4	3.51
	64	0.74	88.2	0.74	1.68	84.9	1.68
	70	0.38	89.9	0.38	0.84	86.4	0.84
	76	0.21	88.3	0.21	0.43	88.8	0.43
20	52	4.08	83.4	4.10	11.35	77.6	11.62
	58	1.89	85.7	1.89	4.99	81.2	5.05
	64	0.91	87.7	0.91	2.35	83.1	2.36
	70	0.46	89.4	0.46	1.16	85.7	1.16
	76	0.25	88.8	0.25	0.56	87.4	0.56
30	52	6.79	80.5	6.89	12.13	78.3	12.39
	58	3.09	82.7	3.11	5.37	80.5	5.44
	64	1.48	85.1	1.49	2.44	83.1	2.45
	70	0.75	87.6	0.75	1.23	85.4	1.23
	76	0.39	89.4	0.39	0.64	87.6	0.64
40	52	8.06	80.0	8.18	13.90	76.5	14.29
	58	3.55	82.7	3.57	6.47	79.4	6.58
	64	1.74	85.2	1.74	3.06	82.0	3.09
	70	0.84	86.8	0.84	1.45	84.6	1.45
	76	0.43	88.9	0.43	0.72	86.9	0.72
50	52	11.54	77.7	11.81	15.62	75.7	16.12
	58	5.46	80.6	5.53	7.53	78.6	7.68
	64	2.51	83.4	2.52	3.39	81.1	3.43
	70	1.16	85.7	1.16	1.60	84.0	1.61
	76	0.60	87.7	0.60	0.82	86.1	0.82
75	52	25.37	73.8	26.42	33.25	72.7	34.83
	58	11.21	77.0	11.50	15.10	75.1	15.63
	64	5.38	79.7	5.47	6 79	78.1	6.94
	70	2.46	82.5	2.48	3.25	80.9	3.29
	76	1.25	85.1	1.25	1.60	84.2	1.61
100	52	49.94	70.2	53.09	49.94	70.2	53.09
	58	23.31	72.6	24.42	23.31	72.6	24.42
	64	10.09	76.1	10.39	10.09	76.1	10.39
	70	4.67	79.4	4.75	4.67	79.4	4.75
	76	2.34	82.5	2.36	2.34	82.5	2.36

Note: 1. The unit for G*/sinδ is kPa.
2. The unit for δ is degree.

Table 2.6 DSR Test Results of RTFO aged Asphalt Binders Blended with Plant C-RAP in 1998.

RAP, %	Temps, C	RTFO Aged					
		PG 58-28			PG 64-22		
		G*	δ	G*/sinδ	G*	δ	G*/sinδ
0	52	6.75	80.1	6.85	14.94	74.6	15.5
	58	3.0	82.7	4.77	6.68	77.8	6.83
	64	1.47	84.7	1.48	3.29	80.8	3.33
	70	0.72	86.6	0.72	1.55	83.2	1.56
	76	0.37	87.5	0.37	0.78	85.2	0.78
10	52	10.01	77.9	10.23	20.78	73.0	21.72
	58	4.71	80.9	4.77	9.44	76.0	9.73
	64	2.22	82.9	2.23	4.40	79.4	4.47
	70	1.05	85.2	1.05	2.03	82.2	2.04
	76	0.54	86.6	0.54	1.04	84.8	1.04
20	52	19.82	73.5	20.67	25.98	71.2	27.45
	58	9.18	76.9	9.42	11.66	74.5	12.1
	64	4.22	79.9	4.29	5.39	78.1	5.5
	70	1.95	82.9	1.96	2.57	81.3	2.6
	76	0.96	85.5	0.96	1.26	84.0	1.27
30	52	22.88	72.9	23.94	35.96	69.4	38.42
	58	10.20	76.6	10.49	16.36	72.7	17.14
	64	4.59	79.6	4.67	7.43	76.0	7.65
	70	2.26	82.6	2.28	3.58	79.3	3.64
	76	1.08	85.3	1.08	1.79	82.4	1.81
40	52	31.41	70.9	33.24	48.60	67.2	52.71
	58	13.92	74.3	14.46	21.15	70.8	22.4
	64	6.11	77.6	6.26	10.19	74.5	10.57
	70	2.91	80.9	2.94	4.06	78.2	4.15
	76	1.48	83.6	1.48	2.32	81.0	2.35
50	52	44.14	68.3	47.50	68.94	65.6	75.73
	58	20.81	72.0	21.88	29.63	69.2	31.71
	64	9.55	75.5	9.87	13.38	72.3	14.04
	70	4.33	78.6	4.42	6.41	76.4	6.59
	76	2.08	82.0	2.10	3.23	79.9	3.28
75	52	84.23	64.6	93.24	130.43	62.1	147.58
	58	38.18	68.5	41.04	59.14	65.2	65.17
	64	18.77	72.2	19.71	26.71	68.2	28.77
	70	8.76	75.9	9.03	13.09	72.7	13.71
	76	4.03	79.4	4.10	6.23	76.2	6.41
100	52	225.49	60.1	260.24	225.49	60.1	260.24
	58	110.88	62.8	124.66	110.88	62.8	124.66
	64	50.11	66.6	54.62	50.11	66.6	54.62
	70	24.91	69.9	26.53	24.91	69.9	26.52
	76	11.13	74.0	11.58	11.13	74.0	11.58

Note: 1. The unit for G*/sinδ is kPa.

2. The unit for δ is degree.

Table 2.7 DSR Test Results of RTFO aged Asphalt Binders Blended with Plant L-RAP in 1998.

RAP, %	Temps, C	RTFO Aged					
		PG 58-28			PG 64-22		
		G*	δ	G*/sinδ	G*	δ	G*/sinδ
0	52	6.75	80.1	6.85	14.94	74.6	15.5
	58	3.07	82.7	4.77	6.68	77.8	6.83
	64	1.47	84.7	1.48	3.29	80.8	3.33
	70	0.72	86.6	0.72	1.55	83.2	1.56
	76	0.37	87.5	0.37	0.78	85.2	0.78
10	52	9.68	78.4	9.88	20.99	72.9	21.96
	58	4.49	81.1	4.55	9.89	76.3	10.18
	64	2.10	83.8	2.11	4.31	79.4	4.38
	70	1.02	86.0	1.02	2.19	82.2	2.21
	76	0.52	87.9	0.52	1.07	84.8	1.07
20	52	14.37	75.9	14.82	27.22	71.7	28.67
	58	6.39	78.8	6.52	12.41	74.5	12.88
	64	3.04	81.6	3.07	5.89	77.8	6.03
	70	1.41	84.3	1.42	2.71	81.1	2.74
	76	0.70	86.5	0.70	1.32	83.7	1.33
30	52	18.52	74.4	19.23	32.40	69.9	34.50
	58	8.69	77.6	8.90	14.77	73.2	15.43
	64	4.01	80.5	4.06	7.00	76.7	7.19
	70	1.86	83.1	1.87	3.45	80.3	3.50
	76	0.94	85.7	0.94	1.59	83.3	1.60
40	52	26.05	72.3	27.34	47.93	68.4	51.55
	58	11.33	75.5	11.70	21.32	71.8	22.44
	64	5.38	78.7	5.48	9.68	75.2	10.01
	70	2.60	81.7	2.63	4.66	78.3	4.76
	76	1.26	84.3	1.27	2.31	81.3	2.34
50	52	39.30	69.9	41.85	57.54	67.6	62.24
	58	18.06	73.3	18.86	25.47	70.0	27.10
	64	8.49	76.8	8.72	12.24	73.9	12.74
	70	4.05	79.8	4.12	5.66	77.1	5.81
	76	1.88	82.7	1.90	2.66	80.6	2.70
75	52	82.62	65.1	91.09	109.69	63.0	123.11
	58	35.84	69.3	38.31	50.97	67.4	55.21
	64	17.76	72.3	18.64	22.95	70.5	24.53
	70	8.57	75.7	8.84	10.76	73.9	11.20
	76	3.83	79.3	3.90	5.07	77.5	5.19
100	52	183.87	64.2	204.23	183.87	64.2	204.23
	58	84.86	63.7	94.66	84.86	63.7	94.66
	64	38.56	67.8	41.65	38.56	67.8	41.65
	70	19.39	71.0	20.51	19.39	71.0	20.51
	76	9.10	74.9	9.43	9.10	74.9	9.43

Note: 1. The unit for G*/sinδ is kPa.
2. The unit for δ is degree.

Table 2.8. Statistical Analyses of Rutting Parameter (G*/sinδ) for RTFO Aged Binders.

Analysis of Variance (ANOVA)

Full Model

Source	DF	Seq SS	Adj SS	Adj MS	F-test	P
Main Effect:						
RC	7	55.195	55.195	7.885	1.4E+04	0.000
T	4	70.711	70.711	17.678	3.2E+04	0.000
AC	1	3.475	3.475	3.475	6203.35	0.000
RS	1	0.167	0.167	0.167	298.01	0.000
Interactions:						
RC*T	28	0.038	0.038	0.001	2.43	0.000
RC*AC	7	0.782	0.782	0.112	199.34	0.000
RC*RS	7	0.083	0.083	0.012	21.10	0.000
T*AC	4	0.001	0.001	0.000	0.40	0.811
T*RS	4	0.002	0.002	0.001	0.89	0.469
AC*RS	1	0.020	0.020	0.020	36.38	0.000
Error	255	0.143	0.143	0.001		
Total	319	130.616	R^2= 99.9%			

Reduced Model

Source	DF	Seq SS	Adj SS	Adj MS	F-test	P
Main Effect:						
RC	7	55.195	55.195	7.885	1959.10	0.000
T	4	70.711	70.715	17.678	4392.21	0.000
AC	1	3.475	3.475	3.475	863.40	0.000
Error	307	1.236	1.236	0.004		
Total	319	130.6160	R^2= 99.2%			

No.	Linear Regression Models for Prediction of G*/sinδ	Adjusted R^2
1	Log G*/sinδ = 1.87 + 0.0132(RC) – 0.0554(T) + 0.0347(AC) – 0.0457(RS)	99.2%
2	Log G*/sinδ = 1.80 + 0.0132(RC) – 0.0554(T) + 0.0347(AC)	99.0%
3	Log G*/sinδ = 1.87 + 0.0132(RC) – 0.0554(T)	96.3%

RC = RAP binder content in percentage (i.e., 0, 10, 20, 30, 40, 50, 75, and 100%)
T = Temperatures in degree Celsius (i.e., 52, 58, 64, 70, and 76°C)
AC = High temperature grade of asphalt type (i.e., 58 and 64°C)
RS = Absolute viscosity value of Plant C and L RAP Source (i.e., 37,477 and 26,789 poises)

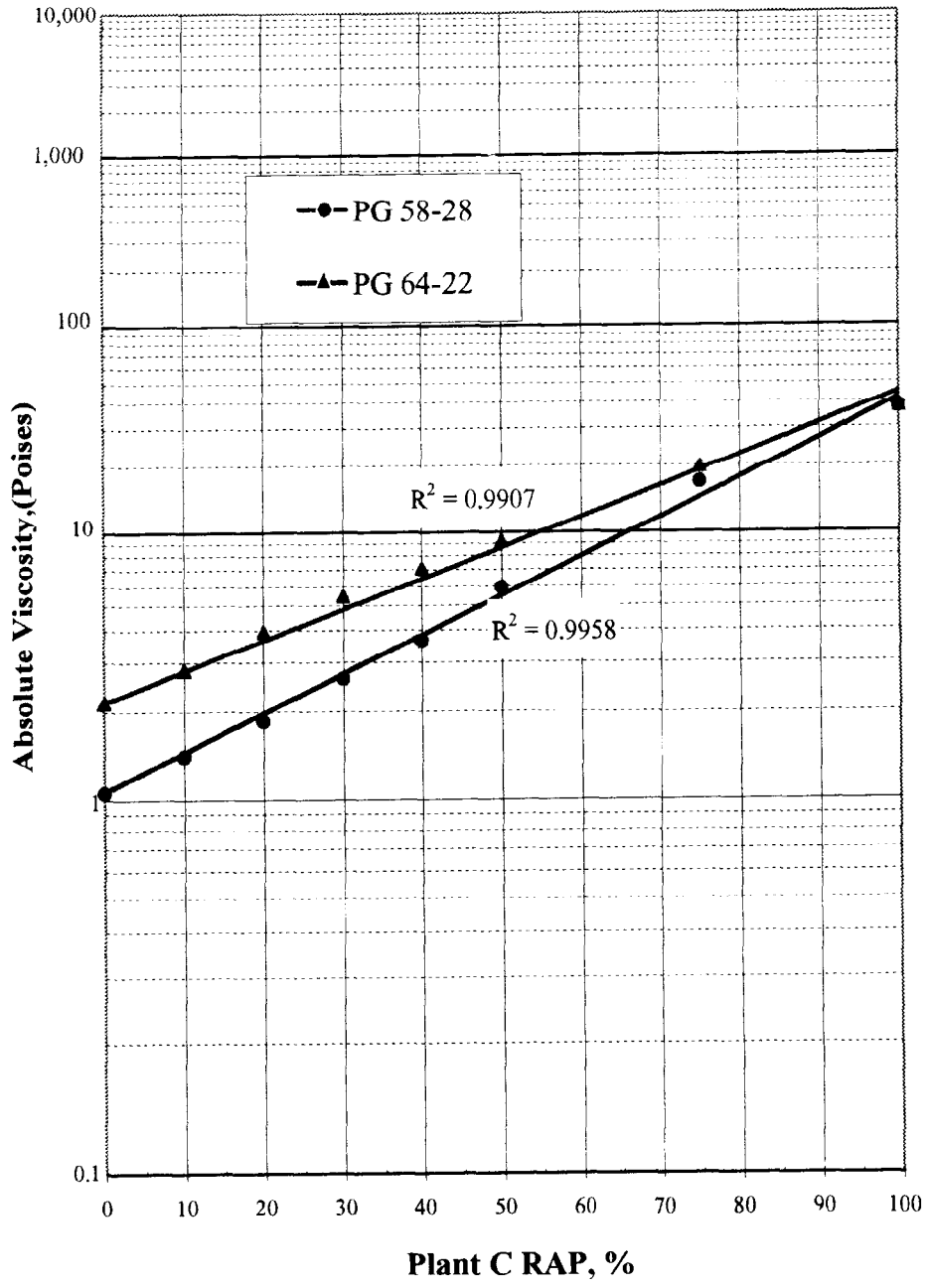

Figure 2.1 Comparison of Absolute Viscosity Test Results of the Asphalt Blend with Plant C RAP Binder in 1998.

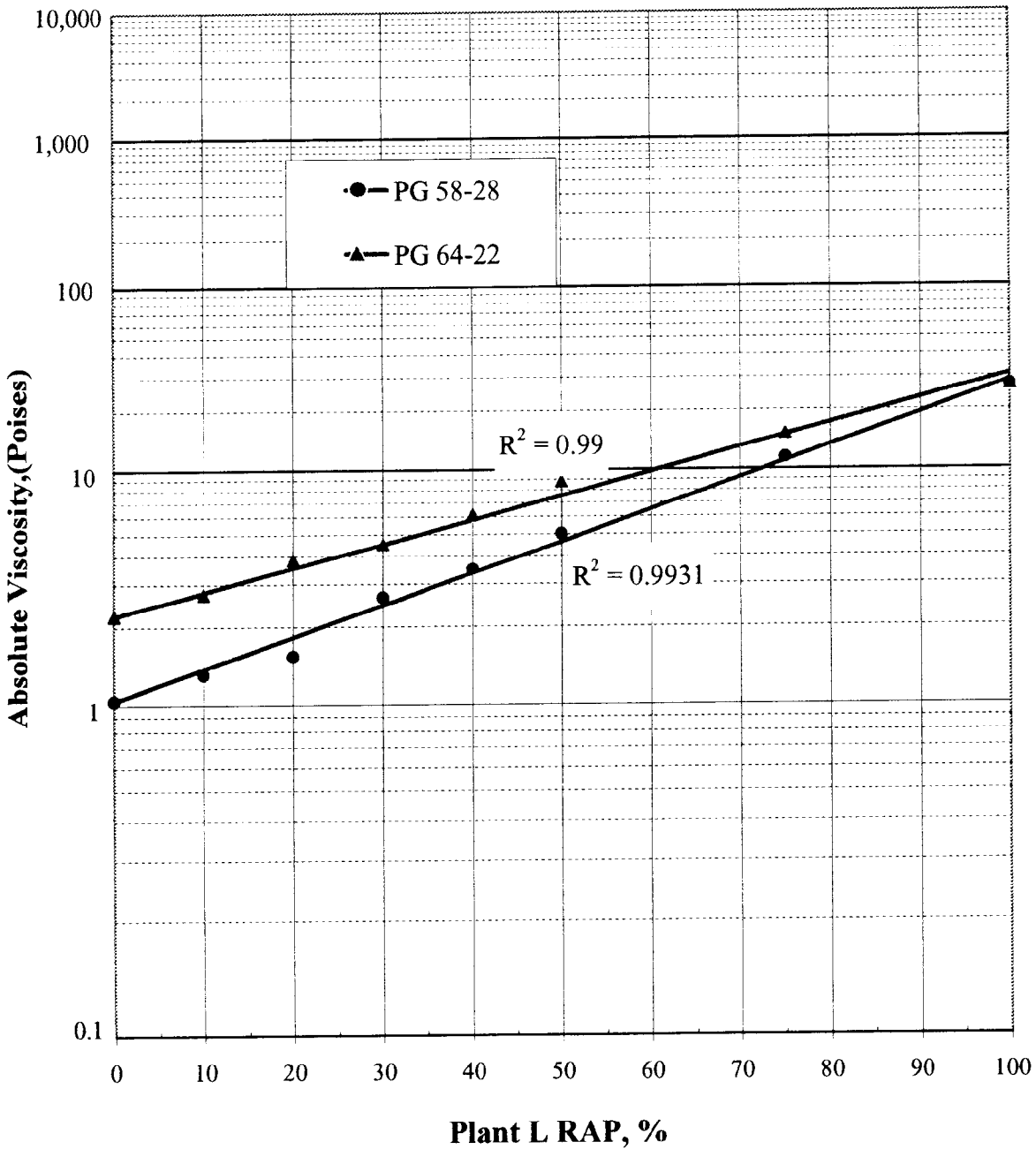

Figure 2.2 Comparison of Absolute Viscosity Test Results of Asphalt Blended with Plant L RAP in 1998.

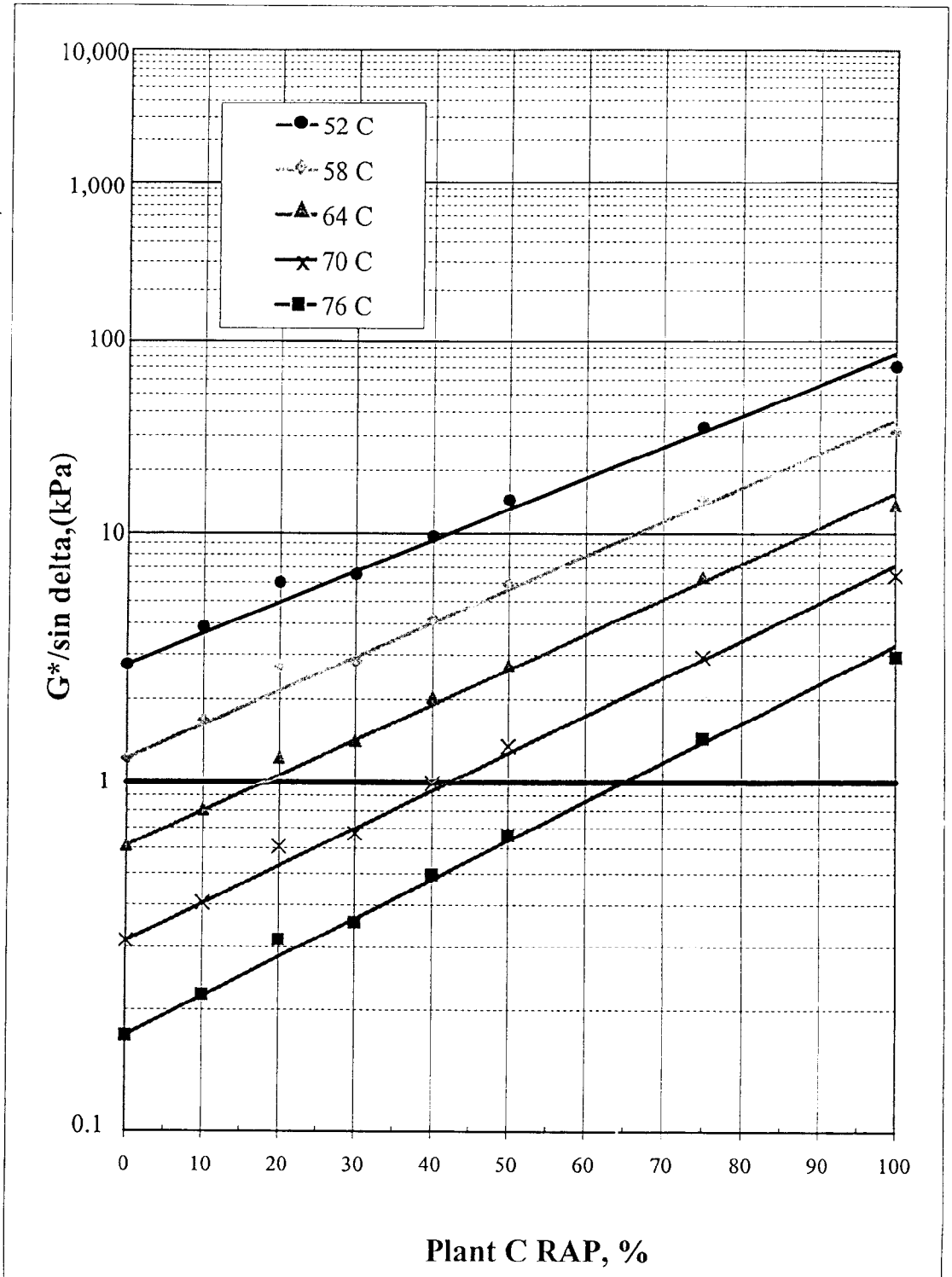

Figure 2.3 Comparison of DSR Test Results for Unaged Binder of PG 58-28 Base Binder Blended with Plant C RAP at Different Temperatures in 1998.

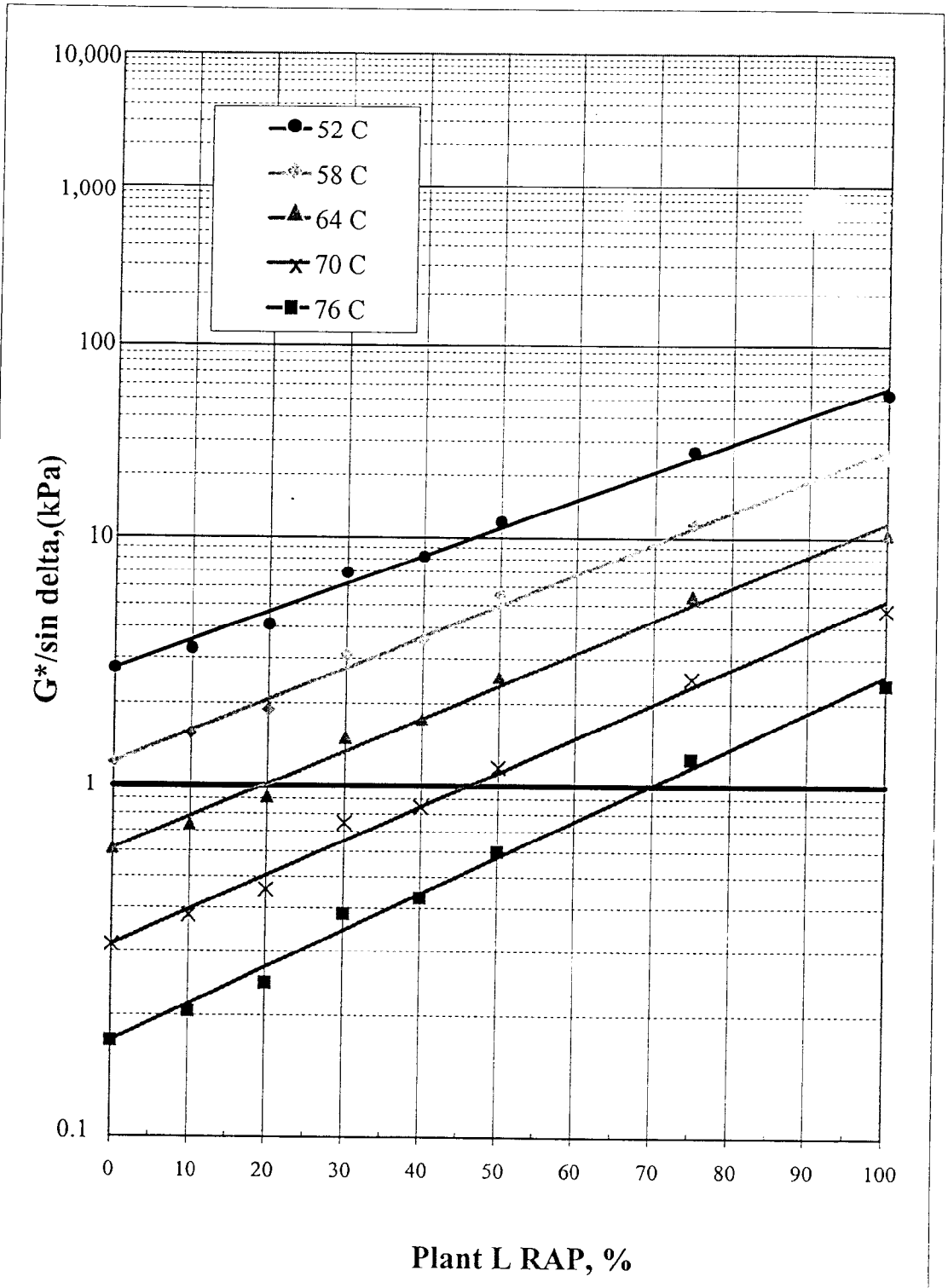

Figure 2.4. Comparison of DSR Test Results for Unaged Binder of PG 58-28 Base Binder Blended with Plant L RAP at Different Temperatures in 1998.

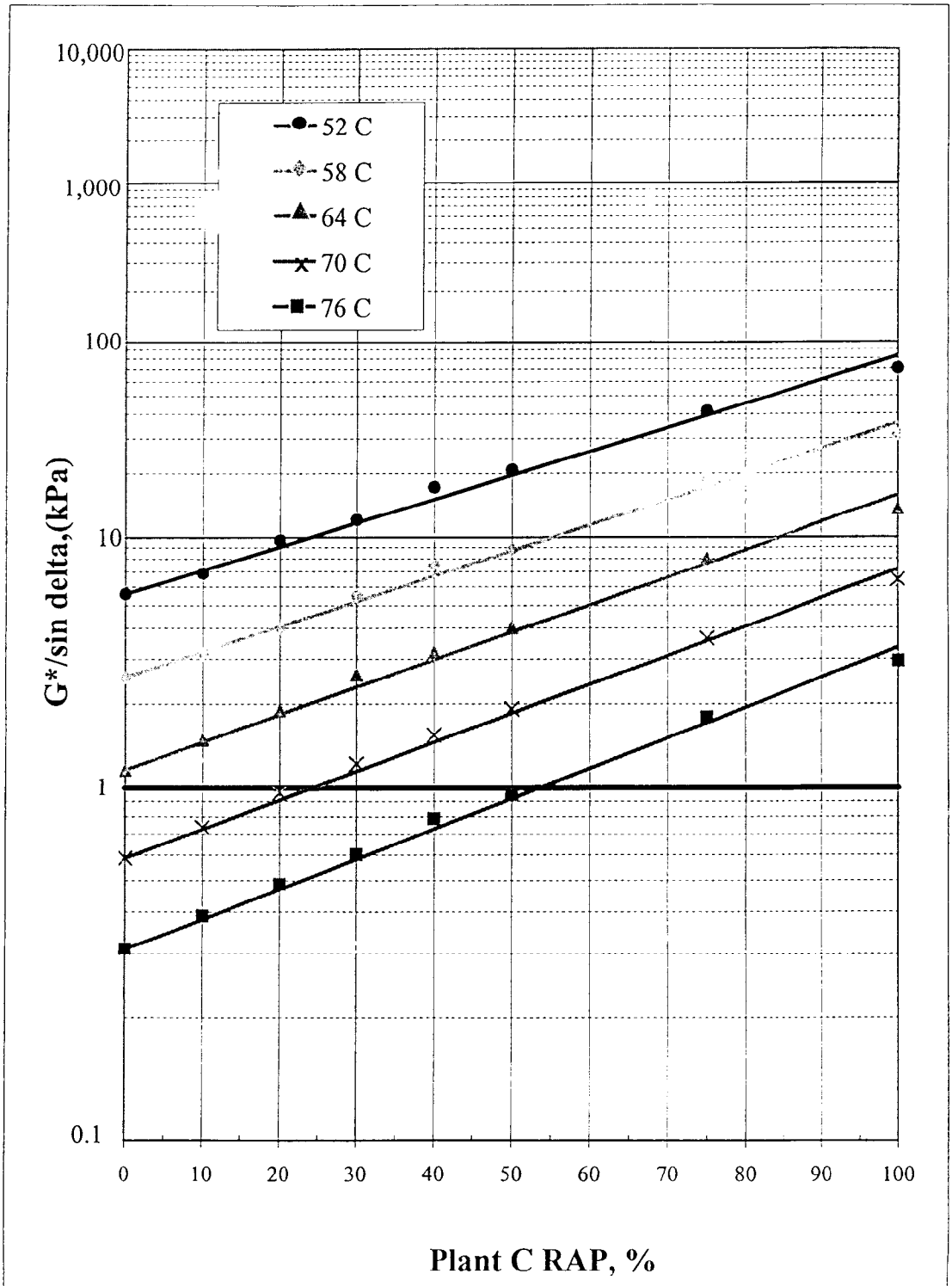

Figure 2.5. Comparison of DSR Test Results for Unaged Binder of PG 64-22 Base Binder Blended with Plant C RAP at Different Temperatures in 1998.

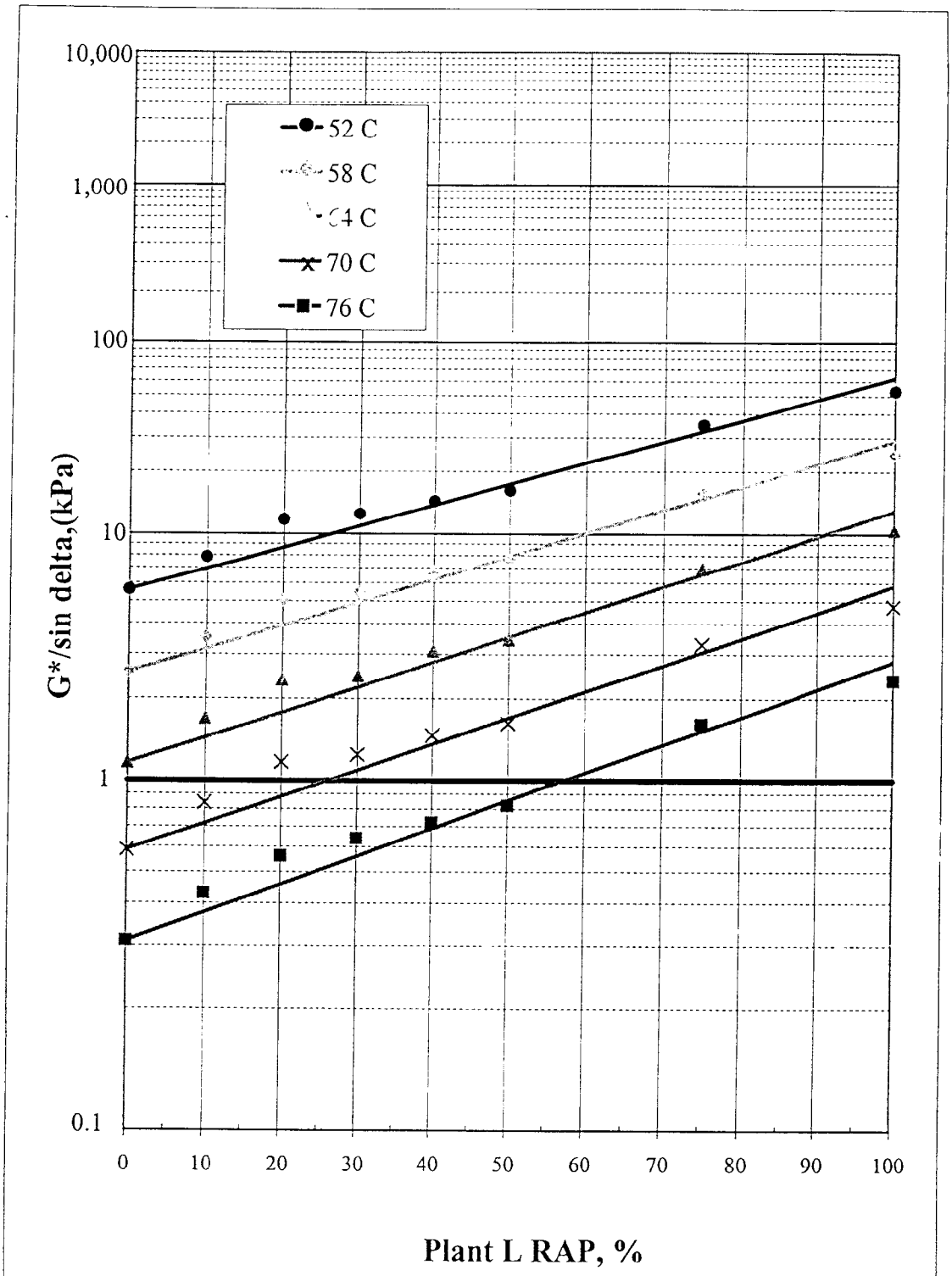

Figure 2.6. Comparison of DSR Test Results for Unaged Binder of PG 64-22 Base Binder Blended with Plant L RAP at Different Temperatures in 1998.

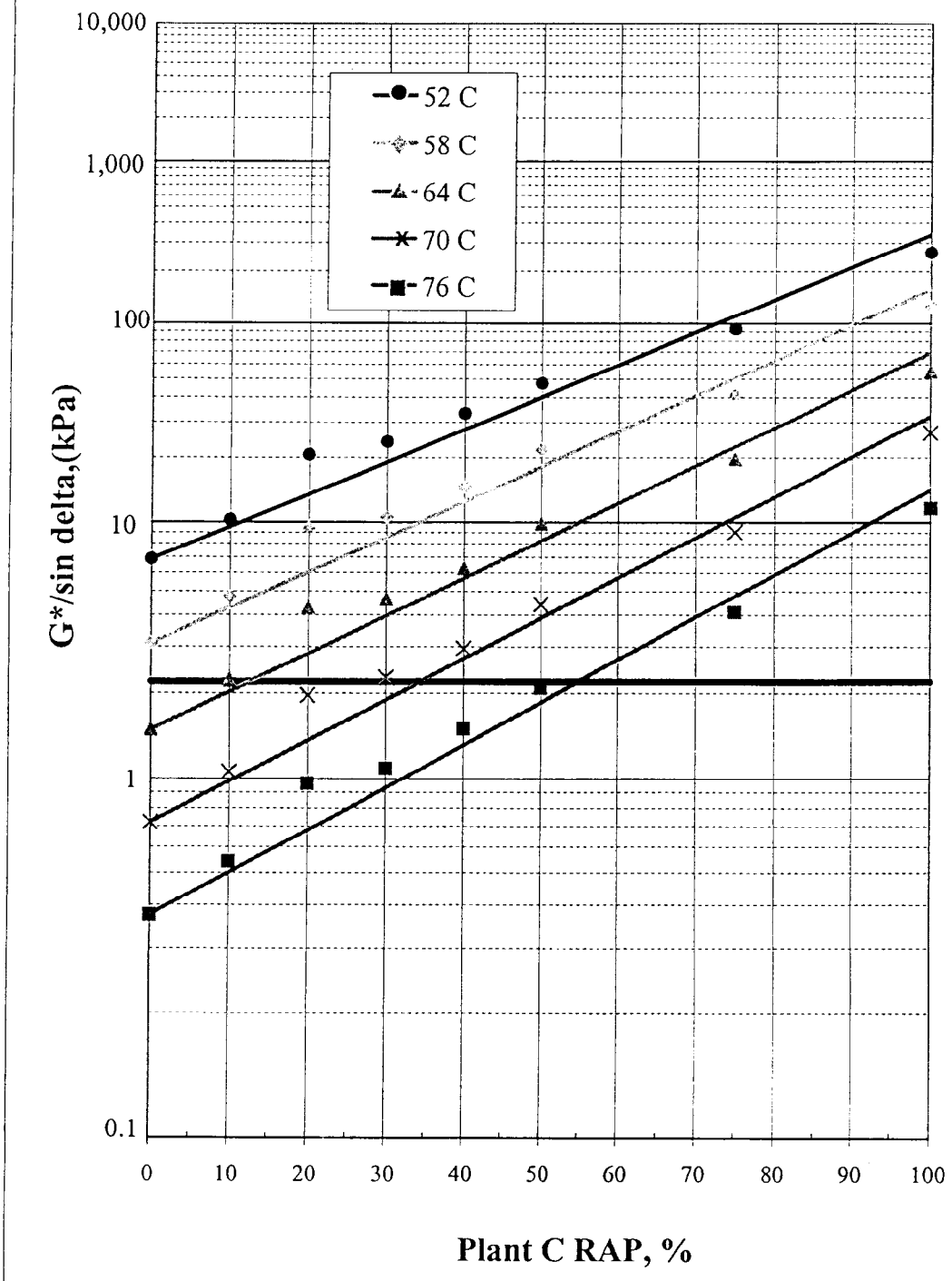

Figure 2.7. Comparison of DSR Test Results for RTFO Aged Binder of PG 58-28 Base Binder Blended with Plant C RAP at Different Temperatures in 1998.

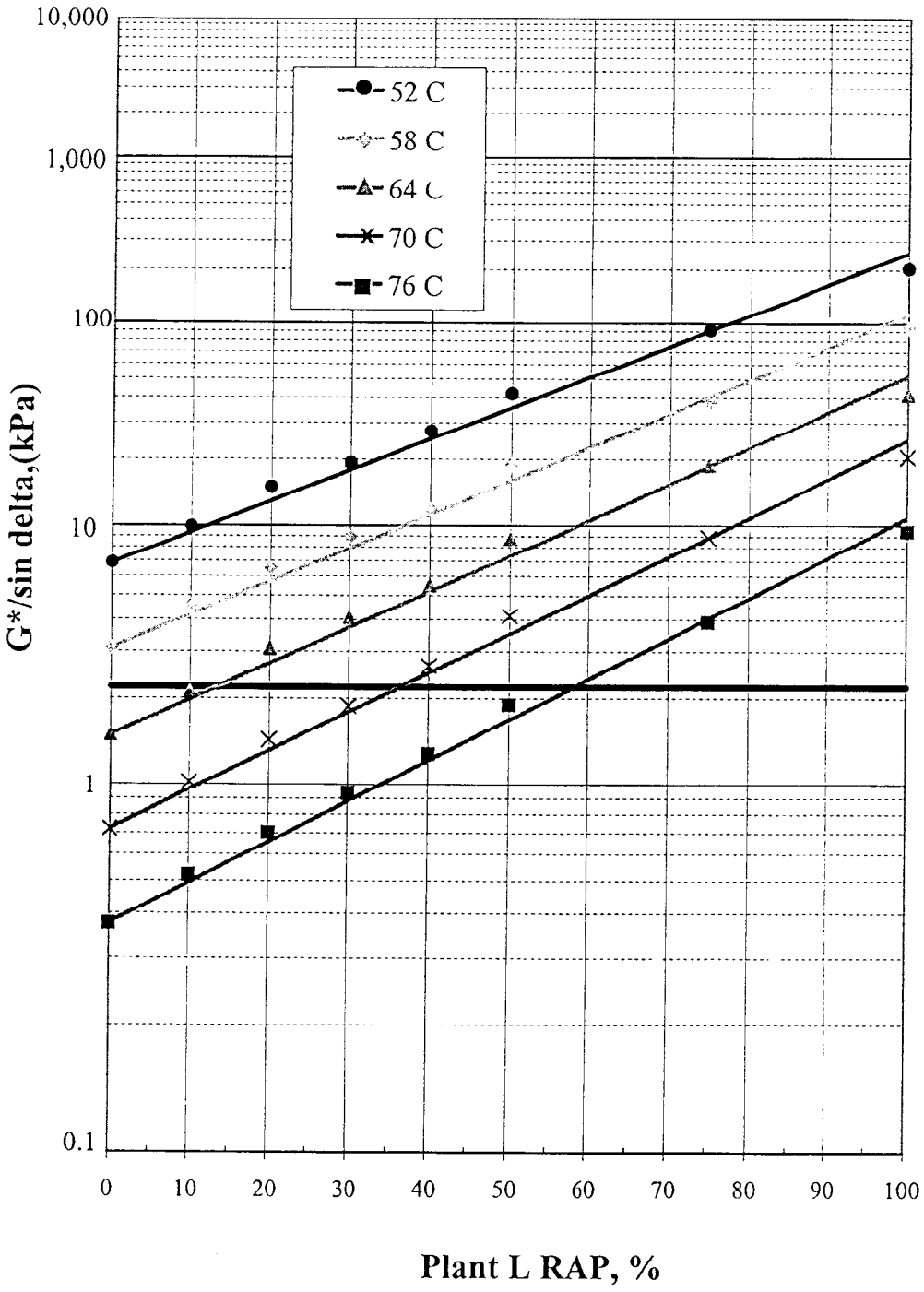

Figure 2.8. Comparison of DSR Test Results for RTFO Aged Binder of PG 58-28 Base Binder Blended with Plant L RAP at Different Temperatures in 1998.

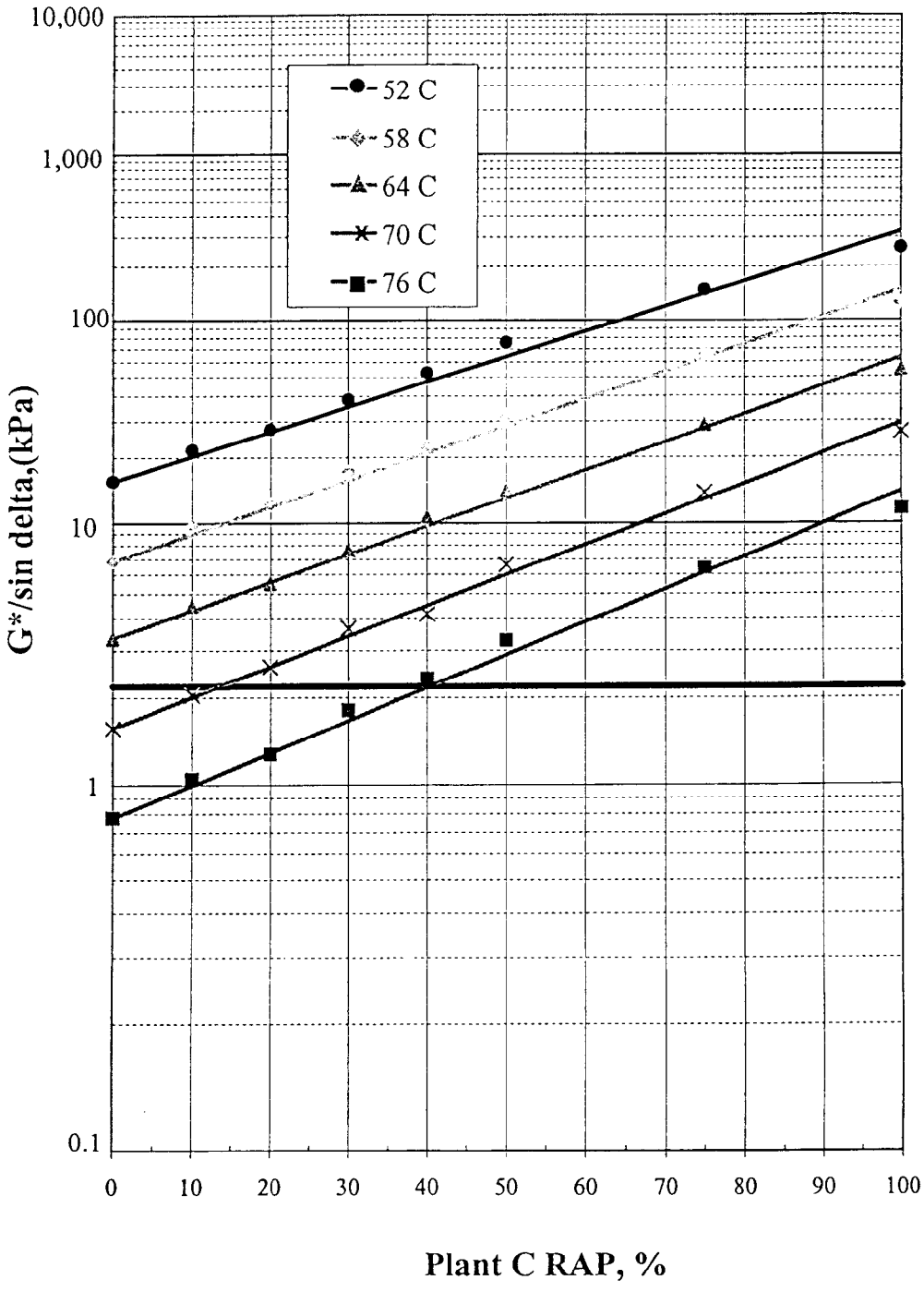

Figure 2.9. Comparison of DSR Test Results for RTFO Aged Binder of PG 64-22 Base Binder Blended with Plant C RAP at Different Temperatures in 1998.

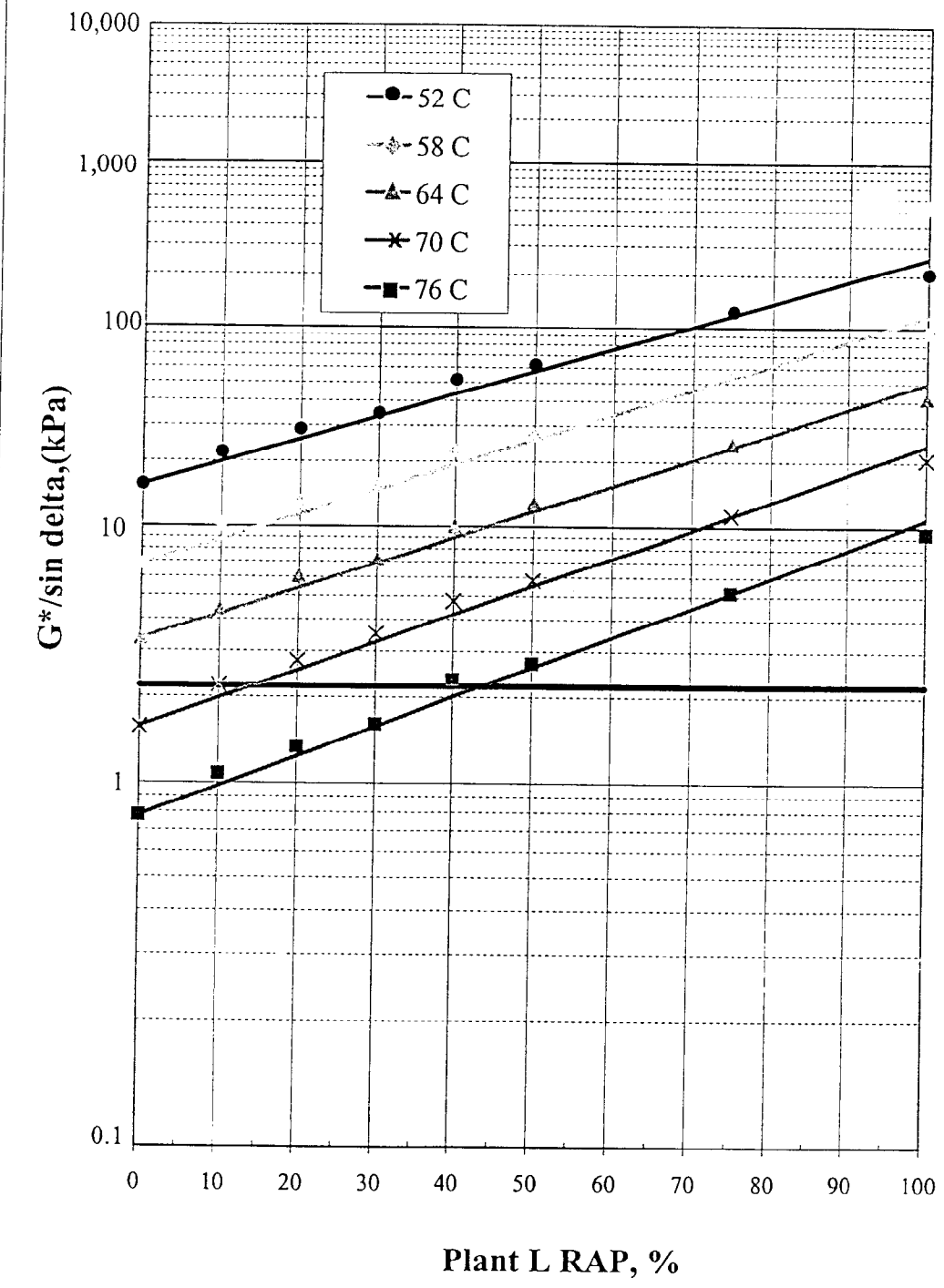

Figure 2.10. Comparison of DSR Test Results for RTFO Aged Binder of PG 64-22 Base Binder Blended with Plant L RAP at Different Temperatures in 1998.

CHAPTER 3. FATIGUE CRACKING

Fatigue cracking is the phenomenon of fracture under repeated or fluctuating stress lower than the tensile strength in the asphalt mixture. The intermittent longitudinal cracks are the early sign of the fatigue cracking, which usually occurs in the wheel path. Furthermore, the cracks will join and cause more cracks to form. The intermediate stage of fatigue cracking is called "alligator cracking", characterized by transverse cracks connecting the longitudinal cracks. In the severe case, the pothole forms when the aggregates and asphalt binder are no longer bonding. Generally speaking, hot mix asphalt (HMA) must have enough tensile strength to withstand the applied tensile stress at the bottom of the asphalt layer, and be resilient enough to withstand repeated load applications without cracking.

3.1 Rheological Properties of PAV Aged Binder

The present study investigated the effect of RAP binder percentage on the rheological properties of asphalt blended with binders extracted from the recycled asphalt pavement (RAP). Then, the rheological property was utilized to evaluate the resistance characteristics of blended asphalt binders against fatigue cracking. This chapter also describes an attempt to utilize mechanical properties of blended asphalt binder to examine the resistance characteristics against fatigue cracking using fracture toughness and split Hopkinson pressure bar tests.

3.1.1 Experimental Plan

Similar to the rutting study in chapter 2, two base asphalts, i.e., PG 58-28 (or AC-10) and PG 64-22 (or AC-20) were blended with different amounts of RAP binders, i.e., 0, 10, 20, 30, 40, 50, 75 and 100% based on the total weight of blended asphalt binders.

Fatigue cracki: :y:cally occurs at normal service temperature about 7 to 10 years after pavement construction. The pressure aging vessel (PAV) was used to simulate the long-term aging process of asphalt binder by means of pressurized air and elevated temperature. Pressure of 2.10 MPa is applied to age the RTFO residue at a temperature of 100°C for 20 hours. Then, the DSR tests were performed on the aged binders to evaluate the fatigue cracking resisting characteristics of asphalt binder with RAP at 19, 22, 25, 28 and 31°C. The PAV aged binder is tested at intermediate temperatures to determine the fatigue cracking parameter, $G^*\sin\delta$. The experimental designs for the year of 1997 and 1998 have been included in Table 2.1 and 2.2, respectively.

3.1.2 Test Results

In 1997, the DSR tests were performed in a constant stress mode. It was observed that the $G^*\sin\delta$ values of asphalt binders blended with Plant C and L RAPs were increased as the amount of RAP binders was increased at all temperatures (Lee et al. 1998). A good linear correlation was observed between the log-log rheological properties of the blended asphalt and RAP binder contents.

In 1998, the DSR test was performed on PAV aged binders similar to the experiments conducted in 1997. The DSR test results are summarized in Table 3.1 and

3.2. Figure 3.1 through 3.4 show the comparison between the log-log G*sinδ and RAP binder content at different temperatures. In addition, a series of statistical analyses was performed on the test data collected in 1998.

3.1.3 Analysis and Discussion

The maximum limit for the fatigue resistance factor, G*sinδ has been set at 5,000 kPa on RTFO and PAV aged binders. The smaller the G*sinδ value, the more elastic the material and the better resistance to fatigue cracking. From the observations in 1997, it was observed that G*sinδ was increased as the amount of RAP binder content increased (Lee et al. 1998). The increase in G*sinδ value was mainly due to G*. Values of δ decreased as the amount of RAP binder content increased, but did not influence the values of G*sinδ significantly. It may be noted that some of the blended asphalt binders did not meet the fatigue resistance criteria. Therefore, the Superpave criteria of G*sinδ may dictate the maximum amount of RAP addition not to have fatigue cracking.

Similar observations were obtained from results of experiments conducted in 1998. It can be seen that G*sinδ was increased as the amount of RAP binder content increased at all temperatures as shown in Figure 3.1 through 3.4. It was also observed that there was no significant difference in slope between Plant C and L RAP binders.

The analysis of variance (ANOVA) and the linear regression analysis were carried out to investigate the effects of the different variables on G*sinδ as shown in Table 3.3. From the ANOVA table, all main effects of the variables (RAP binder content, temperature, asphalt type, and RAP source) are found to be significant as well as other interactions, except for the interaction of temperature with RAP source and asphalt

type with RAP source. However the F-test revealed that only three main effects (RAP binder content, temperature, and asphalt type) were significantly different from others. Therefore, the reduced model was considered only these variables. It can be observed that the R^2 value of the reduced model did not significantly differ from the full model. The RAP source and all interactions were found to be less important than the other factors.

To predict the G*sinδ for different RAP binder contents and different temperatures, an attempt was made to develop linear regression models. The models are shown in Table 3.3. All of the main effects of the variables were included in the first model. The goodness of fit provided an R^2 value of 95.3%. In the second model, the RAP source was eliminated from the first model, and the R^2 is found to be the same as the first model. This indicates that the RAP source is not an important factor. In the third model, the asphalt type variable was eliminated, and the R^2 value did not differ significantly from other models. For simplicity, the third model could be acceptable, i.e., the log G*sinδ is dependent on RAP binder content and temperature.

3.2 Fracture Toughness Characterization

Fracture toughness is the value of the stress intensity factor at which the crack begins to propagate. Early studies on the behavior and performance of bituminous concrete go back to the work of Monismith et al. (1972). The analysis of the experimental results indicated the variation of fracture toughness with asphalt content and consistency as well. The influence of asphalt content on the fracture toughness was found to be dependent upon the test temperature. The concepts of fracture mechanics and

fatigue crack growth have considered the effect of various mixture constituents, such as asphalt cement, filler, polymeric and fibrous additives (Majidzadeh et al. 1976). The stress rate dependency of asphaltic overlays was investigated and the fracture toughness was evaluated at various geometrical and loading conditions. The continuously changing stress distribution during the crack growth process is described by linear elastic fracture mechanics principles using Paris' law (Jacobs et al. 1996). Fatigue life was found to be increased as the magnitude of load decreases. A fracture toughness test was used to measure the resistance of a material to crack initiation in the present study.

Comprehensive research on the assessment of the performance of a series of asphalt mixes with varying recycled asphalt content was conducted by Sulaiman and Stock (1996). The fracture toughness testing was carried out at three different near- and sub-zero temperatures using the three points beam specimen. Test results indicated that the fracture toughness, K_{IC} values at -5°C were greater than at -15°C but less than those obtained at +5°C. The fracture toughness of a mix containing 70% RAP was found to be marginally higher than values obtained for mixes containing pure binder. A factor known as the elastic-plastic region was used to study the elastic-plastic response of the mix. Curiously, the results indicated that the resistance to crack growth was greater at lower temperatures. Also, data showed that RAP content did not have any significant effect on crack growth behavior for the range of mix tested.

3.2.1 ASTM Fracture Toughness Criteria

A fracture toughness test essentially measures the resistance of a material to crack extension. Fracture toughness is that value of the stress intensity at which the crack begins to propagate, catastrophically. The present study utilized the procedure of ASTM

E399 "Standard Test Method for Plane-Strain Fracture Toughness of Metallic Materials" ("Annual" 1996). The standard disk-shaped compact, DC(T), specimen geometry was adopted, mainly because of ease in fabrication. The standard proportions of this geometry are shown in Figure 3.5. The fracture toughness of a material having such a geometry is given by following relation:

$$K_{IC} = \left(\frac{P_{MAX}}{BW^{1/2}} \right) f(a/W) \qquad (3 - 1)$$

Where,

K_{IC} = Fracture Toughness, MPa$\sqrt{m}$

P_{max} = Maximum load to failure, N

B = Thickness of the specimen, m

W = Width of the specimen, m

f(a/W) = a factor dependent upon the geometry

$$f(a/W) = \left[\frac{(2 + a/W)(0.76 + 4.8a/W - 11.58(a/W)^2 + 11.43(a/W)^3 - 4.08(a/W)^4)}{(1 - a/W)^{3/2}} \right] \qquad (3\text{-}1a)$$

The blank specimen had a diameter of 101.6 mm, and had a width of 76.2 mm (D = 1.35W). The thickness of the specimen was 38.1 mm, as per the relation W/B = 2. For an initial crack length of 43.26 mm, and an a/W ratio of 0.57, the f(a/W) factor was calculated as 13.27.

3.2.2 Specimens Fabrication

The specimens were fabricated by using the Marshall Compactor ("Mix" 1993). The aggregates used for this study were obtained from Plant L and sieved to separate the particle sizes. The aggregates passed 0.6 mm (No. 30) and retained on 0.3 mm (No. 50) sieve were used for specimen fabrication. The aggregate size was so chosen that the aggregate would not contribute to the strength of the specimen, and only binder (cohesion) characteristics could be studied (Kennedy et al. 1982).

The asphalt binders blended with the one extracted form Plant C RAP were heated at 135°C, till they started to flow. They were further mixed with 550 grams of heated aggregates. The weight of binder as a percentage of the total weight was established by performing preliminary tests, and the maximum value of fracture toughness was found to occur at 6% binder content. Thus, it was decided to proceed with an optimum binder content of 6% for the entire study. The Marshall molds and asphalt/blended binder were heated in the oven at 135°C for approximately 1 hour. Then the heated aggregates and asphalt/blended binder were mixed thoroughly in the right proportion, such that all the aggregates got coated with asphalt binder. This mixture was then compacted with 55 blows on either face to account for proper compaction. Finally, the specimen was ejected, cured overnight and machined to the required dimensions. The pinned holes were drilled using the 12.7mm endmill with care, so as to keep the edges of the specimen intact. The edge crack was band-sawed and was sharpened using a diamond saw to provide a sharp crack. The Instron testing machine was used to load the specimen.

3.2.3 Fracture Toughness at Room Temperature

The fracture behavior of binders with RAP was studied at room temperature, in order to evaluate fatigue cracking resistance characteristic (Lee et al. 19). The study was carried out at five different RAP binder contents of 0, 25, 50, 75, and 100%. Five specimens were tested at every increment of RAP binder content and at the loading rate of 152.4 mm per minute in the year of 1997. Furthermore, three more specimens were tested at 0 and 100% RAP binder contents and at the same loading rate of 1997 to check the reproducibility of testing procedure in the year of 1998. It was found that the procedure can be reproduced as shown in Figure 3.6. The crack sharpening was consistently maintained in all the cases so as to obtain an accurate estimate of fracture toughness.

The fracture toughness test results obtained from the year of 1997 and 1998 are presented in Table 3.4. Figure 3.6 shows the comparison of the fracture toughness test results between 1997 and 1998 at room temperature. The trends from the 1997 experiments were represented by a quadratic curve fit. It was found that the fracture toughness values increased as a function of RAP binder contents. The single experiment design analysis was used to determine the effect of RAP binder contents and different years on the fracture toughness. After performing the statistical analysis, it was found that RAP binder contents and different years have a significant effect of the fracture toughness values. It can be seen in Figure 3.6 that the fracture toughness value at 100%

for 1998 was observed to be higher than the one for 1997. It may be noted that the RAP binder collected in 1998 had a higher viscosity.

In the light of visual observations of crack propagation in the specimens at room temperature (Figure 3.7) conducted in 1997, the actual numerical values of fracture toughness may be considered invalid due to the presence of plastic zones at room temperature. This is because fracture toughness is estimated based on the principles of linear elastic fracture mechanics. Therefore, the procedure of the ASTM E399 is not applicable for evaluating the fracture toughness of asphalt binder at room temperature.

3.3 Dynamic Constitutive Behavior of Recycled Asphalt Pavement Binder

Asphalt pavements undergo a wide variety of service conditions ranging from temperature extremes due to the environment to impact loads at various strain rates due to traffic. Lee et al. (1998) studied the dynamic response of asphalt mixes with varying percentages of RAP binder at temperature ranging from 22°C to 0°C.

In this experimental study, two systems were utilized during testing: the Split Hopkinson Pressure Bar (SHPB) and the SHPB refrigeration system. The SHPB technique is one of the more widely utilized systems to study material behavior under conditions of uniform deformation. This apparatus is being utilized for this investigation because of its ease of use in conducting experiments, its ability to achieve a wide range of dynamic strain rates (10^2 s^{-1} to 10^4 s^{-1}), and because it is an established and proven method of performing dynamic testing. The SHPB refrigeration system is a unique device that was designed and fabricated specifically for low temperature dynamic testing with the SHPB apparatus. The SHPB refrigeration system was designed and fabricated to

interface with the SHPB apparatus, quickly cool the test specimen to the target temperatures, and maintain the specimen's target temperature during testing.

3.3.1 SHPB Apparatus for High Strain Rate Comparison Testing

The SHPB technique was initiated with Bertram Hopkinson in 1914. Hopkinson was attempting to ch ..tc..ize the dynamic response of metal wires by attaching the metal wires magnetically at one end to a steel rod and impacting the other by a projectile or by the detonation of an explosive. From these experiments, stress-time curves were developed. In 1948, Davies utilized electrical condenser units to measure displacements at the free surface of the bar. The configuration was changed by Kolsky in 1949 from using one bar to two bars which sandwich the specimen.

Since this configuration was established, numerous experiments have been performed on a variety of materials and under various loading conditions. In 1963, Chiddester and L.E.Malvern developed a technique for performing elevated-temperature tests utilizing the SHPB. Since the results of the experiments are affected by temperature gradients in the bars, the temperature variations were restricted to only the ends of the bars interfacing with the specimen. In 1963, Davies and Hunter derived a relation between the specimen geometry and Poisson's ratio in order to minimize errors generated by inertial effects inherent in the SHPB system. Since this period, the majority of advances that have been made with the SHPB technique have been only to refine the system.

3.3.2 SHPB Theoretical Background

The SHPB consists of an incident and transmitter bar (Figure 3.8). A cylindrical specimen is sandwiched between the incident and transmitter bar. The free end of the

incident bar is impacted by a striker bar or an explosive detonation which generates a compressive stress wave heading towards the specimen. When the compressive wave reaches the incident bar-specimen interface, it is partially reflected back down the incident bar and partially transmitted through the specimen. The amount of the incident wave that is reflected into the incident bar is a function of the impedance and area mismatches between the incident bar and the specimen. The remaining portion of the wave passes through the specimen and undergoes a number of reverberations prior to entering the transmitter bar. The pulses traveling through the bars are detected by strain gages. Both the incident and transmitter bars are instrumented with diametrically opposed strain gages to record the surface strain-time histories. The pulses from the strain gages allow the strain and stress within the specimen to be calculated. The amplitude of the transmitted pulse is a measure of the stress in the specimen and the amplitude of the reflected pulse is a measure of the strain in the specimen. When the stress and strain are obtained, the specimen dynamic stress-strain curve is produced.

All of the above relationships have been established utilizing wave theory and verified through testing. From one dimension wave theory, the average specimen stress, strain, and strain rate can be developed respectively by the following equations:

$$\sigma_s = E\frac{A}{A_s}e^{\varepsilon_s}\varepsilon_t \qquad (3-2)$$

$$\varepsilon_s = \frac{-2c_0}{L}\int_0^t \varepsilon_r dt \qquad (3-3)$$

$$\dot{\varepsilon}_s = \frac{-2c_0}{L}\varepsilon_r \qquad (3-4)$$

In the above equations, E is Young's Modulus, A is the cross sectional area of the bars, A_s is the cross sectional area of the specimen, and c_o is the wave speed in the bars. When the above equations are valid, the surface displacements measured by the strain gages are equivalent to the axial displacements of the bars.

3.3.3 SHPB Specimen Design and Fabrication

For comparison purposes, the asphalt test specimens were manufactured in the exact same manner as that of reference (Lee et al. 1998). The asphalt test specimens were fabricated of #30 - #50 aggregate. This form of aggregate assures that they act as a medium of adhesion to the binder by eliminating any aggregate inter-locking. Therefore, the aggregates do not contribute to the strength of the specimen. This design assists in the determination of only the binder properties and failure modes. The specimen diameter and length were selected as 1.739 and .500, respectively. These dimensions were chosen to minimize errors due to longitudinal and radial inertia. This selection of specimen dimensions also determined that the cross-sectional area mismatch between the pressure bars and the specimen was 25% maximum, assuming a maximum strain of 25% in the specimen. This ensured that the specimen diameter did not exceed the diameter of the bars as it expanded radially during testing. The fabrication process of the test specimens are illustrated in the following paragraphs.

The following items are required for fabrication of an asphalt specimen: 35 gm of #30 - #50 aggregate, 2.2 gm of asphalt binder mixture, a surface oven, a steel storage bowl, a steel mixing bowl, a large steel mixing spoon, a steel mold assembly, a weight scale, anti-stick paper, lubricating oil, and an Instron testing machine. As with reference (Lee et al. 1998), the amount of aggregate utilized was 35 gm for consistency and

comparison purposes. The aggregate was placed in a steel bowl and stored in an oven with a temperature of 275°C. Prior to testing, the aggregate was subjected to this temperature for at least an hour. This ensured that the aggregate was properly heated for adequate adhesion to the binder.

The amount of the asphalt binder mixture was selected to be 2.2 gm as in reference (Lee et al. 1998). This ensured that the optimum binder content was maintained at 6% by weight for consistency and comparison purposes. In order to obtain the proper mixtures, the virgin asphalt binder and RAP were premixed by heating both to 60° C for an hour and then mixing them as a liquid in the required proportions (0%, 25%, 50%, 75% and 100%). The mixtures were stored separately in steel containers.

During specimen fabrication, the steel mixing bowl and mixing spoon were allowed to warm up to approximately 275°C on the surface oven. The binder and the mold assembly were allowed to warm up to 275°C for 10 minutes in the oven housing the aggregate prior to mixing. The steel mixing bowl was removed from the oven and placed on the scale. The bowl containing the aggregate was removed from the oven and 35 gm of the aggregate was placed into the mixing bowl. The storage bowl was placed back into the oven and the binder was removed. 2.2 gm of the desired binder mixture was added to the mixing bowl. After being placed in the mixing bowl, the mixture of aggregate and binder was stirred utilizing the mixing steel mixing spoon. The binder and the aggregate were mixed thoroughly until the aggregate was evenly coated and black.

After the aggregate and asphalt were thoroughly mixed, the mold assembly was removed from the oven. Lubricating oil was quickly placed on a disk of non-stick paper which was placed on the bottom of the mold. The mold was then filled with the mixture

and another piece of non-stick paper coated with lubricating oil was placed on top of the mixture. The plunger of the mold assembly was then placed on top of the non-stick paper. The mixture in the mold assembly was then compacted at 6,200 lb. for 20 minutes using the Instron testing machine. After the 20 minutes, the specimen was ejected from the mold and cured for at least 24 hours prior to testing to complete the asphalt fabrication process.

3.3.4 Dynamic Testing of Blended Asphalt Binder at 22°C

Although this study is to determine the low temperature dynamic response of asphalt and RAP mixtures, the initial experiments were conducted at room temperature to establish a baseline for comparison purposes. After a baseline was established, testing was conducted at 0°C, -10°C, and -20°C. All the experiments were carried out at a nominal strain rate of 450^{-s} per reference (Lee et al. 1998). The typical strain pulses obtained in these experiments are indicated in Figure 3.9. The nominal wave speed was estimated to be 220 m/s. This wave speed is approximately 20 times less than the speed of the wave in the steel bars. A typical plot of the stress history for these experiments is provided in Figure 3.10. Finally, a typical plot of the incident and transmitter stress ratio history is provided in Figure 3.11.

3.3.5SHPB Test Results and Discussion

The maximum flow stresses and strains for SHPB testing at 22°C as a function of RAP content are provided in Table 3.5 and Figures 3.12 and 3.13. From the table, one can see that there was an increase in maximum flow stress of 4.3% from the 25% to the 0% RAP mixtures. However, there was a decrease in the maximum flow stress of 17.4% and 8.7% from the 50% and 75% RAP mixtures when compared to the 0% RAP mixture,

respectively. Also, there was an increase in the maximum flow stress of 8.7% from the 100% RAP mixture when compared to the 0% RAP mixture.

From the table, one can see that there was a decrease in the maximum flow strain for all of the RAP mixtures when compared to the virgin asphalt specimen. The average decreases in maximum flow strain are 1.0%, 10%, 4.2% and 6.3% from the 25%, 50%, 75%, and 100% RAP mixtures when compared to the 0% RAP mixture, respectively.

The post-mortem analysis of the specimen revealed that the mechanism of failure was shear dominated. The specimen was compressed and sections of the specimen spalled off leaving an intact core. The sections that spalled off did so as wedge like chunks. These wedges were formed because the specimen developed circumferential, radial and longitudinal cracks as shown in Figures 3.14 and 3.15. The number of wedge shaped segments sheared from the main core increased with an increase in RAP percentage. This observation also indicates that the material becomes more brittle as the RAP content increases. These observations were typical of all the specimens that failed at room temperature.

Table 3.1 DSR Test Results of PAV aged Asphalt Binders Blended with Plant C-RAP in 1998.

RAP, %	Temps, C	PAV Aged					
		PG 58-28			PG 64-22		
		G*	δ	G*sinδ	G*	δ	G*sinδ
0	19	4941	47.9	3666	9446	40.2	6091
	22	3120	51.0	2423	6262	43.0	4267
	25	1961	53.9	1584	4094	45.8	2932
	28	1212	57.0	1015	2632	48.7	1975
	31	716	60.1	621	1629	52.0	1283
10	19	5621	45.8	4030	9279	39.9	5952
	22	3614	48.7	2715	6194	42.6	4193
	25	2258	51.6	1770	4067	45.4	2896
	28	1397	55.0	1144	2655	48.6	1992
	31	840	58.1	713	1668	51.9	1313
20	19	5935	45.3	4215	10374	39.5	6599
	22	3852	48.2	2872	6906	42.0	4621
	25	2456	51.2	1913	4538	44.9	3203
	28	1528	54.0	1235	2935	47.8	2174
	31	907	57.4	764	1825	51.1	1420
30	19	9074	41.5	6013	11409	37.4	6929
	22	6047	44.3	4220	7780	40.0	4996
	25	3958	47.2	2901	5264	42.8	3577
	28	2496	50.1	1914	3501	45.6	2501
	31	1573	52.8	1253	2255	48.6	1690
40	19	11311	38.9	7103	13413	36.6	7987
	22	7677	41.7	5102	9224	39.1	5811
	25	5108	44.2	3561	6269	41.9	4187
	28	3333	47.0	2435	4166	44.5	2920
	31	2138	50.0	1638	2691	47.7	1990
50	19	13307	37.2	8036	15475	35.0	8876
	22	9196	39.6	5855	10830	37.2	6540
	25	6195	42.3	4165	7539	39.8	4821
	28	4083	45.0	2884	5159	42.7	3499
	31	2670	47.9	1980	3444	45.6	2453
75	19	18379	33.8	10211	18015	34.4	10165
	22	13057	36.0	7675	12631	36.7	7549
	25	9148	38.7	5720	8789	39.1	5543
	28	6236	41.4	4120	5970	41.9	3987
	31	4135	44.1	2877	3972	44.8	2799
100	19	27138	29.4	13322	27138	29.4	13322
	22	20036	32.0	10602	20036	32.0	10602
	25	14569	34.0	8147	14569	34.0	8147
	28	10428	36.4	6188	10428	36.4	6188
	31	7299	39.1	4603	7299	39.1	4603

Note: 1. The unit for G*sinδ is kPa.
2. The unit for δ is degree.

Table 3.2 DSR Test Results of PAV aged Asphalt Binders Blended with Plant L-RAP in 1998.

RAP, %	Temps, C	PAV Aged					
		PG 58-28			PG 64-22		
		G*	δ	G*sinδ	G*	δ	G*sinδ
0	19	4941	47.9	3666	9446	40.2	6091
	22	3120	51.0	2423	6262	43.0	4267
	25	[illegible]	53.9	1584	4094	45.8	2932
	28	1212	57.0	1015	2632	48.7	1975
	31	716	60.1	621	1629	52.0	1283
10	19	5377	48.2	4008	9752	39.9	6255
	22	3409	51.3	2660	6356	42.7	4306
	25	2133	54.5	1735	4213	45.4	3000
	28	1302	57.2	1093	2729	48.4	2039
	31	780	60.3	678	1707	51.8	1340
20	19	6990	44.2	4868	10366	39.3	6566
	22	4551	47.3	3345	7114	42.1	4769
	25	2985	50.1	2288	4727	45.1	3345
	28	1886	53.0	1505	3095	48.0	2298
	31	1178	55.8	974	1927	51.0	1498
30	19	9088	41.9	6069	11196	38.0	6893
	22	5992	44.8	4218	7581	40.5	4917
	25	3906	47.5	2879	5177	43.3	3547
	28	2496	50.4	1922	3362	46.0	2416
	31	1601	53.6	1288	2096	49.1	1584
40	19	10449	40.3	6751	13388	36.4	7945
	22	6972	43.2	4768	9226	39.0	5806
	25	4615	45.9	3311	6284	42.0	4205
	28	3007	48.6	2253	4209	44.9	2971
	31	1887	51.7	1481	2763	48.0	2053
50	19	13327	38.0	8205	13915	36.0	8169
	22	9058	40.7	5907	9712	38.6	6052
	25	6023	43.6	4154	6556	41.2	4319
	28	3903	46.2	2813	4371	44.2	3047
	31	2443	49.6	1860	2881	47.1	2109
75	19	16433	35.6	9566	18028	33.3	9899
	22	11992	37.7	7334	12743	36.0	7490
	25	8565	39.6	5460	8825	38.4	5482
	28	6004	42.3	4041	5971	41.2	3933
	31	4159	44.7	2925	3887	44.4	2726
100	19	23543	30.6	11984	23543	30.6	11984
	22	17049	32.9	9261	17049	32.9	9261
	25	12282	35.3	7097	12282	35.3	7097
	28	8581	37.9	5271	8581	37.9	5271
	31	5771	40.9	3779	5771	40.9	3779

Note: 1. The unit for G*sinδ is kPa.
2. The unit for δ is degree.

Table 3.3. Statistical Analyses of Fatigue Cracking Parameter (G*sinδ).

Analysis of Variance (ANOVA)

Source	DF	Seq SS	Adj SS	Adj MS	F-test	P
Main Effect:						
RC	7	10.425	10.425	1.489	1965.63	0.000
T	4	15.416	15.416	3.854	5086.68	0.000
AC	1	1.031	1.031	1.031	1360.73	0.000
RS	1	0.011	0.011	0.011	14.90	0.000
Interactions:						
RC*T	28	0.296	0.296	0.011	13.94	0.000
RC*AC	7	0.634	0.634	0.091	119.52	0.000
RC*RS	7	0.038	0.038	0.005	7.15	0.000
T*AC	4	0.035	0.035	0.009	11.67	0.000
T*RS	4	0.001	0.001	0.000	0.19	0.943
AC*RS	1	0.002	0.002	0.002	3.01	0.084
Error	255	0.193	0.193	0.001		
Total	319	28.082	R^2= 99.3%			

Reduced Model

Source	DF	Seq SS	Adj SS	Adj MS	F-test	P
Main Effect:						
RC	7	10.423	10.425	1.489	377.79	0.000
T	4	15.416	15.416	3.854	977.65	0.000
AC	1	1.031	1.031	1.031	261.53	0.000
Error	307	1.210	1.210	0.004		
Total	319	28.082	R^2= 95.7%			

No.	Linear Regression Models for Prediction of G*sinδ	Adjusted R^2
1	Log G*sinδ = 0.478 + 0.00571(RC) – 0.0517(T) + 0.0189(AC) – 0.0119(RS)	95.3%
2	Log G*sinδ = 0.460 + 0.00571(RC) – 0.0517(T) + 0.0189(AC)	95.3%
3	Log G*sinδ = 1.610 + 0.00571(RC) – 0.0517(T)	91.6%

RC = RAP binder content in percentage (i.e., 0, 10, 20, 30, 40, 50, 75, and 100%)
T = Temperatures in degree Celsius (i.e., 19, 22, 25, 28, and 31°C)
AC = Asphalt type (i.e., PG 58-28 and PG 64-22)
RS = RAP sources (i.e., Plant C and L)

Table 3.4. Fracture Toughness Test Results at Room Temperature.

		RAP Binder Content, %				
		0	25	50	75	100
Room Temperature (22°C)	1997	79	87	85	145	173
	1998	72	N/T	N/T	N/T	255

Note: 1. A unit for all fracture toughness values is $1*e^{-3}$ MPa$\sqrt{m}$.

2. N/T indicates no testing in 1998.

Table 3.5 Values of Maximum Flow Stress and Maximum Flow Strain for SHPB Testing of Various Percentages of Plant C RAP Binder at Room Temperature.

	0% RAP	25% RAP	50% RAP	75% RAP	100% RAP
Max. Flow Stress	23	22	19	21	25
Max. Flow Strain	9.6	9.5	8.6	9.2	9

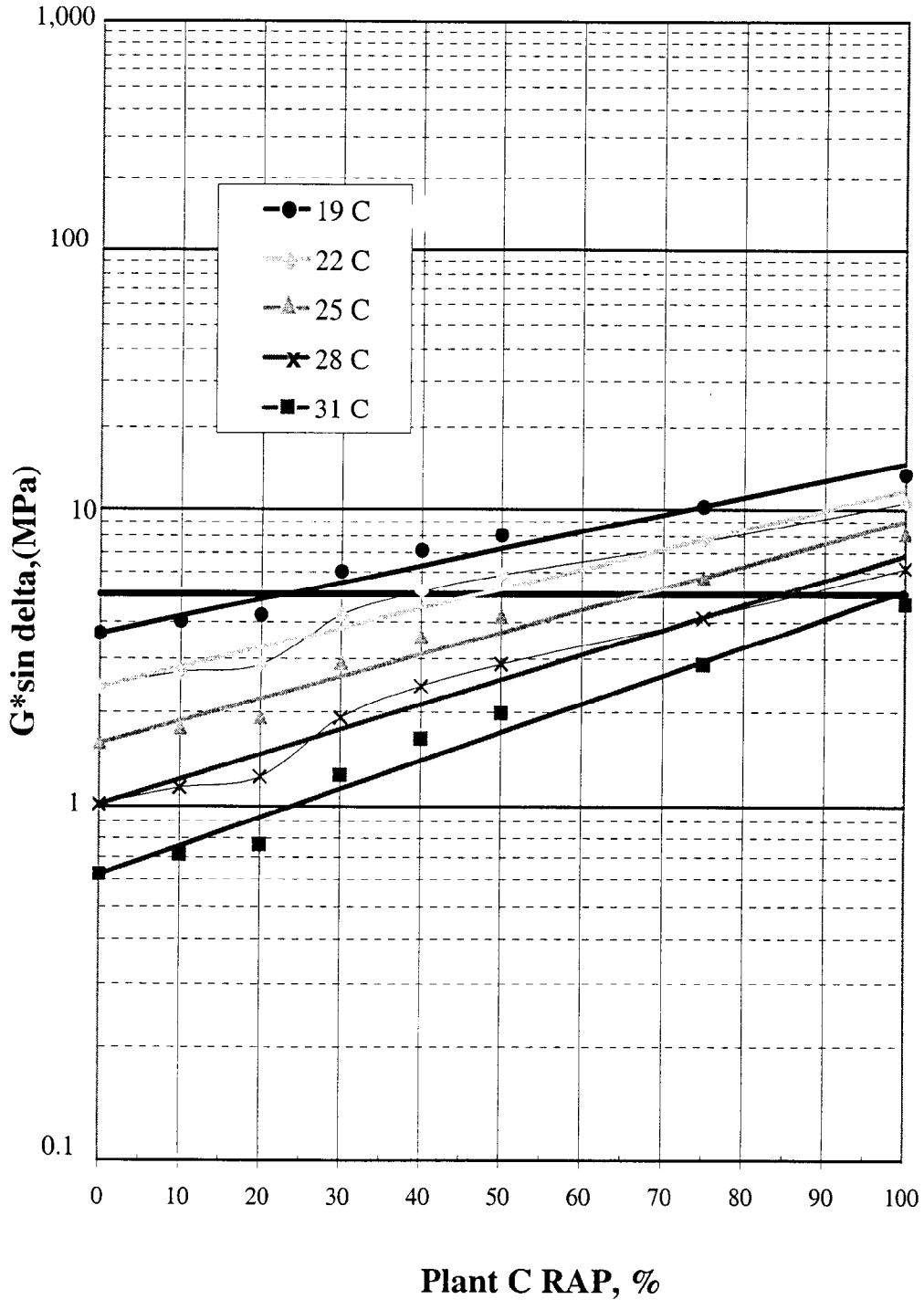

Figure 3.1. Comparison of DSR Test Results for PAV Aged Binder of PG 58-28 Base Binder Blended with Plant C RAP at Different Temperatures in 1998.

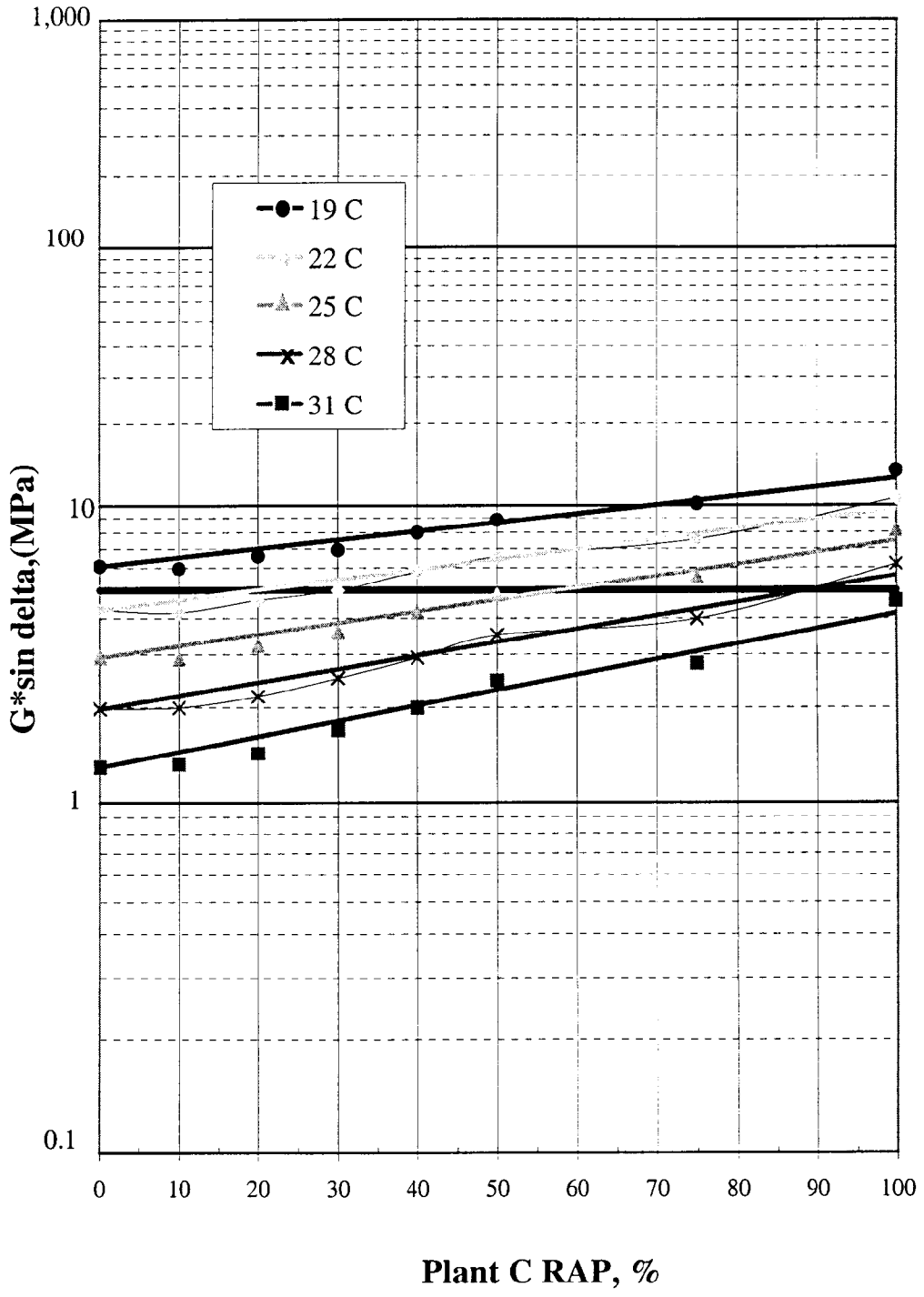

Figure 3.2. Comparison of DSR Test Results for PAV Aged Binder of PG 64-22 Base Binder Blended withPlant C RAP at Different Temperatures in 1998.

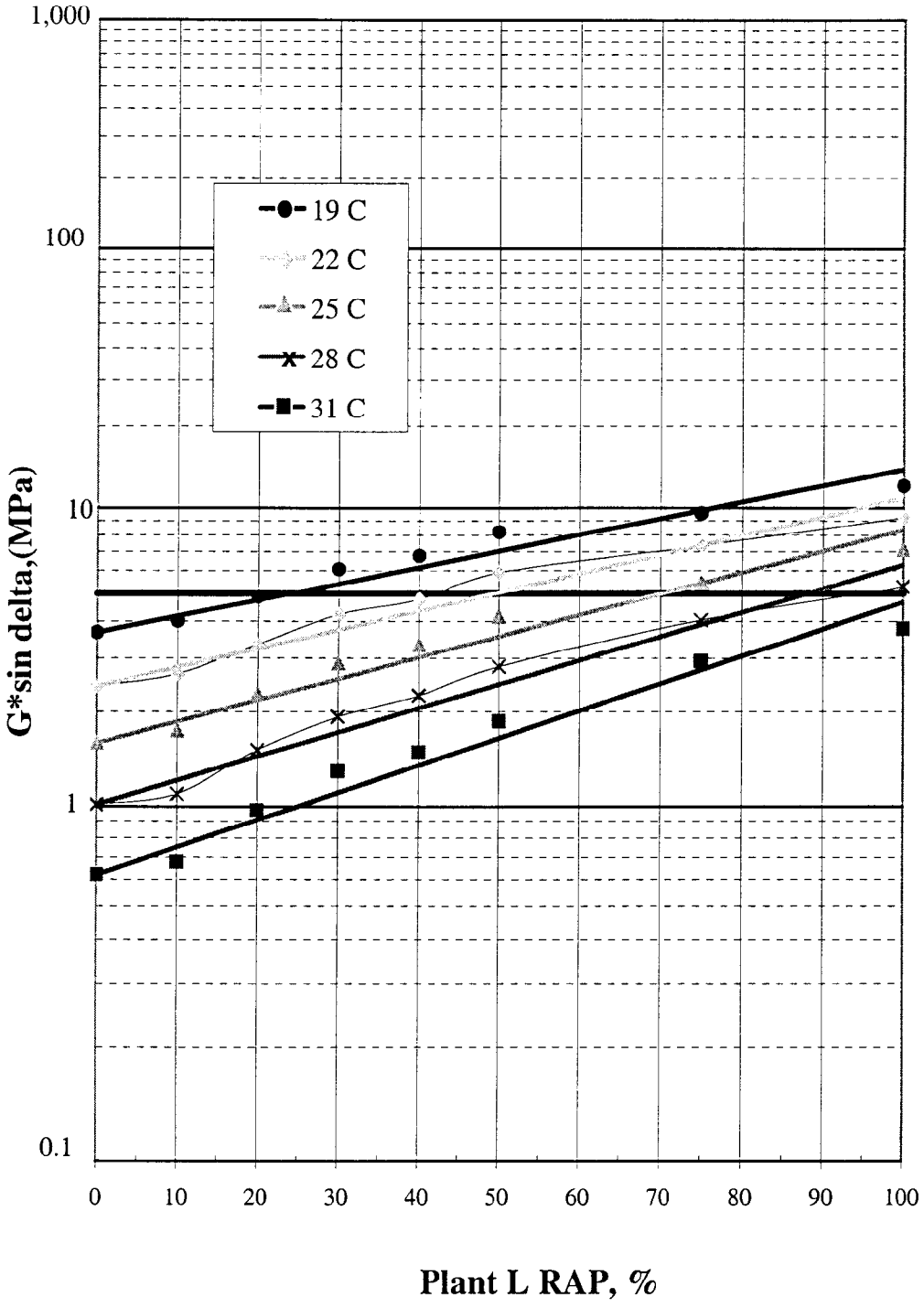

Figure 3.3. Comparison of DSR Test Results for PAV Aged Binder of PG 58-28 Base Binder Blended with Plant L RAP at Different Temperatures in 1998.

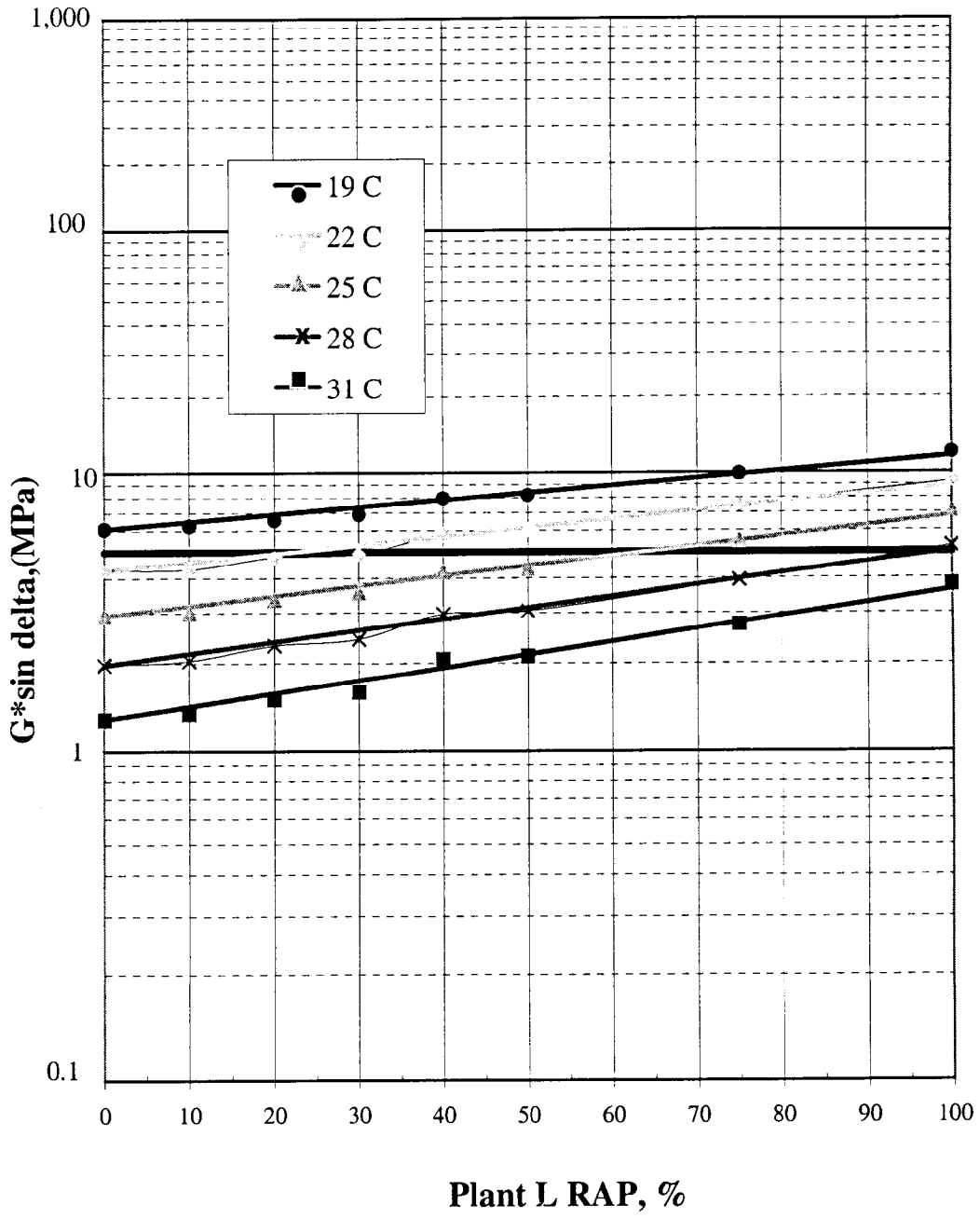

Figure 3.4. Comparison of DSR Test Results for PAV Aged Binder of PG 64-22 Base Binder Blended with Plant L RAP at Different Temperatures in 1998.

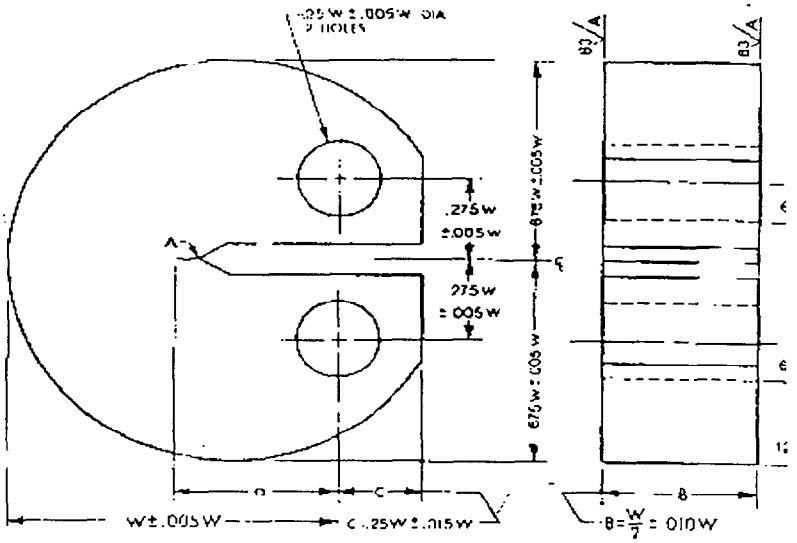

(a) Disk Shaped Compact Tension – DC(T) Specimen with Standard Proportion and Tolerances.

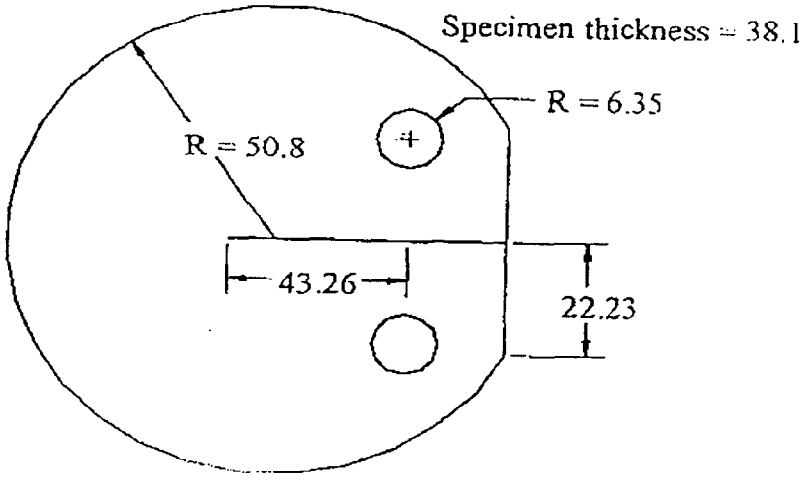

(b) Fracture Toughness Specimen Dimensions.

Figure 3.5. Disk Shaped Compact Specimen DC(T) Standard and the Specimen Dimensions.

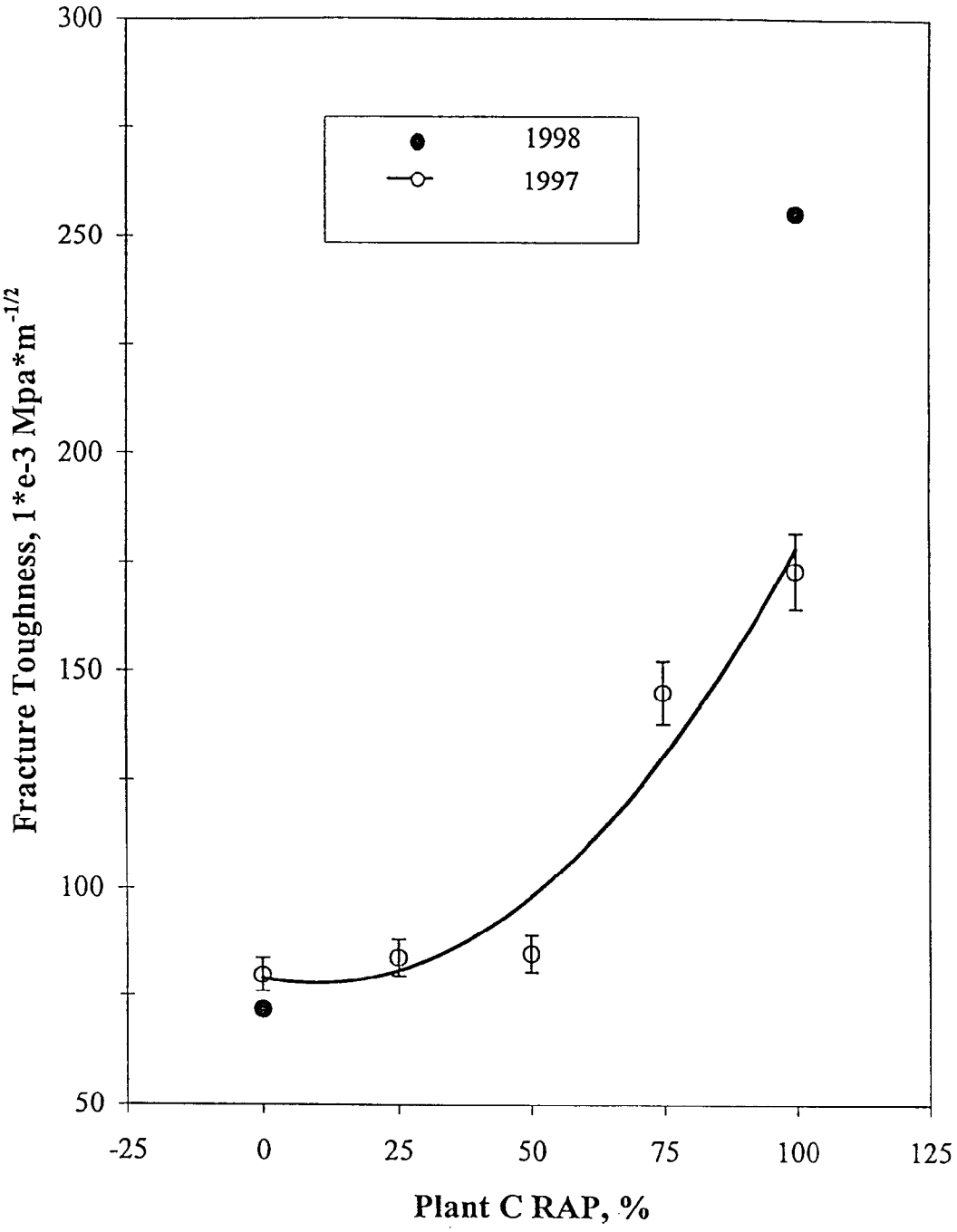

Figure 3.6. Comparison of Fracture Toughness Test Results Between 1997 and 1998 at Room Temperature (22 degree C).

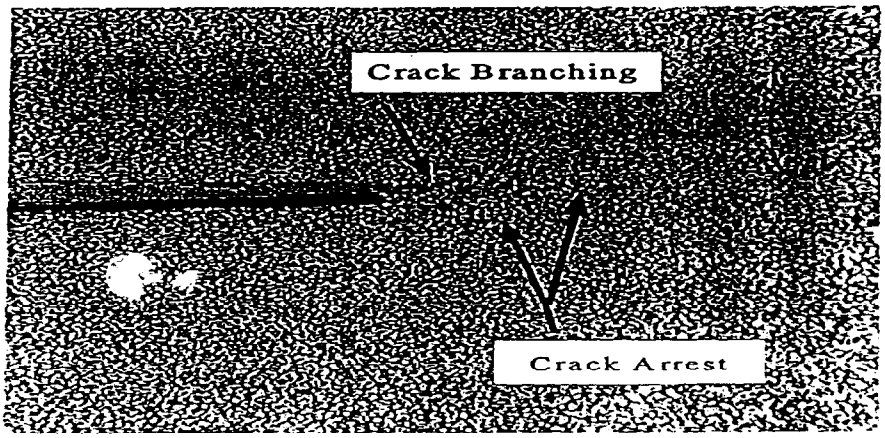

(a) Crack Propagation in the 0% RAP Binder Specimen at 22°C.

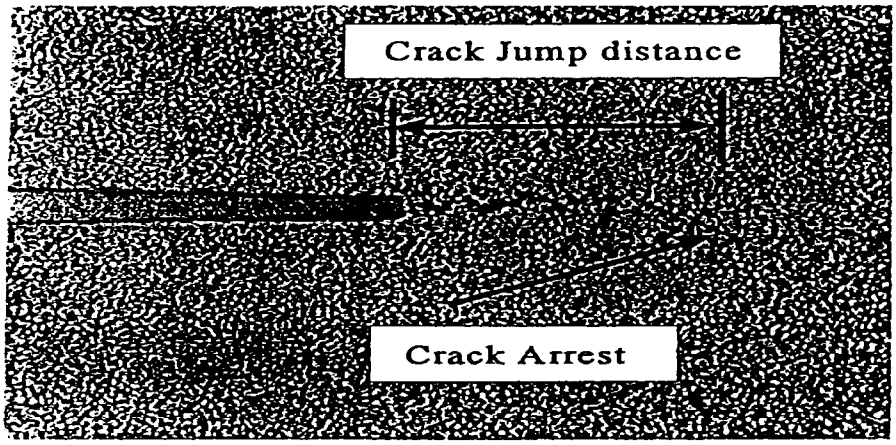

(b) Crack Propagation in the 50% RAP Binder Specimen at 22°C.

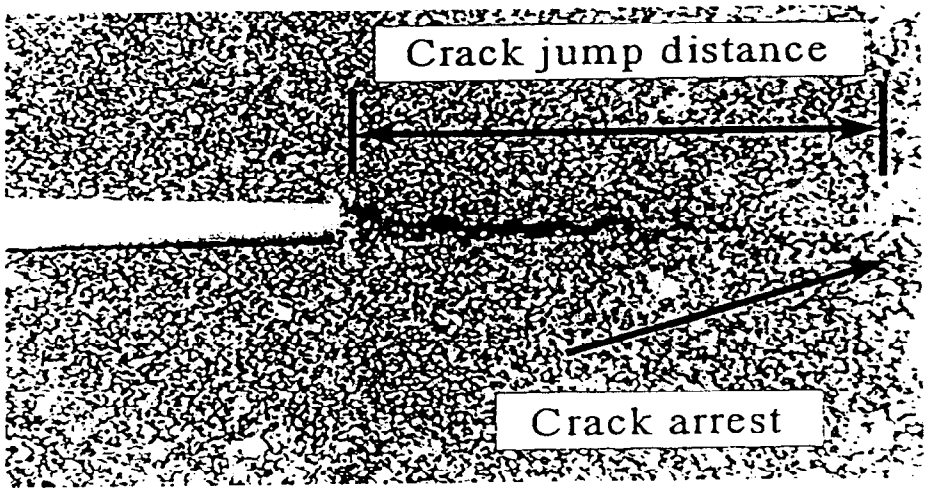

(c) Crack Propagation in the 100% RAP Binder Specimen at 22°C.

Figure 3.7. Crack Propagation in the Specimens at 22°C.

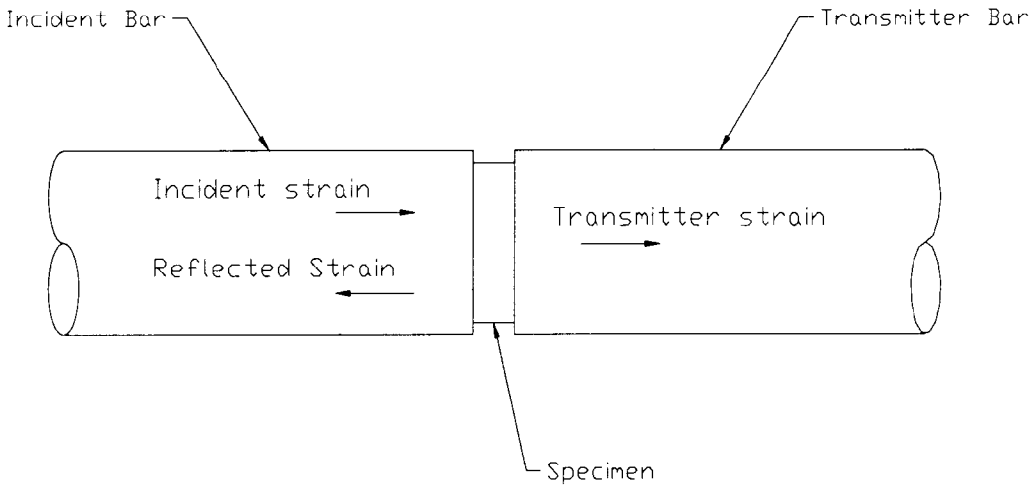

Figure 3.8 Schematic of the Incident Bar-Specimen and Transmitter Bar-Specimen Interfaces of the SHPB.

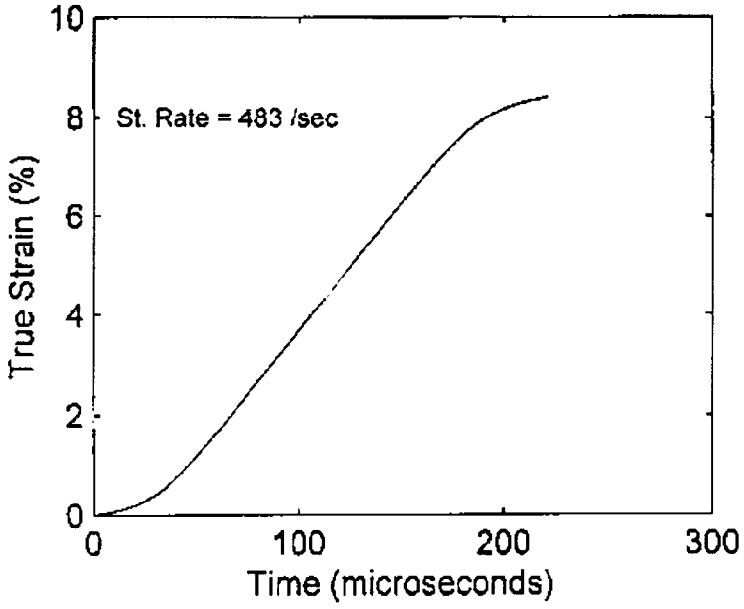

Figure 3.9 Typical Strain History for SHPB Testing of Asphalt.

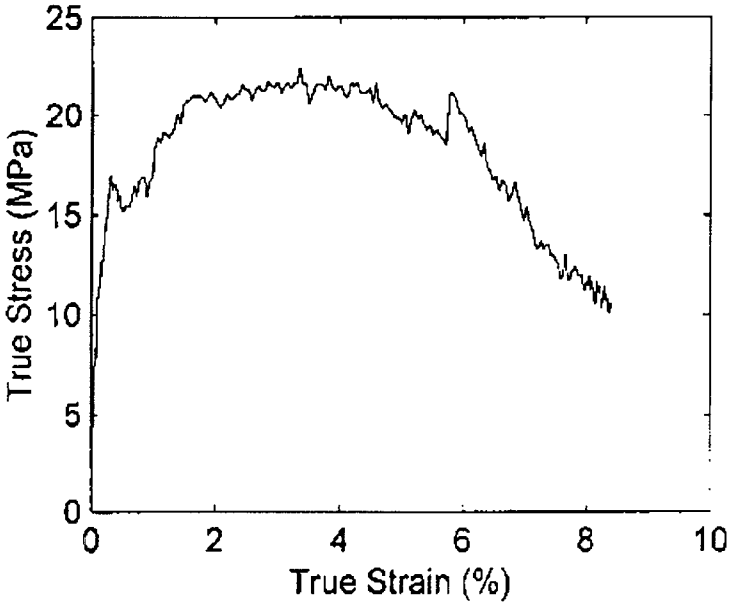

Figure 3.10 Typical stress history for SHPB testing of asphalt.

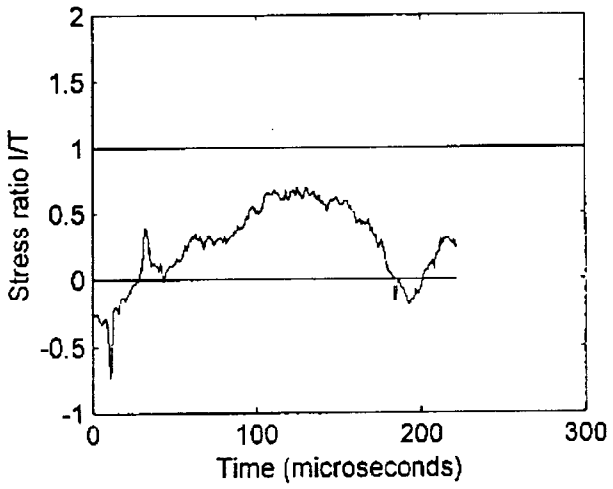

Figure 3.11 Plot of the Incident and Transmitter Stress Ratio History.

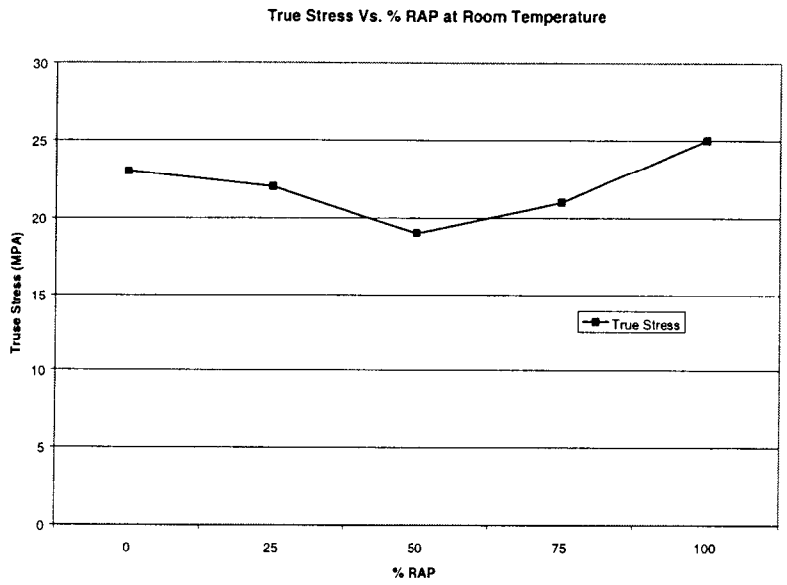

Figure 3.12 Plot of Maximum Flow Stress for SHPB testing of Various Percentages of Asphalt and RAP mixtures at room temperature.

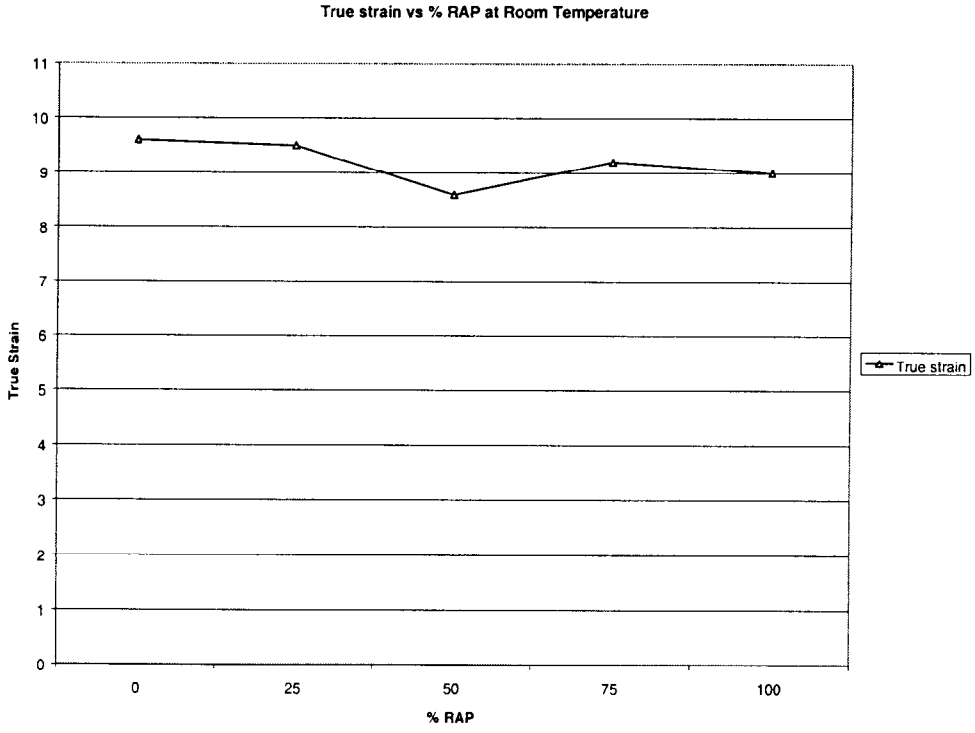

Figure 3.13. Plot of Maximum Flow Strain for SHPB Testing of Various Percentages of Asphalt and RAP Mixtures at Room Temperature.

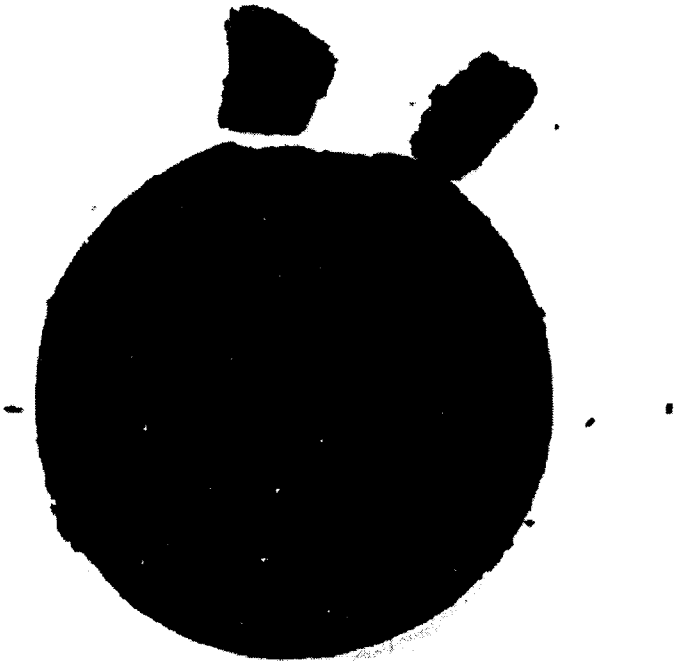

Figure 3.14 Typical 100% RAP Specimen Tested at 22 degrees C.

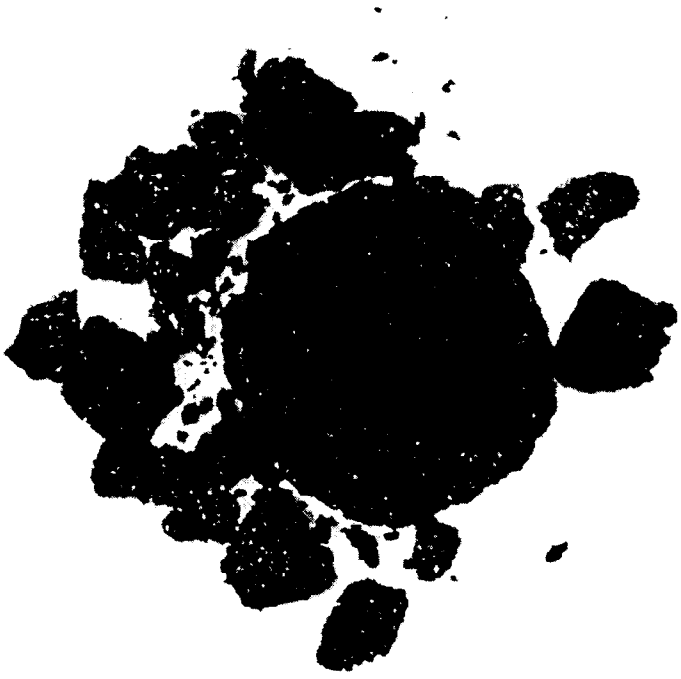

Figure 3.15. Typical 100% RAP Specimen Tested at 22 degrees C.

CHAPTER 4. LOW TEMPERATURE CRACKING

Low temperature cracking is a distress type that is caused by adverse environmental conditions rather than by applied traffic loads. It is characterized by intermittent transverse cracks (i.e., perpendicular to the direction of traffic) that occur at a surprisingly consistent spacing. Low temperature cracks form when an asphalt pavement layer shrinks in cold weather. As the pavement shrinks, tensile stress builds within the layer. At some point along the pavement, the tensile stress exceeds the tensile strength and the asphalt layer cracks. Thus, low temperature cracks occur primarily from a single cycle of low temperature. Some engineers, however, also believe it is a fatigue phenomenon due to the cumulative effect of many cycles of cold weather.

Most engineers agree that asphalt binders play the central role in low temperature cracking. In general, hard asphalt binders are more prone to low-temperature cracking than soft asphalt binders. Asphalt binders that are excessively oxidized, either before or after construction, or both, are more prone to low temperature cracking. Thus, to overcome low temperature cracking engineers must use a soft binder, a binder that is not overly prone to aging, and control in-place air void content so that the binder is not excessively oxidized.

Low temperature cracking will join, which in turn, causes even more cracks to form. In some extreme cases, the final stage of low-temperature cracking is disintegration when potholes form. A pothole forms when several of the pieces become dislodged and removed under the action of traffic.

4.1 Bending Beam Rheometer (BBR) Testing

This section describes the detailed investigations of the rheological properties of asphalt binders blended with extracted binders from the recycled asphalt pavement (RAP) at low temperatures. Then, the rheological property was evaluated to determine the resistance characteristics of blended asphalt binders against low temperature cracking.

4.1.1 Experimental Plan

The asphalt binder blending process was followed in accordance with the procedure described in the section 2.1. Then, two replicates of blended asphalt binders were tested in accordance with the procedure of American Association of State Highway and Transportation Officials (AASHTO) TP1 at Superpave low temperatures, i.e., -6, -12, -18, and -24°C ("Provisional" 1996). The experimental design for BBR testing can be seen in Table 2.2.

4.1.2 Sample Preparation

After blended asphalt binders have been aged through the RTFO and PAV tests, the aged binders are heated in the oven until the sample is sufficiently fluid to pour. It should be noted that over heating should be avoided because the samples will harden due to oxidation and volatilization.

In this study, the aluminum mold was selected for BBR specimen preparation. To prepare aluminum molds, there are a couple of materials needed for the mold preparation. The plastic sheeting (transparency film) was cut for lining the interior faces of the three long aluminum mold sections. The petroleum based grease was used to hold the plastic strip to the interior faces of the aluminum mold. Also, the glycerol-talc mixture was used to coat the end pieces of aluminum molds.

Before the aluminum mold preparation, it is very important that the molds should be cleaned. Then, a very thin layer of petroleum based grease was spread, only sufficient to hold the plastic strips to the aluminum mold sections. The plastic strips were placed over the aluminum faces, and it was rubbed with firm finger pressure. The glycerol-talc mixture was contacted to the end pieces, and the molds were assembled using the elastic bands to hold the mold together. After assembled, the asphalt binder was poured from one end of the mold and moved toward the other end, slightly overfilling the mold. The mold was allowed to cool for approximately 45 minutes to 1 hour at room temperature before trimming. The heated spatula was used to trim the specimen and store the mold in the freezer (approximately 0 to -10°C) for 10 minutes. Just prior to testing, the aluminum mold and the plastic strips were removed, and the specimen was inserted in the BBR bath. If the plastic strips could not be removed from the asphalt beam, the beam was put back in the freezer for 3 to 5 minutes more or was put in the BBR bath for 5 to 20 seconds.

4.1.3 Laboratory Testing

The BBR is a tool to evaluate the properties of binders at low temperature in Superpave binder specification. A constant load of 100 grams is applied for 4 minutes at the center of the asphalt beam, which is supported at both ends. The deflection of the beam is measured continuously during the loading and the stiffness is calculated. At very low temperatures, the binder gets brittle and this leads to cracking. To avoid this, the Superpave binder specification has set the limits for the creep stiffness S(t) not to exceed 300 MPa and the m-value m(t) to be at least 0.300 after 60 seconds of loading. A higher

m-value indicates better relaxation characteristics; therefore the thermal stresses do not accumulate to produce cracks.

4.1.4 Test Results and Analysis

The characterization of RAP binder with the BBR has shown an increase in the creep stiffness and decrease in m-value for all temperatures as the amount of RAP binder increases. Table 4.1 and 4.2 show the BBR test results. The effect of RAP binder content on the creep stiffness and the m-value can be seen from Figures 4.1 through 4.4. It should be noticed that Y-axis is in log-log scale. Both the PG 58-28 and PG 64-22 blends have a similar trend, but the slope for the PG 58-28 blend appears to be steeper than the one for PG 64-22 blend. This indicates that the addition of RAP binder did not improve the thermal cracking resistance of the resulting binder over the base binders.

Table 4.3 summarizes the analysis of variance and linear regression analysis for the creep stiffness. It has been observed from the ANOVA table that the three main effects of the variables (RAP binder content, temperature and asphalt type) were found to be significant. It can be seen that the R^2 value of the full model and the reduced model did not differ significantly. From the F-test, however, the effect of the temperature variable was significantly differed from the effects of the RAP binder content and asphalt type. This indicates that the effect of temperature is stronger than the effects of the RAP binder content and asphalt type.

The linear regression models were developed to predict the creep stiffness for different amounts of RAP binder content at different temperatures. All three linear regression models are shown in Table 4.3. It was observed that the R^2 value for the first and second models were similar. Since the RAP source variable was found not to be important factor from the ANOVA table, the third model did include this variable. The

R^2 value was decreased slightly, but did not differ significantly. In this case, the third model was selected to be an accepted model to predict the creep stiffness as a function of RAP binder content at different temperatures.

As observed from the ANOVA of the m-value in Table 4.4, the three main effects of the variables were found to be significant. Similar to the creep stiffness, the R^2 value did not show significant difference between the full and reduce models, and also found that the effect of the temperature was significantly different from the effects of temperature and asphalt type.

Again, the linear regression was used to model the slope (m-value) for different amounts of RAP binder content at different temperatures. It can be seen that the R^2 values for all three models showed no significant difference. For simplicity of the model, the third model was considered to be acceptable to predict the m-value for different amount of RAP binder content at different temperatures.

4.2 Superpave Grading of Blended Asphalt Binders

From the results of DSR and BBR testing, there appears to be a difference in how the different/same RAP sources react with base asphalt binders. As shown before, the addition of RAP has a significant effect on the $G^*/\sin\delta$ and $G^*\sin\delta$ for all temperatures. An addition of RAP binder may improve the rutting resistance properties. According to BBR testing results, the creep stiffness increased and m-value decreased as the amount of RAP binder content increased. The resistance against low temperature cracking was not improved with the increase in RAP binder amount.

The SUPERPAVE performance based grading for asphalt containing Plant C and

L RAP binders are reported in Table 4.5 and 4.6, respectively. A general trend is that the addition of RAP binder has increased the high temperature grade for all binders. The increase in the high temperature grade was due to the increase of stiffness at high temperatures and was evident from the measured values of $G^*/\sin\delta$. The low temperature grade for the PG 58-28 blend remained the same until it decreased at 30 percent RAP binder. Interestingly, an increase in RAP binder amount had little effect in the performance grade at low temperatures for PG 64-22 base binder. The low temperature grade remained the same until it decreased at 75 percent RAP binder. It may be noticed that the low temperature grade was controlled by the m-value. The SUPERPAVE performance based grading for asphalt containing Plant C and L RAP binder did not change, except for 75 and 100% RAP binder content blended with PG 64-22. This indicates that the effect of RAP source was not significant.

4.3 Fracture Toughness at Low Temperatures

The methodology adopted in conducting this set of experiments remained much the same as the previous one in the year of 1997 except the low testing temperature ($0^{\circ}C$). Thus, the cured specimens were soaked in ice for a period of 24 hours, before testing. Three specimens each were tested at every increment of RAP binder content and an average of the results was reported in Table 4.7.

In the year of 1998, three specimens each were also tested at every increment of RAP binder contents at 0, -10 and -20°C. It should be noticed that the temperature control was significantly different between 1997 and 1998. Before conducting the experiments, a control specimen was made to measure the core temperature by inserting

the thermal couple inside a specimen. First, a control specimen was cured in the dry ice to measure the cooling temperatures as a function of times. Then, the control specimen was removed from the dry ice, and the temperature was measured as a function of times. Figures 4.5 and 4.6 show the cooling and decooling rate, respectively. In addition, the environmental chamber box was used to maintain the temperature during testing. The chamber was designed using the insulation and plywood. The nitrogen gas was applied inside the environmental chamber box to adjust the temperature. Figure 4.7 shows the comparison of the fracture toughness values conducted at 0°C in the years of 1997 and 1998. The statistical analyses indicated that there is a significant difference between their mean values in both 1997 and 1998. In addition, multiple comparisons were performed using Duncan's test to make comparison between their means. In 1997, this analysis indicated that the mean values of fracture toughness were not significantly different for all RAP binder contents, but at 100 % RAP binder content it was significantly different from others in 1998. It can be seen that the fracture toughness values for 1998 were higher than the ones in 1997, because the experiments were conducted at a higher temperature than 0°C in 1997. The difference in the fracture toughness values between the 1997 and 1998 appeared to be due to the temperature control during the testing. In 1997, the specimens were soaked in ice sprinkled with salt, for a period of 24 hours, before testing. The experiments had no control on the temperature when the specimens were removed from the ice sprinkled with salt, because the temperature increased rapidly. Therefore, it might be concluded that the experiments conducted in 1997 were not performed at 0°C. However, the trends appeared to be not significantly different between the two.

Figure 4.8 shows the comparison of the fracture toughness at different low temperatures. The trends from the experiments are presented by the linear regression fit. The errors in the average values are effectively between ±5%. It can be observed that the trends were decreased or weakened as the RAP binder increased, and the fracture toughness values was also decreased as the temperature decreased. The crack propagated straight through the pre-crack rapidly for all specimens. From the visual observations, the crack opening displacement was also found lesser at low temperature than what was observed at room temperature. However, the K_{IC} values obtained at low temperatures seem to be valid as the binder behaves as a true brittle material at these temperatures. Hence, the increasing trends of K_{IC} with RAP binder content at room temperature can be considered to be the leading into brittle behavior. More importantly, it is plausible that there is a ductile to brittle transition in the behavior of the binder as the temperature is varied from room to low temperatures. Thus, the results from these experiments can be considered to truly represent the fracture toughness of the material, and linear elastic fracture mechanics is completely valid to characterize RAP binder properties at low temperatures.

The Statistical analyses were performed to compare the fracture toughness as a function of RAP binder contents and temperatures. In these analyses, the two-factor factorial design and multiple regression were used to analyze test results utilizing the statistical software called MINITAB. It should be noted that these analyses were performed only on the experiments conducted in 1998.

From the two-factor factorial design, it was found that RAP binder contents and temperatures had significant effect on the mean fracture toughness values but not their

interaction. The insignificant interaction was indicated by the parallelism of the trends. In general, higher fracture toughness values were attained at 0% RAP binder specimen, regardless of temperatures. Since it was concluded that the means of the fracture toughness differed, it could be interesting to make comparison between the mean fracture toughness values at the specific RAP binder content and temperature. However, this study was concentrated on the fracture behavior as a function of RAP binder contents. Therefore, the Duncan's multiple range test was conducted to evaluate the specific differences at each increment of RAP binder content for all low temperatures. The analysis indicated that the mean fracture toughness values from 0 through 75% RAP binder specimens had no significant differences. In another word, only 100% RAP binder specimen differed from others for all temperatures.

The multiple regression analysis was used to develop the regression model for the fracture toughness. The regression equation was obtained as follows:

$$Y = 299 - 0.21X_1 + 3.12X_2 \qquad (4\text{-}1)$$

$$R^2 = 0.938$$

where, Y = Fracture Toughness, Mpa$\sqrt{m}$ (psi$\sqrt{in}$),

X_1 = RAP Binder Content, %, and

X_2 = Temperature, °C.

ANOVA indicated that all predictors in the regression model were significant. This means that all predictors are needed in the regression model, and the model indicated a good correlation between the X_1, X_2, and Y variables.

4.4 Dynamic Response of Blended Asphalt Binder at Low Temperatures

Although the properties of asphalt and RAP have been studied by DOT at low strain rates and under room temperature conditions, few studies have been performed under dynamic loading at low temperatures. The study of the response of asphalt and RAP to dyn.. .ic compressive stress pulses at low temperatures plays an important role in understanding the durability and failure modes of asphalt pavements. This knowledge assists in designing structurally sound pavements in regions where the environmental temperature is below freezing. This report illustrates a series of compressive impact loading experiments that were performed to assess the dynamic response of asphalt mixes with varying percentages of RAP binder at temperature ranging from 0°C to -20°C.

4.4.1 Split Hopkinson Pressure Bar (SHPB) Refrigeration System

The second system utilized during asphalt testing was the SHPB refrigeration system. This system consists of the Nitrogen Delivery System (NDS), the Low Temperature Chamber (LTC), and a Specimen Cooling Chamber (SCC). The NDS supplies nitrogen gas at a chosen flow rate and output pressure which is specified and manually controlled by the user. The nitrogen gas is transferred from the NDS into the LTC where it is cooled to approximately -74°C (-101°F). After the nitrogen is cooled, it is transferred from the LTC to the SCC. The SCC houses the specimen and interfaces with the SHPB apparatus. Further details of the SHPB refrigeration system are illustrated in the following paragraphs.

4.4.2 Nitrogen Delivery System for the SHPB Refrigeration System

The first subassembly of the SHPB refrigeration system is the NDS. The NDS is

composed of a compressed gas cylinder, a gas cylinder regulator, a digital pressure gage, and a 10 ft. long plastic (polyethylene) hose with a ¼ in. outer diameter. The gas for this system is used as a heat transfer fluid. Nitrogen was chosen as the heat transfer fluid because it is readily available, inexpensive, relatively safe to handle, and has an extremely low freezing point. The freezing point of nitrogen is approximately -209 °C (-346°F).

The gas cylinder regulator chosen for the system was a typical regulator used for compressed gas cylinders. The actual type of cylinder regulator was not significant although it plays a significant role in the refrigeration system. The regulator controls the output pressure of the gas cylinder which controls the nitrogen flow rate. The flow rate of the nitrogen controls the cooling rate of the refrigeration system and the specimen temperature during testing.

Since the output pressure is important, it is necessary to determine the output pressure quickly and accurately during testing. Therefore, a digital versus analog pressure gage was utilized as part of the NDS. It is this pressure gage that is used in conjunction with the gas cylinder regulator to monitor and adjust the output pressure, cooling rate, and specimen temperature during testing.

The last piece of equipment utilized in the NDS is a plastic tube. This plastic tubing is the conduit for transferring the nitrogen gas out of the NDS and into other components of the refrigeration system. Plastic tubing was chosen because its thermal conductivity was less than that of the copper tubing typically utilized in conjunction with this equipment. Since the material is less conductive, there will be less heat loss to the atmosphere during testing.

4.4.3 Low Temperature Chamber for the SHPB Refrigeration System

The second subassembly of the SHPB refrigeration system is LTC. LTC is made of 7/16 in. thick plywood and 1 in. thick Owens Corning FOAMULAR® 150 extruded polystyrene rigid foam insulation. The internal volume of the LTC is approximately 432 in^3 (.25 ft^3). Within the LTC is approximately 50 ft. of ¼ in. outer diameter flexible copper tubing. This copper tubing is wound into 3 in. and 4 in. inner diameter spirals. Both ends of the copper tubing penetrate the top cover of the LTC via two 3/8 in. holes. The nitrogen that flows out of the NDS flows into the LTC via one end of the copper tube and out of the LTC via the other end.

During the refrigeration process, the LTC is filled with dry ice (CO_2) chunks that are no greater than 1 cu. in. When the nitrogen gas from the NDS is transferred into the LTC, the nitrogen gas is cooled to approximately -74°C (-101°F). After being cooled in the LTC, the nitrogen gas is transferred out of the LTC via a 6 in. long ¼ in. outer diameter plastic (polyethylene) tube.

4.4.4 Specimen Cooling Chamber for the SHPB Refrigeration System

The third and final subassembly of the SHPB refrigeration system is the SCC. The SCC is made of 7/16 in. thick plywood and 1 in. thick Owens Corning FOAMULAR® 150 extruded polystyrene rigid foam insulation. The internal volume of the SCC is approximately 81 in^3 (.05 ft^3). The front and rear walls of the SCC contain 2 ¼ in. diameter holes that allow the 2 in. diameter SHPB incident and transmitter bars to enter the chamber and sandwich the specimen. Besides the two holes for the SHPB, the SCC also contains two 3/8 in. diameter holes. These holes allow access for the plastic tube transferring the cooled nitrogen gas from the LTC into the SCC and for two

thermocouples. The cooled nitrogen gas cools the sandwiched specimen prior to and during testing. The thermocouples are needed to monitor the temperature within the SCC and the surface temperature of the specimen.

4.4.5 SHPB Refrigeration System Calibration

The SHPB refrigeration system was assembled and various temperatures versus time profiles for NDS output pressures of 10, 20, 30, 40 and 50 psi were obtained in order to calibrate the system. The temperatures versus time profiles are illustrated in Figures 4.9 through 4.13. From these profiles one can see that the NDS output pressure has a significant effect on the cooling rate of the system up to 30 psi. Once this level is reached, the heat losses in the system prevent the cooling rate to increase or the minimum temperature in the SCC to decrease. However, the cooling rate and the minimum SCC temperature capabilities of the SHPB refrigeration system are sufficient to cool specimens down to –20°C.

Although the SHPB refrigeration system is capable of lowering and maintaining the asphalt's temperature down to the required temperature, this process is time consuming due to the low thermal conductivity and diffusivity rate of asphalt. With materials having low thermal conductivity and diffusivity rates, it is recommended that the specimens be pre-cooled prior to being placed in the SHPB refrigeration system. To pre-cool the asphalt specimen, it should be placed in a thin plastic bag and submersed in an insulated container that is filled with dry ice. Figure 4.14 shows the typical temperature versus time profile for an asphalt specimen with an outer diameter of 1.739 in. and a thickness of 0.5 in. From this profile, one can see that an asphalt specimen initially at room temperature requires 885 seconds (14.8 minutes) of submersion in dry

ice before the specimen core reaches -40°C (-40°F). After the asphalt is pre-cooled, it can be placed in the SHPB refrigeration system. While in this system the specimen's temperature would be exposed to the desired temperature until its temperature has equilibrated. Once thermal equilibrium has been achieved throughout the specimen, testing can begin.

4.4.6 Dynamic Testing of Asphalt at 0°C

Testing of asphalt at 0°C was performed in order to determine the low temperature performance of RAP binders under dynamic loading conditions. These experiments were conducted in the same manner as the room temperature experiments. The only difference was that the specimens were pre-soaked in a dry ice bath until their core temperatures were at 0°C. After pre-soaking the specimens, they were placed in the SHPB apparatus and the SHPB refrigeration system was utilized to maintain a 0°C specimen temperature during testing. Also, each of these experiments were performed twice with respect to RAP content,.

The maximum flow stresses and strains as a function of RAP content are provided in Tables 4.8 and 4.9. The average values of the maximum flow stress and strain as a function of RAP content is provided in Table 4.10 and Figures 4.15 and 4.16. From this table, one can see an increase in the average maximum flow stresses of 5.3% from the 25%, 50%, and 100% RAP mixtures when compared to the 0% RAP mixture. However, there was an increase in the average maximum flow stress of 11% when comparing the 75% RAP mixture to the 0% RAP mixture.

From the table, one can see that there was a decrease in maximum flow strain for all of the RAP mixtures when compared to the virgin asphalt specimen. The maximum

flow strains for the 50% and 75% RAP mixtures decreased by 7.8% when compared to the 0% RAP mixture. However, there was a 3.3% maximum flow strain decrease from 25% and 100% RAP mixtures when compared to the 0% RAP mixture.

The post-mortem analysis of the specimen revealed that the mechanism of failure was shear dominated. With the virgin specimens, the specimen was compressed and sections of the specimen spalled off leaving an intact core. The sections that spalled off did so as chunks of asphalt as depicted in Figure 4.17. As the RAP content increased, there was less of a core and the number of asphalt chunks increased and the size of the chunks decreased. The 100% RAP specimen had no core and consisted of small chunks of asphalt and black sand as depicted in Figure 4.18. This observation also indicates that the material becomes more brittle as the RAP content increases. This observation is definitely indicative of brittle failure.

4.4.7 Dynamic Testing of Asphalt at -10°C

Testing of asphalt at -10°C was conducted to determine the low temperature performance of RAP binders under dynamic loading conditions. The maximum flow stresses and strains as a function of RAP content are provided in Tables 4.11 and 4.12. The average values of the maximum flow stresses and strains as a function of RAP content are provided in Table 4.13 and Figures 4.19 and 4.20. There was an increase in the average maximum flow stresses of 8.7% and 4.3% from the 25% and 75% RAP mixtures to the 0% RAP mixture respectively. However, there was a decrease in maximum flow stress of 8.7% and 13% from the 50% and 100% RAP mixtures to the 0% RAP mixture respectively.

The table also shows an increase in maximum flow strain for all of the RAP mixtures when compared to the 0% RAP specimen. The average maximum flow strains for the 25%, 50%, 75% and 100% RAP mixtures increase 3.8%, 3.8%, 10.1% and 8.9%, respectively when compared to the 0% RAP mixture.

In this set of experiments, the specimens could not be recovered for postmortem analysis. All of them had turned into black sand with a very small amount of minute chunks of the specimen remaining intact as shown in Figures 4.21 and 4.22. This observation is definitely indicative of brittle failure.

4.4.8 Dynamic Testing of Asphalt at -20°C

Testing of asphalt at -20°C was conducted to determine the low temperature performance of RAP binders under dynamic loading conditions.

The maximum flow stresses and strains as a function of RAP content are provided in Tables 4.14 and 4.15. Also, the average values for the maximum flow stresses and strains as a function of RAP content are provided in Table 4.16 and Figures 4.23 and 4.24. There was a decrease in the average maximum flow stress of 23.1%, 3.8%, and 4.3% from the 25%, 50%, and 75% RAP mixtures to the 0% RAP mixture. However, there was an increase in maximum flow stress of 19.2% from the 100% RAP mixture to the 0% RAP mixture. From this data, one can see that there is a significant amount of scatter. The average maximum flow stress deviations for 50% and 75% RAP mixtures are within experimental error unlike that for the 25% and 100% RAP mixtures.

The table shows that there was a decrease in maximum flow strain for all of the RAP mixtures when compared to the 0% RAP specimen. The average maximum flow strain deviations are 1.1%, 9.7%, 13%, and 17% for the 25%, 50%, 75% and 100% RAP

mixtures when compared to the 0% RAP mixture, respectively. There is a linear decrease in the average maximum flow strain as the RAP content is increased at -20°C. Therefore, the material becomes stiffer and more brittle as the RAP percentage is increased at -20°C.

In this set of experiments, the specimens could not be recovered for postmortem analysis. All of them had turned into fine black sand as shown in Figures 4.25 and 4.26.

4.4.9 Dynamic Testing Summary

Experiments were conducted to characterize the dynamic constitutive behavior of RAP binders at low temperatures. From the analysis of the experimental data, one can conclude that the performance of the binder was not affected by the addition of RAP at room nor at low temperatures. Both the average maximum flow stresses and strains experienced no significant deviation due to the addition of RAP at 22°C, 0°C, and -10°C. The majority of the average maximum flow stress and strain deviations for these temperatures were within experimental error. The deviations for those values that were not within experimental error, were attributed to the randomness inherent of the material. At -20° C, the average maximum flow stress experienced no significant deviation due to the addition of RAP. However, the maximum flow strain decreased as the RAP content increased. Therefore, at -20°C, an increase in RAP content increases the degree of brittle failure of the specimen.

A postmortem analysis of all of the specimens illustrated that the dynamic failure modes were shear dominated and of a brittle nature. It also revealed that asphalt becomes more brittle as the temperature of the specimen decreases. At 22°C, the specimen was compressed and sections of the specimen spalled off in wedge like chunks leaving an intact core behind. These wedges were formed because the specimen developed

circumferential, radial and longitudinal cracks that are shear dominated. At 0°C, -10°C, and -20°C, the specimens could not be recovered for postmortem analysis. At 0°C, the specimens had crumbled into moderate chunks and black sand. At -10°C, the specimen had crumbled into small chunks and black sand. At -20°C, the specimens crumbled into black sand. The above failures are indicative of brittle failure.

Table 4.1 BBR Test Results of PAV aged Asphalt Blended with Plant C-RAP Binder in 1998.

RAP, %	Temps, C	PAV Aged			
		PG 58-28		PG 64-22	
		Stiffness, S(t)	Slope, m-value	Stiffness, S(t)	Slope, m-value
0	-6	38.890	0.432	59.897	0.394
	-12	95.975	0.380	128.929	0.341
	-18	216.290	0.323	273.495	0.296
	-24	456.385	0.274	546.935	0.247
10	-6	41.428	0.435	60.712	0.383
	-12	94.258	0.378	136.573	0.366
	-18	227.754	0.319	277.344	0.289
	-24	504.672	0.264	551.592	0.233
20	-6	41.364	0.436	61.204	0.380
	-12	101.470	0.376	140.131	0.332
	-18	217.127	0.330	284.061	0.286
	-24	482.462	0.273	572.346	0.231
30	-6	59.446	0.396	74.554	0.359
	-12	125.733	0.334	156.374	0.322
	-18	263.476	0.277	311.409	0.275
	-24	529.045	0.225	606.237	0.230
40	-6	68.153	0.371	80.858	0.348
	-12	144.470	0.332	165.996	0.318
	-18	301.393	0.283	332.711	0.273
	-24	583.025	0.235	606.260	0.227
50	-6	76.960	0.355	94.439	0.344
	-12	161.023	0.316	182.741	0.306
	-18	332.856	0.278	374.909	0.263
	-24	647.638	0.221	642.605	0.200
75	-6	101.575	0.315	100.353	0.340
	-12	188.188	0.298	202.737	0.305
	-18	410.511	0.264	392.229	0.258
	-24	691.664	0.209	711.108	0.194
100	-6	150.923	0.285	150.923	0.285
	-12	237.467	0.262	237.467	0.262
	-18	485.816	0.237	485.816	0.237
	-24	805.924	0.187	805.924	0.187

Note: 1. The unit for S(t) is MPa.

2. The m-value is unitless.

Table 4.2 BBR Test Results of PAV aged Asphalt Blended with Plant L-RAP Binder in 1998.

RAP, %	Temps, C	PAV Aged			
		PG 58-28		PG 64-22	
		Stiffness, S(t)	Slope, m-value	Stiffness, S(t)	Slope, m-value
0	-6	38.890	0.432	59.897	0.394
	-12	95.975	0.380	128.929	0.341
	-18	216.290	0.323	273.495	0.296
	-24	456.385	0.274	546.935	0.247
10	-6	39.960	0.545	62.378	0.390
	-12	96.680	0.388	134.929	0.343
	-18	229.831	0.326	272.364	0.303
	-24	447.308	0.254	535.967	0.246
20	-6	47.978	0.415	63.085	0.377
	-12	111.562	0.366	134.645	0.322
	-18	250.461	0.316	289.730	0.283
	-24	497.055	0.251	559.401	0.249
30	-6	57.528	0.396	72.494	0.369
	-12	127.828	0.355	142.430	0.329
	-18	255.703	0.301	301.854	0.276
	-24	523.443	0.247	604.075	0.221
40	-6	60.713	0.388	77.093	0.359
	-12	137.146	0.345	160.581	0.319
	-18	280.647	0.290	304.546	0.274
	-24	606.913	0.248	611.458	0.218
50	-6	69.267	0.368	85.927	0.346
	-12	151.950	0.324	170.784	0.310
	-18	295.204	0.281	343.413	0.263
	-24	601.664	0.235	618.985	0.221
75	-6	96.118	0.332	91.096	0.329
	-12	192.792	0.304	204.246	0.297
	-18	352.668	0.266	390.662	0.250
	-24	600.639	0.240	638.094	0.216
100	-6	133.137	0.301	133.137	0.301
	-12	228.581	0.277	228.581	0.277
	-18	416.003	0.244	416.003	0.244
	-24	723.379	0.199	723.379	0.199

Note: 1. The unit for S(t) is MPa.
2. The m-value is unitless.

Table 4.3. Statistical Analyses of Creep Stiffness S(t).

Analysis of Variance (ANOVA)						
Source	DF	Seq SS	Adj SS	Adj MS	F-test	P
Main Effect:						
RC	7	2.61345	2.61354	0.37336	679.58	0.000
T	3	30.12839	30.12839	10.04280	1.8E+04	0.000
AC	1	0.28208	0.28208	0.28208	513.44	0.000
RS	1	0.01555	0.01555	0.01555	28.30	0.000
Interactions:						
RC*T	21	0.30272	0.30272	0.014442	26.24	0.000
RC*AC	7	0.11499	0.11499	0.01643	29.90	0.000
RC*RS	7	0.02764	0.02764	0.00395	7.19	0.000
T*AC	3	0.03461	0.03461	0.01154	21.00	0.000
T*RS	3	0.00180	0.00180	0.00060	1.09	0.354
AC*RS	1	0.00022	0.00022	0.00022	0.40	0.527
Error	201	0.11043	0.11043	0.00055		
Total	255	33.6320	R^2= 99.7%			
Reduced Model						
Main Effect:						
RC	7	2.6135	2.6135	0.3734	149.85	0.000
T	3	30.1284	30.1284	10.0428	4030.63	0.000
AC	1	0.2821	0.2821	0.2821	113.21	0.000
Error	244	0.6080	0.6080	0.0025		
Total	255	33.6320	R^2= 98.2%			

No.	Linear Regression Models for Prediction of G*/sinδ	Adjusted R^2
1	Log S(t) = 0.772 + 0.00319(RC) – 0.0511(T) + 0.0111(AC) – 0.0156(RS)	98.1%
2	Log S(t) = 0.749 + 0.00319(RC) – 0.0511(T) + 0.0111(AC)	98.0%
3	Log S(t) = 1.420 + 0.00319(RC) – 0.0511(T)	97.2%

RC = RAP binder content in percentage (i.e., 0, 10, 20, 30, 40, 50, 75, and 100%)
T = Temperatures in degree Celsius (i.e., -6, -12, -18, and –24°C)
AC = Asphalt type (i.e., PG 58-28 and PG 64-22)
RS = RAP sources (i.e., Plant C and L)

Table 4.4. Statistical Analyses of m-value m(t).

Analysis of Variance (ANOVA)						
Source	DF	Seq SS	Adj SS	Adj MS	F-test	P
Main Effect:						
RC	7	0.43689	0.43689	0.06241	356.36	0.000
T	3	1.46648	1.46648	0.48883	2791.09	0.000
AC	1	0.05051	0.05051	0.05051	288.41	0.000
RS	1	0.00501	0.00501	0.00501	28.60	0.000
Interactions:						
RC*T	21	0.00936	0.00936	0.00045	2.55	0.000
RC*AC	7	0.01675	0.01675	0.00239	13.66	0.000
RC*RS	7	0.00528	0.00528	0.00075	4.31	0.000
T*AC	3	0.00016	0.00016	0.00005	0.30	0.822
T*RS	3	0.00127	0.00127	0.00042	2.42	0.067
AC*RS	1	0.00024	0.00024	0.00024	1.38	0.241
Error	201	0.03520	0.03520	0.00018		
Total	255	2.02715	R^2= 98.2%			
Reduced Model						
Main Effect:						
RC	7	0.43689	0.43689	0.06241	207.84	0.000
T	3	1.46648	1.46648	0.48883	1627.83	0.000
AC	1	0.05051	0.05051	0.05051	168.21	0.000
Error	244	0.07327	0.07327	0.00030		
Total	255	2.02715	R^2= 96.4%			

No.	Linear Regression Models for Prediction of G*/sinδ	Adjusted R^2
1	Log m(t) = 2.96 - 0.0031(RC) + 0.0112(T) - 0.00468(AC) + 0.00885(RS)	95.2%
2	Log m(t) = 2.98 - 0.0031(RC) + 0.0112(T) - 0.00468(AC)	94.9%
3	Log m(t) = 2.69 - 0.0031(RC) + 0.0112(T)	92.4%

RC = RAP binder content in percentage (i.e., 0, 10, 20, 30, 40, 50, 75, and 100%)
T = Temperatures in degree Celsius (i.e., -6, -12, -18, and –24°C)
AC = Asphalt type (i.e., PG 58-28 and PG 64-22)
RS = RAP sources (i.e., Plant C and L)

Table 4.5 SUPERPAVE Performance Grading of Asphalt Blended with Plant C RAP Binder in 1998.

RAP (%)	DSR			BBR		PG Grade
	Unaged	RTFO Aged	PAV Aged	Stiffness	Slope	
	G*/sinδ (Kpa)	G*/sinδ (KPa)	G*sinδ (Kpa)	S (MPa)	m-value	
PG 58-28						
0	1.21@58°C	3.09@58°C	3666@19°C	216@-18°C	0.323	PG 58-28
10	1.67@58°C	4.77@58°C	4030@19°C	228@-18°C	0.319	PG 58-28
20	1.22@64°C	4.29@64°C	2872@22°C	217@-18°C	0.330	PG 64-28
30	1.40@64°C	4.67@64°C	2901@25°C	126@-12°C	0.334	PG 64-22
40	2.03@64°C	6.26@64°C	3561@25°C	144@-12°C	0.332	PG 64-22
50	1.34@70°C	4.42@70°C	2884@28°C	161@-12°C	0.316	PG 70-22
75	1.43@76°C	4.10@76°C	N/A	102@-6°C	0.315	PG 76-16
100	2.95@76°C	11.58@76°C	N/A	151@-6°C	0.285	-
PG 64-22						
0	1.15@64°C	3.33@64°C	2932@25°C	129@-12°C	0.341	PG 64-22
10	1.47@64°C	4.47@64°C	2896@25°C	136@-12°C	0.336	PG 64-22
20	1.90@64°C	5.50@64°C	3203@25°C	140@-12°C	0.332	PG 64-22
30	1.21@70°C	3.64@70°C	2501@28°C	156@-12°C	0.322	PG 70-22
40	1.53@70°C	4.15@70°C	2920@28°C	166@-12°C	0.318	PG 70-22
50	1.92@70°C	6.59@70°C	3499@28°C	183@-12°C	0.306	PG 70-22
75	1.79@76°C	6.41@76°C	N/A	203@-12°C	0.305	PG 76-22
100	2.95@76°C	11.58@76°C	N/A	151@-6°C	0.285	-

NOTE: 1. N/A means that the data is not available.
2. - indicates that the value is insufficient to determine the PG Grading.

Table 4.6 SUPERPAVE Performance Grading of Asphalt Blended with Plant L RAP Binder in 1998.

RAP (%)	DSR			BBR		PG Grade
	Unaged	RTFO Aged	PAV Aged	Stiffness	Slope	
	G*/sinδ (KPa)	G*/sinδ (KPa)	G*sinδ (Kpa)	S (MPa)	m-value	
PG 58-28						
0	1.21@58°C	3.09@58°C	3666@19°C	216@-18°C	0.323	PG 58-28
10	1.54@58°C	4.55@58°C	4008@19°C	230@-18°C	0.326	PG 58-28
20	1.89@64°C	3.07@64°C	3345@22°C	250@-18°C	0.316	PG 64-28
30	1.49@64°C	4.06@64°C	2879@25°C	128@-12°C	0.355	PG 64-22
40	1.74@64°C	5.48@64°C	3311@25°C	137@-12°C	0.345	PG 64-22
50	1.16@70°C	4.12@70°C	2812@28°C	151@-12°C	0.324	PG 70-22
75	1.25@76°C	3.90@76°C	N/A	96@-6°C	0.333	PG 76-16
100	2.36@76°C	9.43@76°C	N/A	133@-6°C	0.301	-
PG 64-22						
0	1.15@64°C	3.33@64°C	2932@25°C	129@-12°C	0.341	PG 64-22
10	1.68@64°C	4.38@64°C	3000@25°C	135@-12°C	0.343	PG 64-22
20	2.36@64°C	6.03@64°C	3345@25°C	135@-12°C	0.322	PG 64-22
30	1.23@70°C	3.50@70°C	2416@28°C	142@-12°C	0.329	PG 70-22
40	1.45@70°C	4.76@70°C	2971@28°C	161@-12°C	0.319	PG 70-22
50	1.61@70°C	5.81@70°C	3047@28°C	171@-12°C	0.310	PG 70-22
75	1.61@76°C	5.19@76°C	N/A	91@-6°C	0.329	PG 76-16
100	2.36@76°C	9.43@76°C	N/A	133@-6°C	0.301	PG 76-16

NOTE: 1. N/A means that the data is not available.
2. - indicates that the value is insufficient to determine the PG Grading.

Table 4.7 Average Fracture Toughness Test Results at Room and Low Temperatures.

		RAP Binder Content, %				
		0	25	50	75	100
Low Temperatures (°C)	0	296	283	293	284	267
	-10	275	265	263	267	252
	-20	232	231	220	217	211

Note: 1. A unit for all fracture toughness values is $1*e^{-3}$ MPa$\sqrt{m}$.
2. N/A indicates that the data is not applicable.

Table 4.8 First Set of Test Values of Maximum Flow Stress and Maximum Flow Strain for SHPB Testing of Various Percentages of Asphalt and RAP Specimens at 0°C.

	0% RAP	25% RAP	50% RAP	75% RAP	100% RAP
Max. Flow S ss	21	24	20	20	21
Max. Flow Strain	8.8	8.6	7.9	8.2	8.7

Table 4.9 Second Set of Test Values of Maximum Flow Stress and Maximum Flow Strain for SHPB Testing of Various Percentages of Asphalt and RAP Specimens at 0°C.

	0% RAP	25% RAP	50% RAP	75% RAP	100% RAP
Max. Flow Stress	18	17	20	22	19
Max. Flow Strain	9.1	8.8	8.7	8.3	8.6

Table 4.10 Average Test Values of Maximum Flow Stress and Maximum Flow Strain for SHPB Testing of Various Percentages of Asphalt and RAP Specimens at 0°C.

	0% RAP	25% RAP	50% RAP	75% RAP	100% RAP
Max. Flow Stress	19	20	20	21	20
Max. Flow Strain	9.0	8.7	8.3	8.3	8.7

Table 4.11 First Set of Test Values of Maximum Flow Stress and Maximum Flow Strain for SHPB Testing of Various Percentages of Asphalt and RAP Specimens at -10°C.

	0% RAP	25% RAP	50% RAP	75% RAP	100% RAP
Max. Flow Stress	22	23	19	22	19
Max. Flow Strain	8.6	8.7	8.5	8.7	8.6

Table 4.12 Second Set of Test Values of Maximum Flow Stress and Maximum Flow Strain for SHPB Testing of Various Percentages of Asphalt and RAP Specimens at -10°C.

	0% RAP	25% RAP	50% RAP	75% RAP	100% RAP
Max. Flow Stress	23	26	24	22	20
Max. Flow Strain	7.1	7.6	7.9	8.6	8.6

Table 4.13 Average Test Values of Maximum Flow Stress and Maximum Flow Strain for SHPB Testing of Various Percentages of Asphalt and RAP Specimens at -10°C.

	0% RAP	25% RAP	50% RAP	75% RAP	100% RAP
Max. Flow Stress	23	25	21	22	20
Max. Flow Strain	7.9	8.2	8.2	8.7	8.6

Table 4.14 First Set of Test Values of Maximum Flow Stress and Maximum Flow Strain for SHPB Testing of Various Percentages of Asphalt and RAP Specimens at -20°C.

	0% RAP	25% RAP	50% RAP	75% RAP	100% RAP
Max. Flow Stress	27	19	24	20	23
Max. Flow Strain	8.8	8.3	7.7	8.0	8.2

Table 4.15 Second Set of Test Values of Maximum Flow Stress and Maximum Flow Strain for SHPB Testing of Various Percentages of Asphalt and RAP Specimens at -20°C.

	0% RAP	25% RAP	50% RAP	75% RAP	100% RAP
Max. Flow Stress	26	20	25	29	19
Max. Flow Strain	9.8	10.1	9.1	7.9	7.1

Table 4.16 Average Test Values of Maximum Flow Stress and Maximum Flow Strain for SHPB Testing of Various Percentages of Asphalt and RAP Specimens at -20°C.

	0% RAP	25% RAP	50% RAP	75% RAP	100% RAP
Max. Flow Stress	26	20	25	25	21
Max. Flow Strain	9.3	9.2	8.4	8.0	7.7

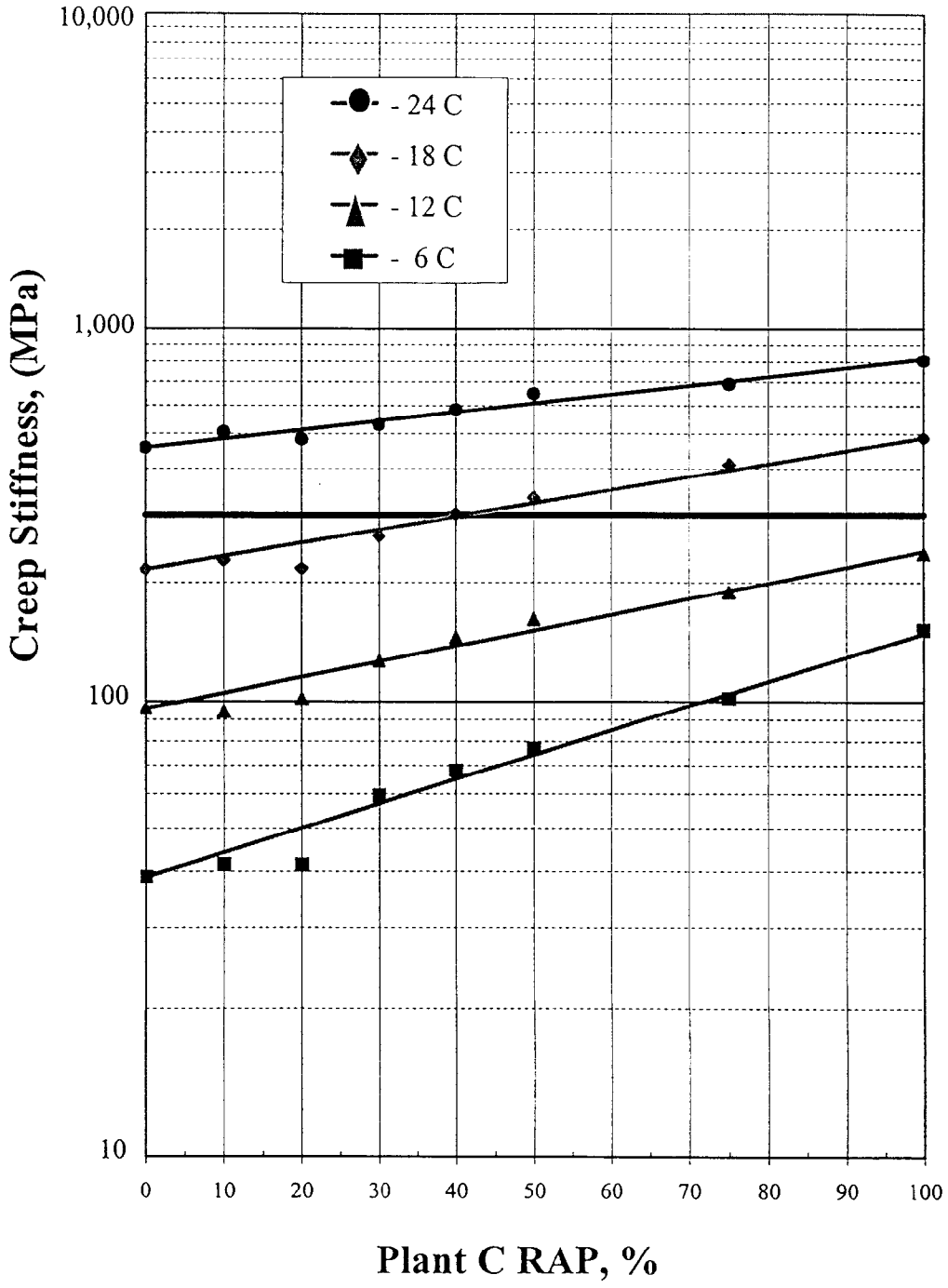

Figure 4.1. Comparison of the Creep Stiffness for PAV Aged Asphalt of PG 58-28 Blended with Plant C RAP Binder at Different Temperatures in 1998.

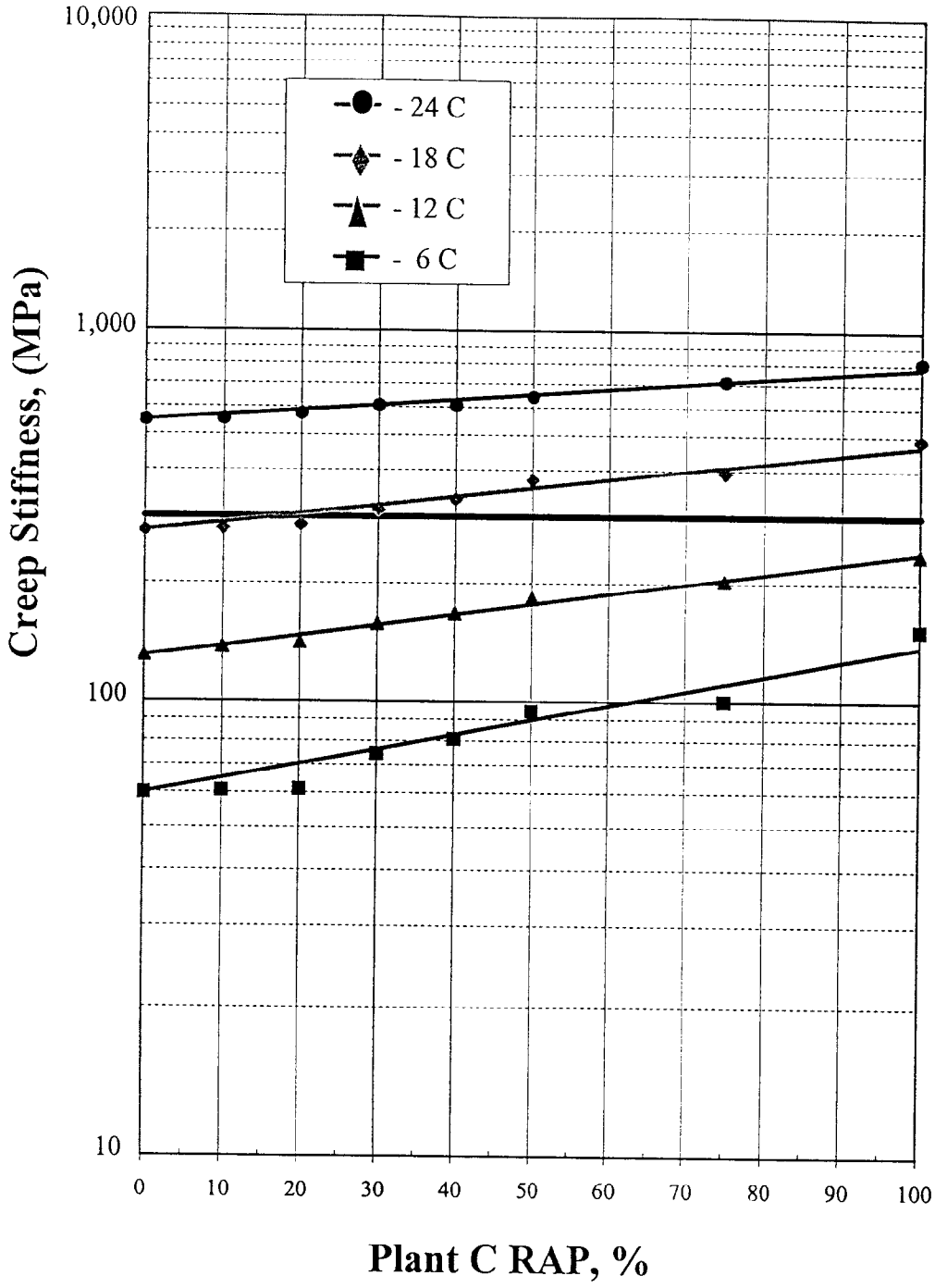

Figure 4.2. Comparison of the Creep Stiffness for PAV Aged Asphalt of PG 64-22 Blended with Plant C RAP Binder at Different Temperatures in 1998.

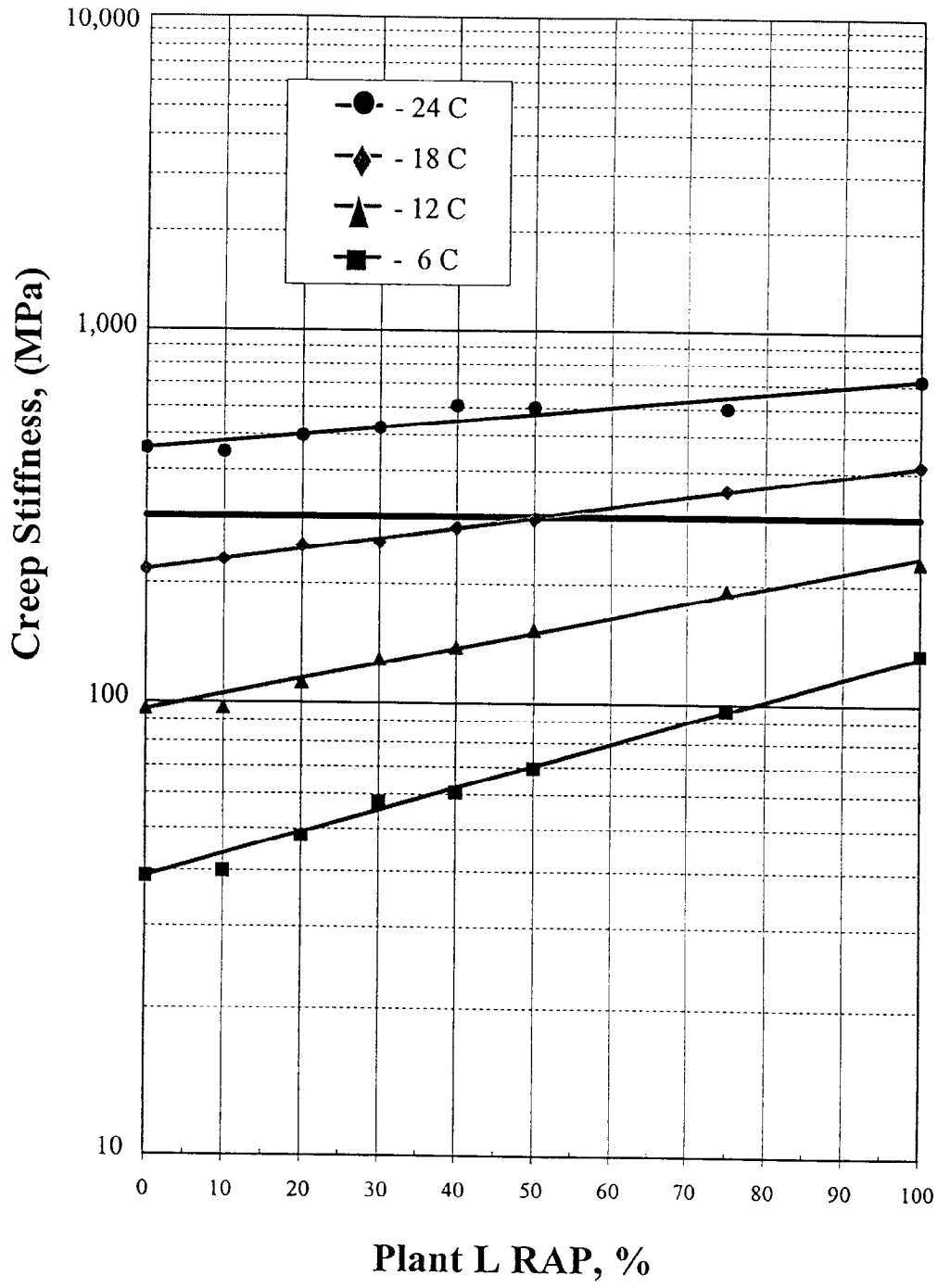

Figure 4.3. Comparison of the Creep Stiffness for PAV Aged Asphalt of PG 58-28 Blended with Plant L RAP Binder at Different Temperatures in 1998.

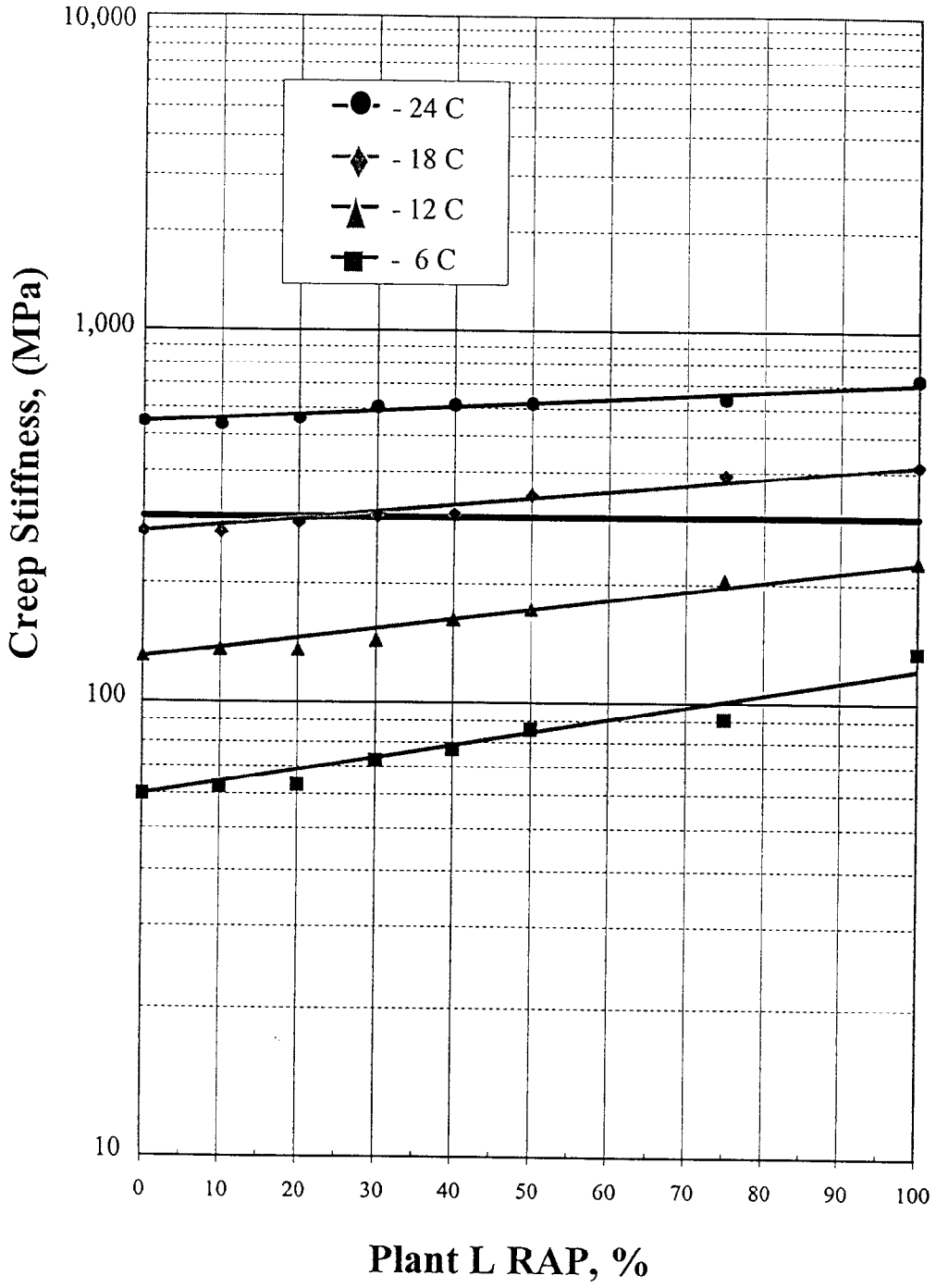

Figure 4.4. Comparison of the Creep Stiffness for PAV Aged Asphalt of PG 64-22 Blended with Plant L RAP Binder at Different Temperatures in 1998.

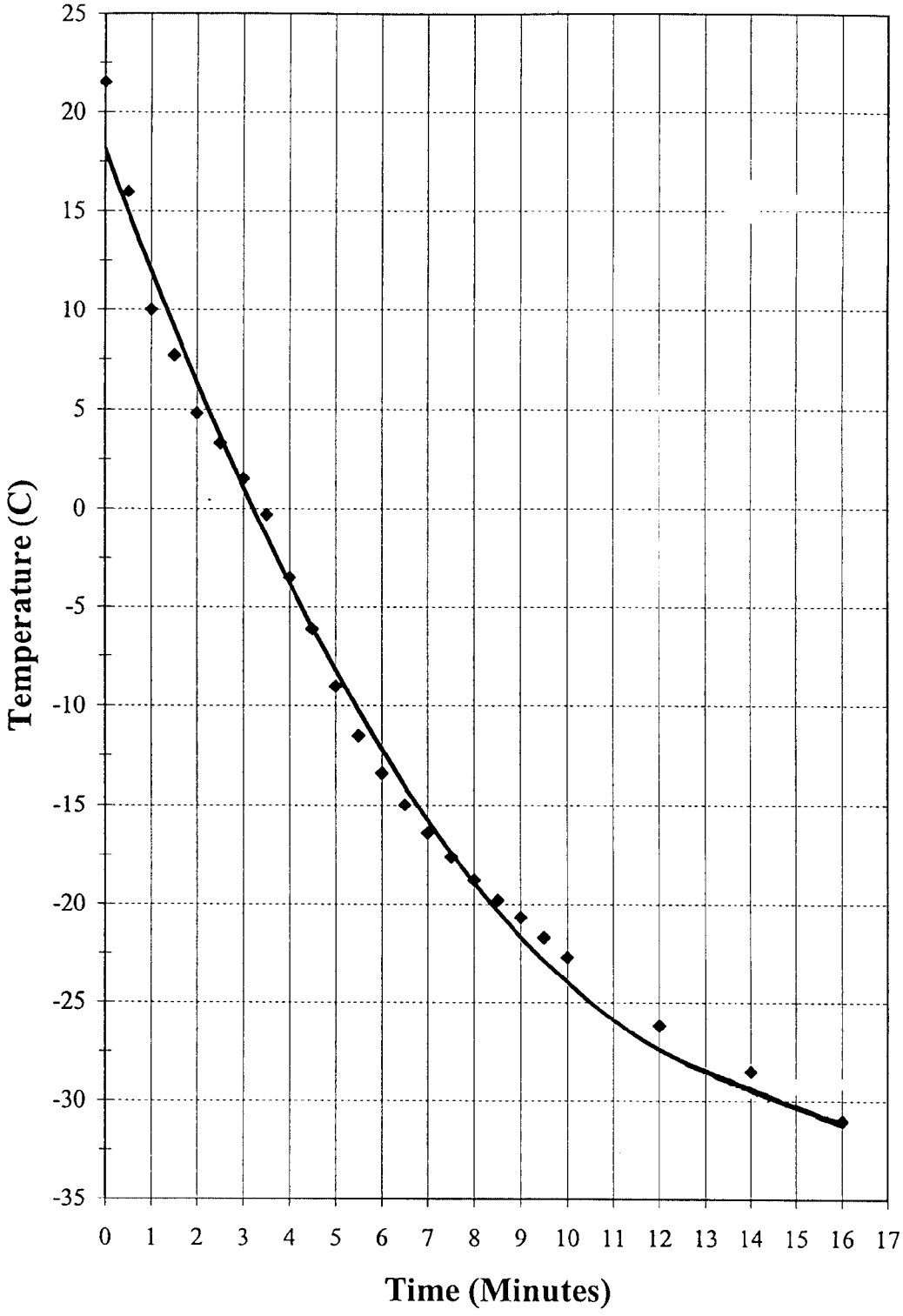

Figure 4.5. The Cooling Rate of the Control Specimen.

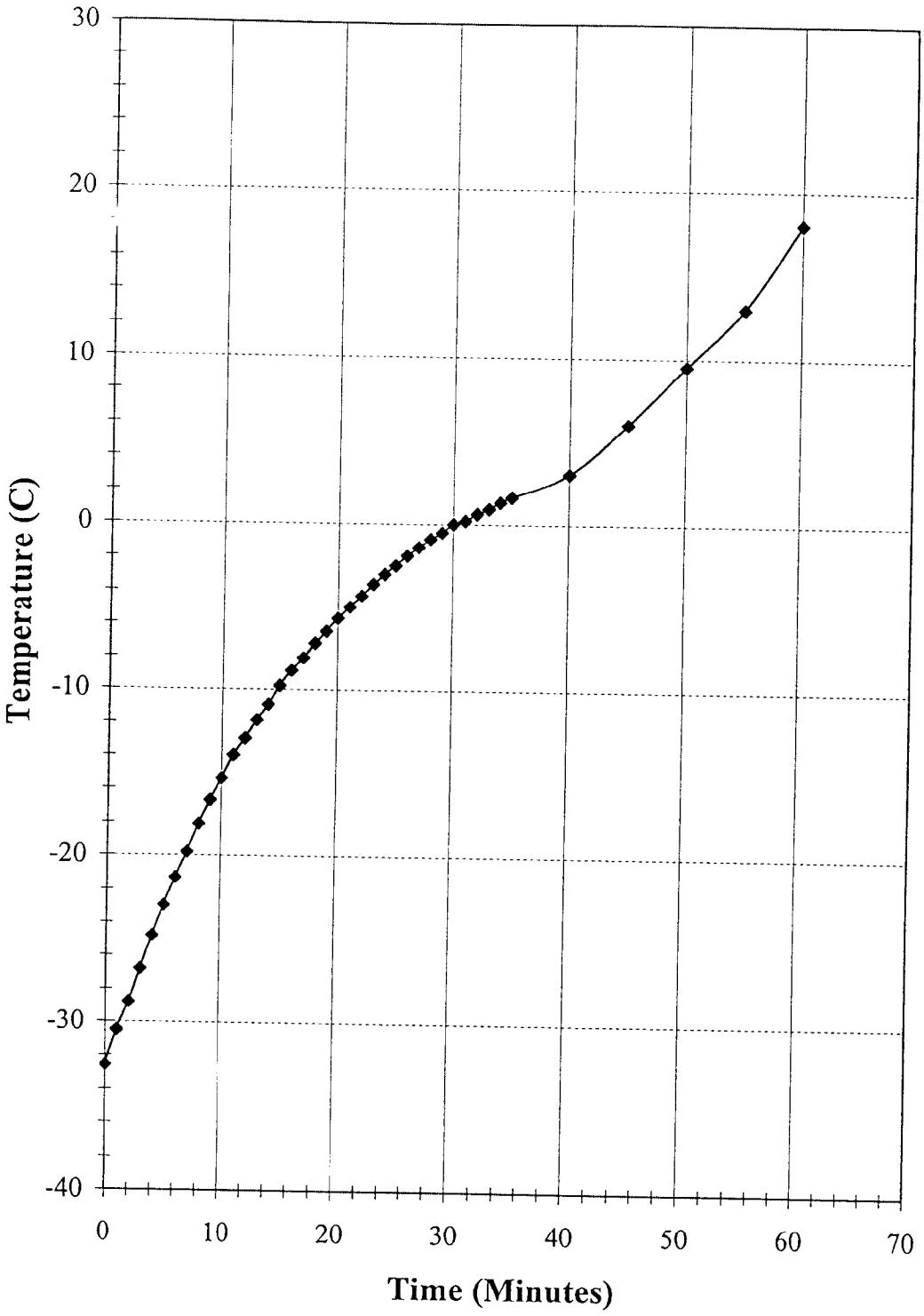

Figure 4.6. The Decooling Rate of the Control Specimen.

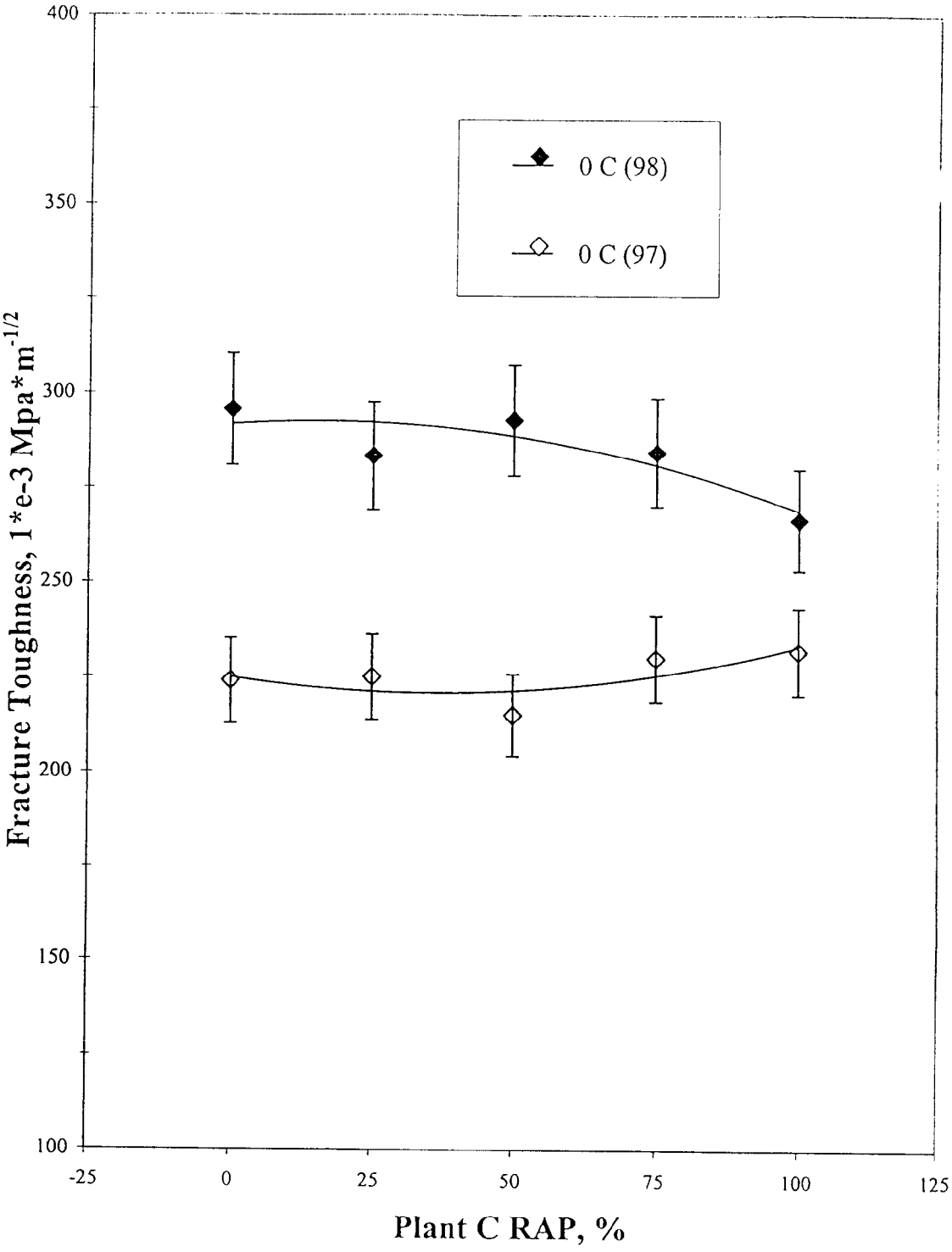

Figure 4.7. Comparison of Fracture Toughness Test Results Between 1997 and 1998 at 0 C.

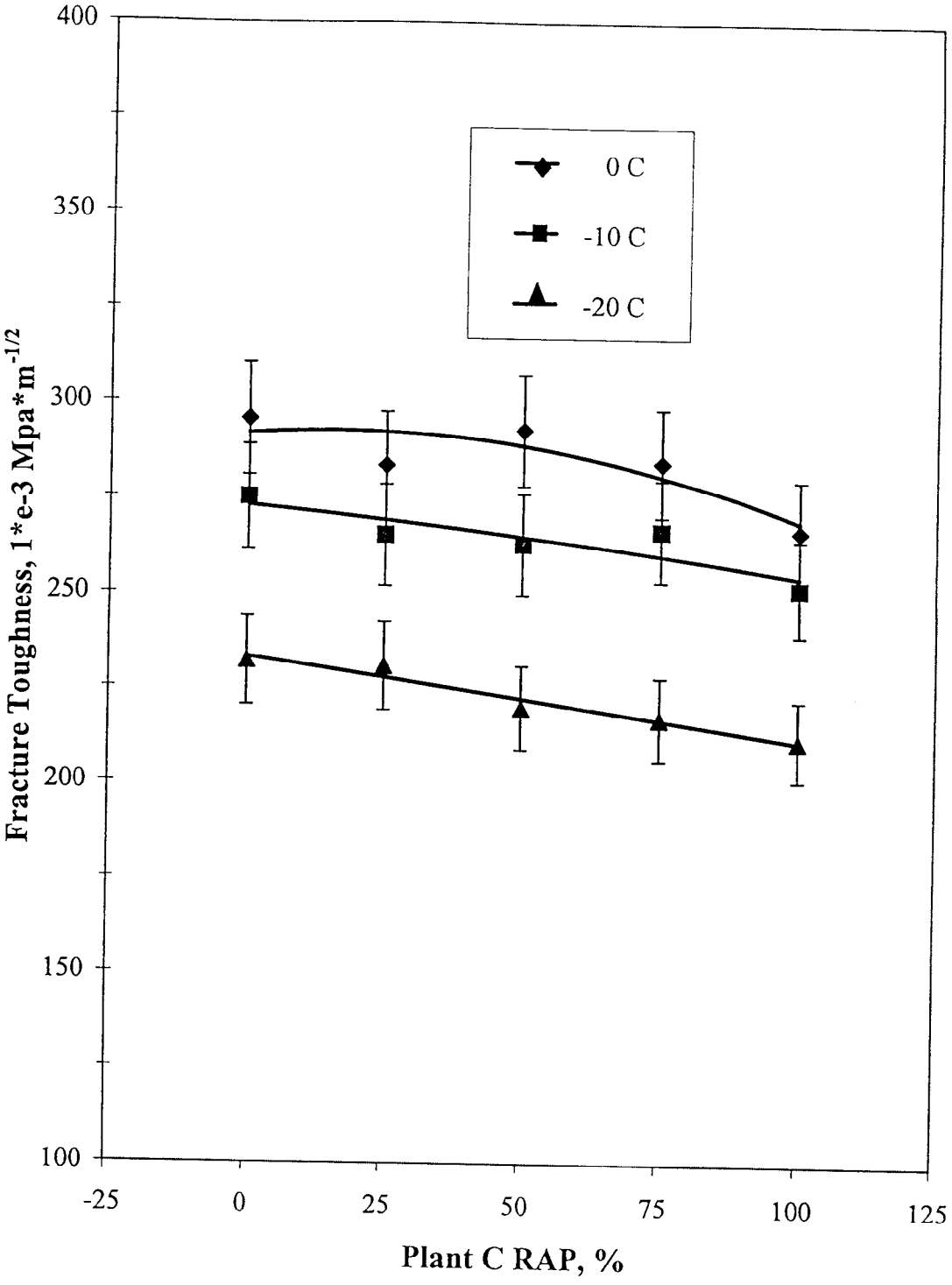

Figure 4.8. Comparison of Fracture Toughness Test Results at Low Temperatures in 1998.

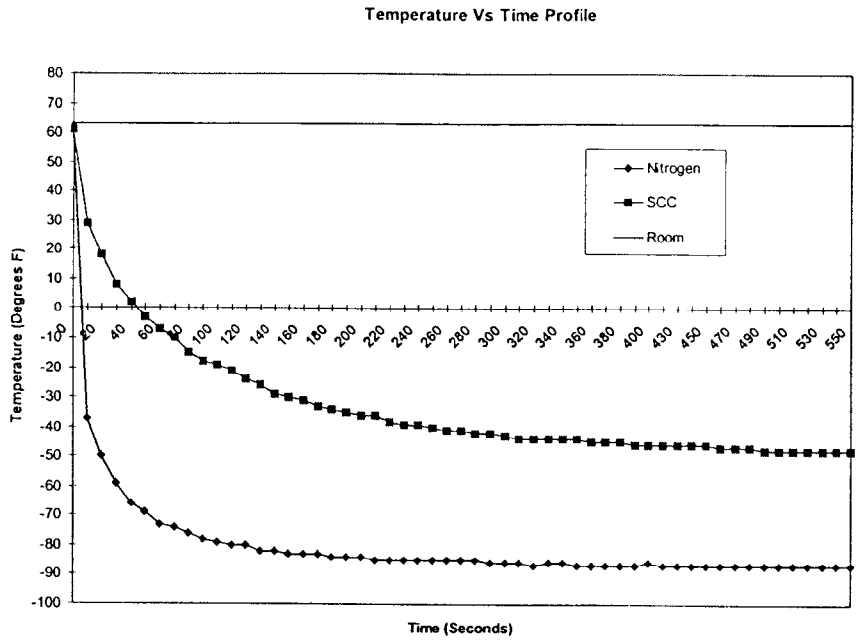

Figure 4.9 SHPB Refrigeration System's Temperature Versus Time Profile for a 10 psi Nitrogen Outlet Pressure.

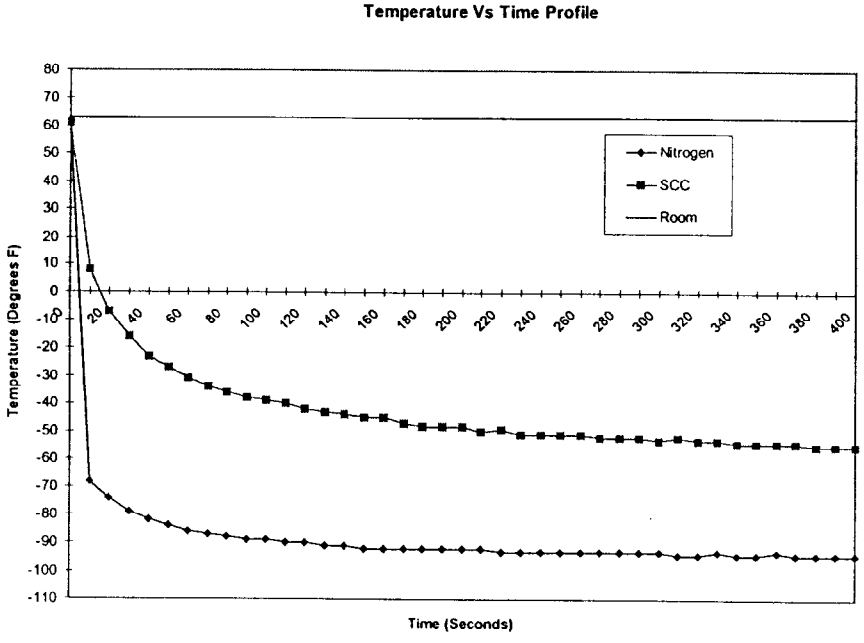

Figure 4.10 SHPB Refrigeration System's Temperature Versus Time Profile for a 20 psi Nitrogen Outlet Pressure.

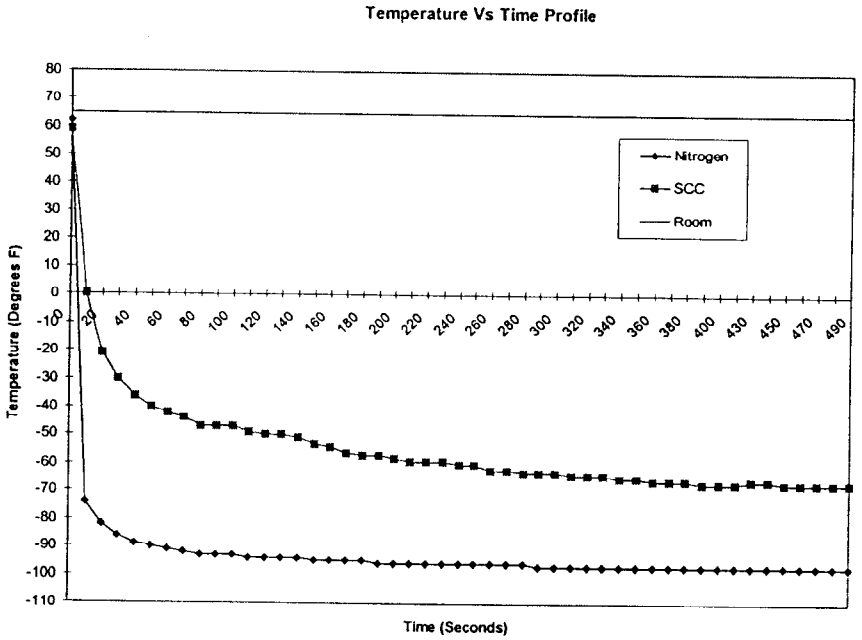

Figure 4-11 SHPB Refrigeration System's Temperature Versus Time Profile for a 30 psi Nitrogen Outlet Pressure.

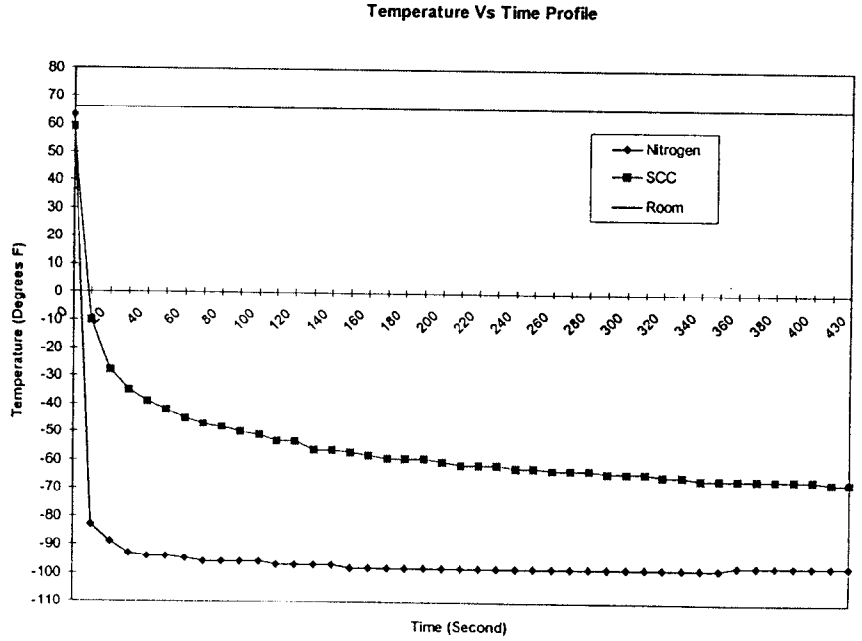

Figure 4-12 SHPB Refrigeration System's Temperature Versus Time Profile for a 40 psi Nitrogen Outlet Pressure.

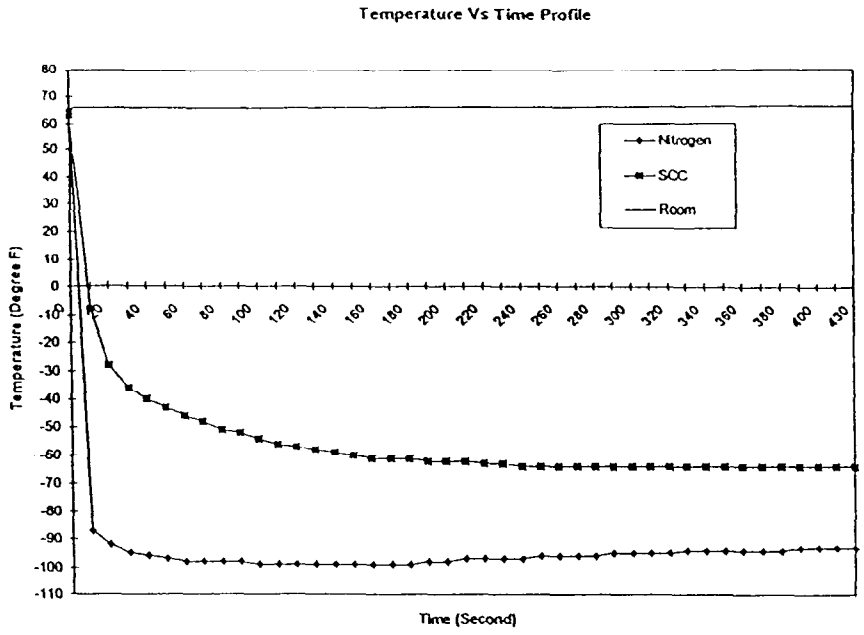

Figure 4-13 SHPB Refrigeration System's Temperature Versus Time Profile for a 50 psi Nitrogen Outlet Pressure.

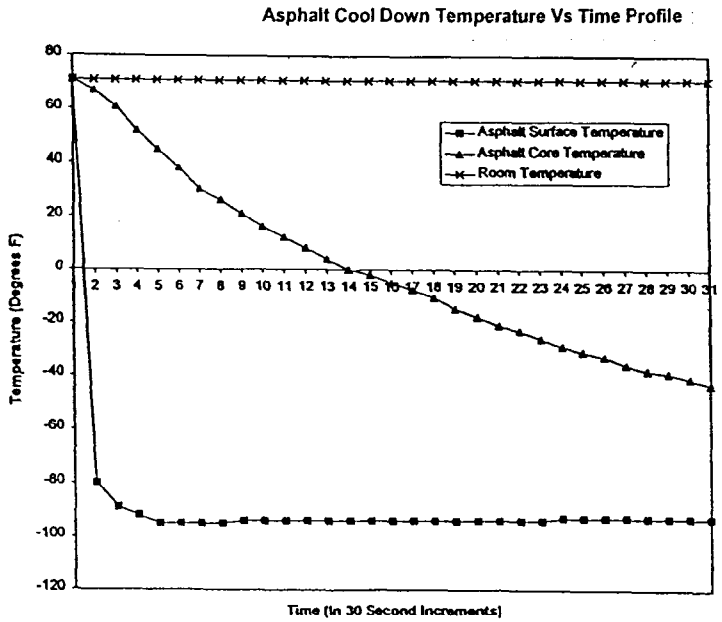

Figure 4-14 Typical Temperature versus Time Profile for an Asphalt Specimen Submersed in Dry Ice.

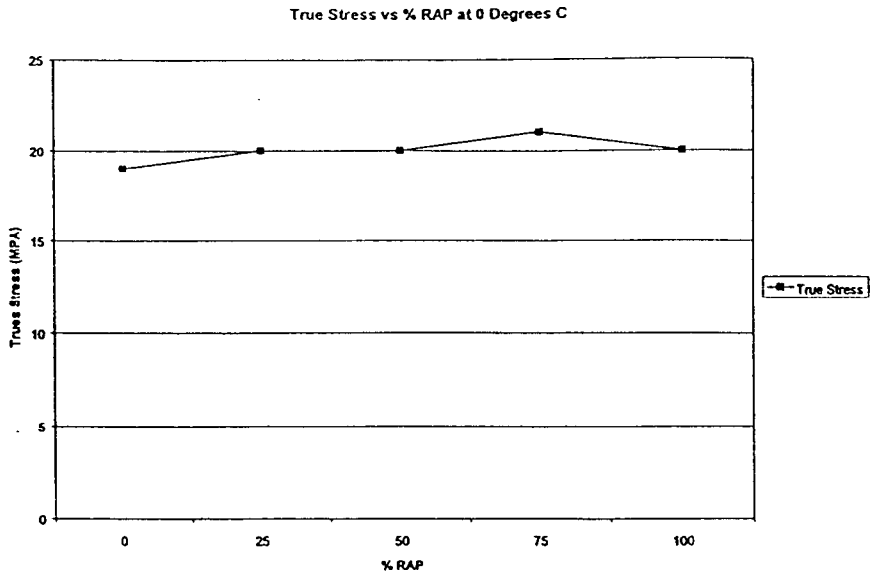

Figure 4-15 Plot of Maximum Flow Stress for SHPB Testing of Various Percentages of Asphalt and Plant C RAP Binder Specimen at 0°C.

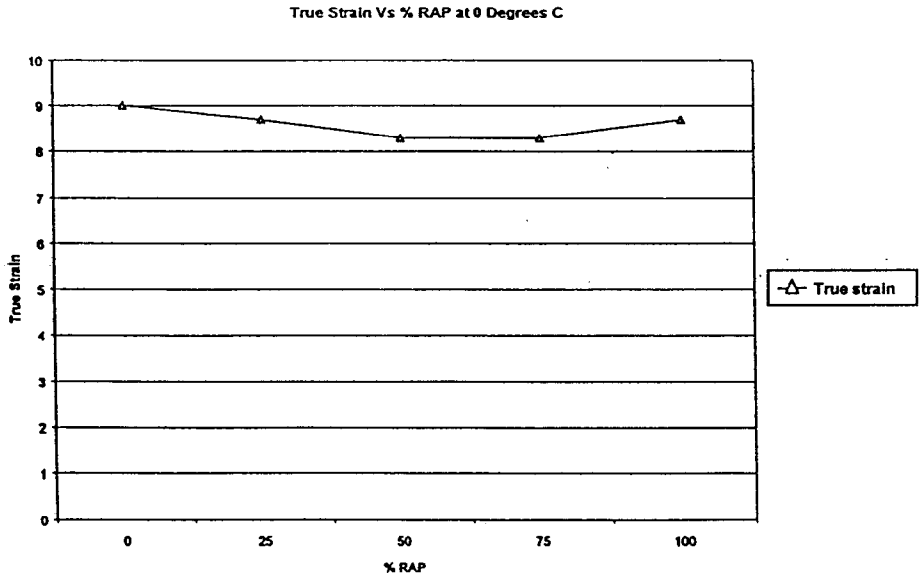

Figure 4-16 Plot of Maximum Flow Strain for SHPB Testing of Various Percentages of Asphalt and Plant C RAP Binder Specimen at 0°C.

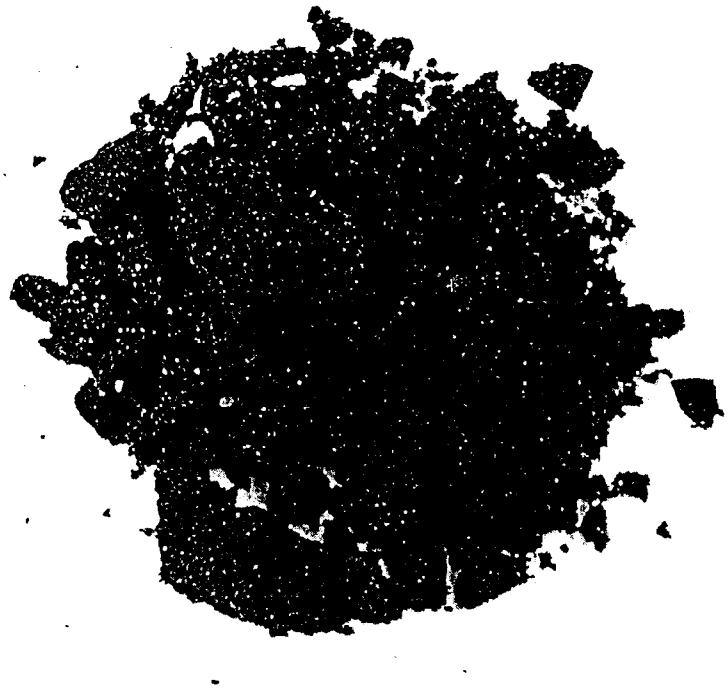

Figure 4.17 Typical Virgin Asphalt Specimen Tested at 0°C.

Figure 4.18 Typical 100% RAP Specimen Tested at 0°C.

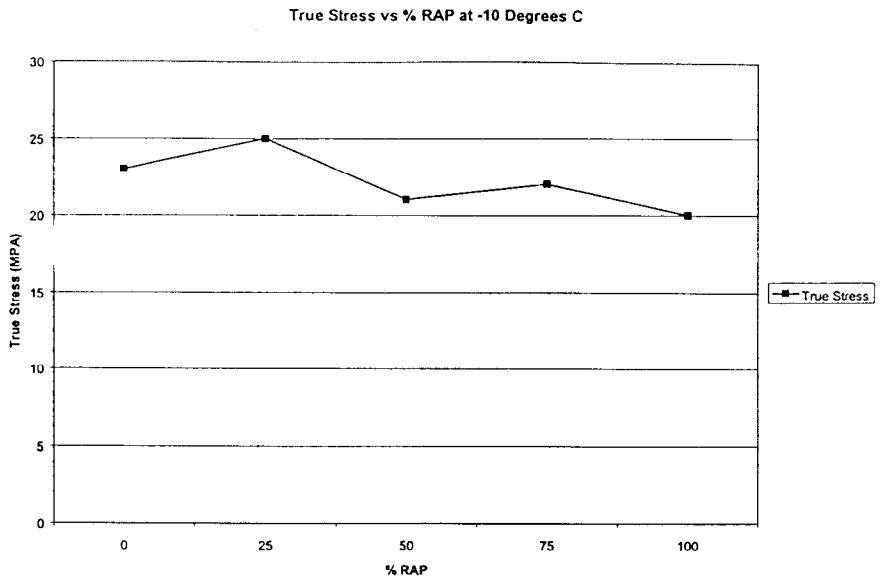

Figure 4.19 Plot of Maximum Flow Stress for SHPB Testing of Various Percentages of Asphalt and Plant C RAP Binder Specimen at –10°C.

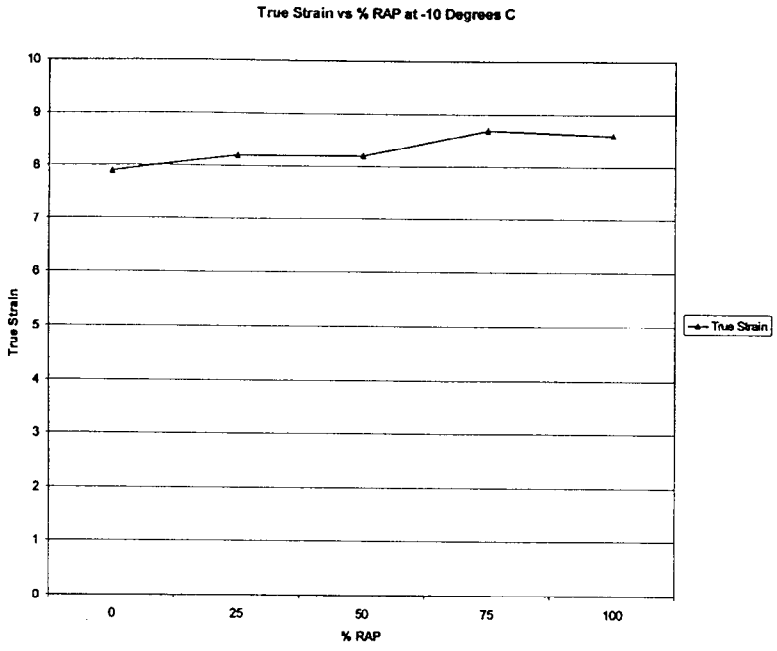

Figure 4.20 Plot of Maximum Flow Strain for SHPB Testing of Various Percentages of Asphalt and Plant C RAP Binder Specimen at –10°C.

Figure 4.21Typical Virgin Asphalt Specimen Tested at -10°C.

Figure 4.22Typical 100% RAP Specimen Tested at -10°C.

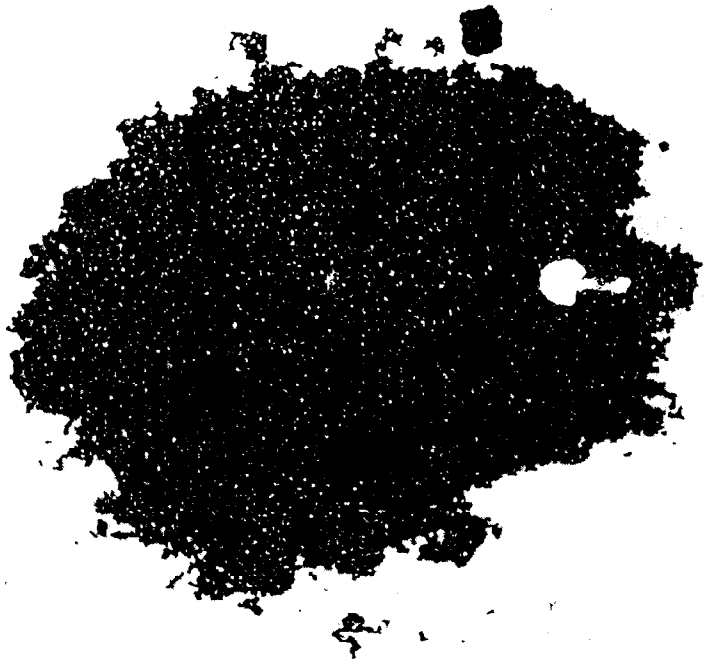

Figure 4.25 Typical Virgin Asphalt Specimen Tested at -20°C.

Figure 4.26 Typical Virgin Asphalt Specimen Tested at -20°C.

CHAPTER 5. CONCLUSIONS AND RECOMMENDATIONS

The following conclusions and recommendations can be drawn from the finding of the present investigation:

1. It was observed that the values of viscosity of blended asphalt were increased as the RAP binder amount was increased for both experiments in 1997 and 1998. It was also noticed that the Plant C RAP binder secured in 1998 has slightly higher values than the Plant L RAP one. However, it may be noted that the one secured from Plant L in 1997 had much higher values than the one from Plant C. Thus, there are significant variations in properties of RAP binder.
2. A good linear relationship between log-log rheological properties of blended asphalt and the amount of RAP binders was obtained.
3. The values of $G^*/\sin\delta$ of asphalt blended asphalt were increased as the RAP binder amount was increased. It was observed that the blended asphalt with Plant C RAP binder exhibited the higher $G^*/\sin\delta$ and steeper slope than the one with Plant L RAP binder in 1998. It may be noted that this is reversed from 1997.
4. The log transformation of $G^*/\sin\delta$ was found to give the best fit and could be applicable for all blended asphalt binders. Statistically, it was observed that the effects of all variables were found significant. But, the RAP source variable was found significantly lower than the RAP binder content, temperature, and asphalt type.
5. All values of $G^*/\sin\delta$ at 58°C for PG 58-28 (or AC-10) base binders met the Superpave minimum requirement, i.e., 1.00 and 2.20 kPa for unaged and RTFO

aged binders, respectively. This was also true for the PG 64-22 (or AC-20) base binders at 64°C. Furthermore, the addition of RAP binders increased the Superpave high temperature grade, and could improve the resistance against rutting.

6. An increase in RAP binder content caused an increase in $G^*\sin\delta$. Therefore, the Superpave criteria of $G^*\sin\delta$ may dictate the maximum amount of RAP addition not to have fatigue cracking.

7. The analysis of variance for log transformation of $G^*\sin\delta$ indicated that all main effects of the variables were found significant as well as other interactions, expect for the interaction of temperature with RAP source and asphalt type with RAP source. The dynamic shear value was found to be dependent on the RAP binder content, temperature, and asphalt type.

8. The fracture toughness was increased as the amount of RAP binder increased at room temperature in 1997 and 1998. However, it was observed that RAP contents had a significant effect on the crack propagation. The crack propagation tended towards instability as the amount of RAP increased, which increased the crack jump distance in the specimen. In other words, RAP binder addition reduced ductility in a specimen.

9. The room temperature dynamic flow stress values of 100% RAP specimen were increased by 8.7% when compared to the 0% RAP specimen. The maximum flow strains for all of the RAP specimens were lower than the one of 0% RAP specimen. However, it was found that average maximum flow stresses and strains

experienced no significant deviation due to the addition of RAP binder at room temperature.

10. An increase in RAP binder content caused an increase in creep stiffness, and a decrease in m-value. It appears that the addition of RAP binders did not enhance the binder's resistance characteristics against low-temperature cracking. Furthermore, the Superpave criteria of s(t) and m(t) may dictate the maximum amount of RAP not to have thermal cracking.

11. The three main variables (RAP binder content, temperature and asphalt type), were found significant for the creep stiffness and m-value. The effect of the temperature was significantly different from the effects of the RAP binder content and asphalt type. This indicates that the creep stiffness and m-value were highly dependent on the temperature.

12. It was general trend that the addition of RAP binder has increased the high temperature grade for all binders. The increase in the high temperature grade was due to the increase of stiffness at high temperatures and is evident from the measured values of $G^*/\sin\delta$. The low temperature grade for the PG 58-28 blend remained the same up to 20 percent RAP binder. Interestingly, an increase in RAP binder amount had little effect on the performance grade at low temperatures for PG 64-22 base binder. The low temperature grade remained the same up to 50 percent RAP binder. It may be noticed that the low temperature grade was controlled by the m-value. There was no difference in the SUPERPAVE performance based grading for blended asphalt with Plant C and L RAP binder, except the PG 64-22 based one containing 75 and 100% RAP binder.

13. The dynamic performance of the binder was not affected by the addition of RAP at room nor at low temperatures. Both the average maximum flow stresses and strains experienced no significant deviation due to the addition of RAP at 22°C, 0°C, and -10°C. The majority of the average maximum flow stress and strain deviations for these temperatures were within experimental error. At -20° C, the average maximum flow stress experienced no significant deviation due to the addition of RAP. However, the maximum flow strain decreased as the RAP content increased. Therefore, at -20°C, an increase in RAP content increases the degree of brittle failure of the specimen.

14. A postmortem analysis of all of the specimens illustrated that the dynamic failure modes were shear dominated and of a brittle nature. It also revealed that asphalt becomes more brittle as the temperature of the specimen decreases.

15. It is recommended that further research should be performed with asphalt mixture to incorporate the finding from the binder study.

REFERENCES

1. *Annual Book of ASTM Standards.* (1997). American Society of Testing and Materials (ASTM). Philadelphia, Pa.

2. Brown, R., Kandhal, P., Lee, D. and Lee, K.W. (1996) "Significance of Tests for Highway Materials," ASCE Journal of Materials in Civil Engineering, Vol.8, No.1, pp. 26-40.

3. Chiddester, J.L. and Malvern, L.E., "Compression-Impact Testing of Aluminum at Elevated Temperatures," Experimental Mechanics, Vol. 3 (1963), pp. 81-90.

4. Davies, R. M., "A Critical Study of the Hopkinsons Pressure Bar," Philosophical Transactions of the Royal Society of London, Series B, Vol. 140 (1948), pp. 375 - 457.

5. Hopkinson, B., "A Method of Measuring the Pressure Produce in the Detonation of Explosives or by the Impact of Bullets," Philosophical Transactions of the Royal Society of London, Series A, Vol. 213 (1914), pp. 437 - 456.

6. Jacobs, M., Hopman, P., and Molenaar, A. (1996). "Application of Fracture Mechanics Principles to Analyze Cracking in Asphalt Concrete," Journal of AAPT, pp. 1-39.

7. Kennedy, T., Roberts, F. and Lee, K.W. (1982). "Evaluation of Moisture Susceptibility of Asphalt Mixtures Using the Texas Freeze-Thaw Pedestal Test," Proc. of AAPT. Vol.51.

8. Kolsky, H. (1949). "An Investigation of the Mechanical Properties of Materials at Very High Rates," Philosophical Transactions of the Royal Society of London, Series B, Vol.62, pp 676-700.

9. Lee, K.W., Shukla, A., Venkatram, S., and Soupharath, N. (1998). "Evaluation of Permanent Deformation and Fatigue Cracking Resistance Characteristics of Recycled Asphalt Pavement Binders," Final Research Report to RIDOT, Kingston, RI.

10. Majidzadeh, K., Dat, M. and Makdisi-Ilyas, F. (1976). "Application of Fracture Mechanics for Improved Design of Bituminous Concrete," Report No. FHWA-RD-76-92.

11. May, R. and McGennis, R. (1996) "Superpave Asphalt Mixture Analysis," The Asphalt Institute Research Center, Lexington, KY.

12. McGennis, R., Shuler, S. and Bahia, H. (1994). "Background of SUPERPAVE Asphalt Binder Test Methods," Report No. FHWA-SA-94-069, Washington, D.C.

13. *Mix Design Methods for Asphalt Concrete and Other Hot Mix Types.* (1993). Asphalt Institute MS-2, 6th ed., Lexington, KY.

14. Monismith, C.L., Hicks, R.G. and Salam, Y.M., (1972) "Basic Properties of Pavement Components," Report FHWA-RD-72-19.

15. *Provisional Standards.* (1996). Am. Assoc. of State Hwy. And Transp. Officials (AASHTO), Washington, D.C.

16. *Standard Specifications for Transportation Materials and Methods of Sampling and Testing.* (1995). 16th ed., Part II, AASHTO, Washington, D.C.

17. Sulaiman, F. and Stock, A. (1996), "The Use of Fracture Mechanics for the Evaluation of Asphalt Mixes," Journal of AAPT, Vol. 64. pp 500-533.